Comparison of the DNA damage response and mechanisms of treatment resistance in stem cells originating from malignant and benign prostate tissues and their differentiated counterparts

Sandra Klein

The University Of Sheffield.

A thesis submitted for the degree of Doctor of Philosophy

Department of Oncology, The University of Sheffield

March 2013

IN PRINTED THESIS FIND 'ACCESS TO THESIS FORM' IN HERE

We don't know whether there is light at the end of the tunnel, but we are pretty convinced that there is a tunnel.

–Unknown

Table of contents

Figures Introduction

Figures Results

ACKNOWLEDGEMENTS

For my family

I would like to thank my supervisors Norman J. Maitland and Mark Meuth for enabling me to come to the UK to undertake this PhD project. Many thanks for your guidance and support during the past years by giving me at the same time the freedom to make own decisions and experiences.

Some PhD students have one postdoc they would owe a big part of their thesis to. In this context I would like to thank Fiona M. Frame for being a great teacher and giving me her time even though she had a busy schedule by herself. Thanks for valuable advice in many different aspects.

Thank you to the laboratory members at the CRU at the University of York and the ICS at the University of Sheffield for supporting and advising me during my PhD and creating a nice working environment. Many of you developed from colleagues into friends and played an important role in my private life. You will be missing now that my work has finished. In this context I would like to give special thanks to Dominika E. Butler for her support.

I also would like to thank the patients for their willingness to donate samples for research and the surgeons for their cooperation. Without them the completion of this work would not have been possible.

Many thanks to the White Rose Consortium for funding this project and linking researchers from different universities to each other to provide additional support to their PhD students.

Last but not least, I would like to thank my friends who no matter whether they lived inside or outside the UK constantly kept in touch with me by writing, calling and visiting me.

Abstract

Prostate cancer is the most frequently diagnosed malignant disorder in men and despite intensive research there is little effective therapy against tumour recurrence and metastatic disease. Recent findings direct the origins of prostate cancer to cancer stem cells (CSCs). The CSC model proposes that tumours are hierarchically organized and sustained by CSCs that act as an undifferentiated reservoir within the tumour. Similar to their normal counterparts, CSCs are thought to be highly protected against DNA damage, which might play a crucial role in therapy failure and tumour recurrence. Our findings indicate that $CD133^{+}/\alpha_2\beta_1 integrin^{high}$ stem cells (SCs) from malignant and benign prostate tissues are more effectively protected against DNA damage introduced by etoposide than $CD133^{-}/\alpha_2\beta_1 integrin^{high}$ transit amplifying (TAs) and $CD133^{-}/\alpha_2\beta_1 integrin^{low}$ committed basal cells (CBs). Furthermore, the colony forming efficiency in prostate SCs was less affected by the drug. The assessment of ABC-transporters revealed that these are unlikely to be mediators of the enhanced resistance in SCs. However, according to a cell cycle analysis a higher proportion of SCs was quiescent when compared to TA or CB populations. Hence, cellular dormancy might be one factor contributing to therapy survival. Further research is required to determine the role of CSCs in treatment resistance. Future therapies that target specifically prostate CSCs might be a key to prevent tumour relapse.

Abbreviations

ABC	ATP-binding cassette
ADT	Androgen deprivation therapy
AP-Atg	Autophagosome-autophagy-related gene
AML	Acute myeloid lymphoma
AR	Androgen receptor
ATM	Ataxia telangiectasia mutated
ATR	Ataxia telangiectasia and Rad3 related
Bcl-2	B-cell lymphoma 2
BER	Base excision repair
BSA	Bovine serum albumin
BPH	Benign prostatic hyperplasia
BRCA-1	Breast cancer -1
Cat. no.	Catalogue number
CB	Committed basal cell
CFGE	Constant field gel electrophoresis
Chk1	Checkpoint kinase 1
Chk2	Checkpoint kinase 2
CML	Chronic myelogenous leukemia
CRPC	Castration resistant prostate cancer
CRU	Cancer Research Unit
CRUK	Cancer Research UK
CSC	Cancer stem cell
CT	Computer tomography
DAPI	4',6-diamidino-2-phenylindole
dCTP	Deoxycyidine triphosphate

DMEM	Dulbeccos´s modified eagle medium
DMSO	Dimethyl sulfoxide
DNA	Deoxyribonucleic acid
DNA-PKcs	DNA dependent protein kinase catalytic subunit
DNA-PK	DNA dependent protein kinase
DSB	Double strand break
dTTP	Deoxythymidine triphosphate
ECM	Extracellular matrix
FANCD2	Fanconi anemia complementation group D2
FCS	Fetal calf serum
FDA	Food and drug administration
FITC	Fluorescein isothiocyanate
FM	Freezing media
GC-rich	Guanine/Cytosine-rich
GS	Gleason score
G-CSF	Granulocyte colony-stimulating factor
GSTP1	Glutathione S-transferase P1
h	Hour
HGPIN	High grade prostate intraepithelial neoplasia
HIFU	High-intensity focused ultrasound
HR	Homologous recombination
ICS	Institute for Cancer Studies
IL-6	Interleukin 6
JAK-STAT	Janus Kinase/Signal transducer and activator of transcription
KEGG	Kyoto Encyclopedia of Genes and Genomes

KSFM	Keratinocyte serum-free medium
LA	Left apex
LB	Left base
LIF	Leukemia inhibitory factor
LM	Left mid
LRP	Laparoscopic radical prostatectomy
MACS	Magnetic cell sorting
MDC1	Mediator of DNA damage checkpoint protein 1
ml	Millilitre
µl	Microlitre
mM	Millimole
µM	Micromole
min	Minute
MRE-11	Meiotic recombination 11
MRI	Magnetic resonance imaging
mTOR	Mammalian target of rapamycin
MTS	3-(4,5-dimethylthiazol-2-yl)-5-(3-carboxy methoxyphenyl) -2-(4-sulfophenyl)-2H-tetrazolium
NE	Neuroendocrine cell
NER	Nucleotide excision repair
NFKb	Nuclear factor kappa b
NHEJ	Non-homologous end joining
ORP	Open radical prostatectomy
PAP	Prostate acid phosphatase
PDT	Photodynamic therapy
PED	Phosophoprotein Enriched in Diabetes over-expression

PFA	Paraformaldehyde
PI	Pan-nuclear intermediate
PIN	Prostate intraepithelial neoplasia
PI3K	Phosphoinositide-3-kinase
PIKK	PI3K -related protein kinases
PL	Pan-nuclear light
PNK	Polynucleotide kinase
PS	Pan-nuclear strong
PSA	Prostate specific antigen
PTEN	Phosphatase and tensin homolog
RA	Right apex
RB	Right base
RP	Radical prostatectomy
RT	Room temperature
SC	Stem cell
SCF	Stem cell factor
SCM	Stem cell media
SSB	Single strand break
TA	Transit amplifying cell
TIMP-2	Tissue inhibitor of metalloproteinases-2
TMPRSS2-ERG	Transmembrane protease, serine 2 - Ets related gene
TURP	Transurethral resection of the prostate
RNA	Ribonucleic acid
PARP1	Poly (ADP-ribose)-Polymerase 1
PBS	Phosphate buffered saline
PIK3	Phosphatidylinositol 3-kinase

PIKK   PI3K-related protein kinase

ROS   Reactive oxygen species

ssDNA   Single stranded DNA

ut   Untreated

UV   Ultraviolet

Chapter I

INTRODUCTION

1. INTRODUCTION

1.1 The prostate

The prostate is a walnut-sized gland of the mammalian reproductive system that produces ~30% of the seminal fluid [1]. The function of this secretion is to provide nutrients and anticoagulants for the spermatozoa, which are mixed in the urethra. According to McNeal's classification, the prostate consists of four zones (Figure 1-1) [2]. The **peripheral zone** constitutes more than 70% of the prostate and surrounds the urethra [2, 3]. The majority of prostate carcinomas arise from here [2]. The second largest zone is the **central zone**, which surrounds the ejaculatory ducts [2, 3]. The **transitional zone** makes up 5% of the prostate [2, 3]. It is the zone where benign prostatic hyperplasia (BPH) and approximately 25% of prostate carcinomas occur [2, 3]. The **anterior zone** contains mainly fibrous and muscular tissue and has no secretory function [2]. The normal prostate epithelium consists of three major cell types: **luminal** cells, **basal** cells and **neuroendocrine** cells (NEs) (Figure 1-2) [3, 4]. The predominant cell type are the luminal cells [4]. They are terminally differentiated and produce prostate specific antigen (PSA), a serine-protease that prevents the coagulation of seminal fluid. Furthermore, they secrete prostatic acid phosphatase (PAP) and beta microseminoprotein [3, 5]. As their growth and survival depends on androgens e.g. testosterone, they express the androgen receptor (AR) [6, 7]. The population of luminal cells has a high apoptotic rate and hence a short life time leading to a fast turn-over [3, 8].

The basal cells of the prostate epithelium are less differentiated and do not have secretory activity [4]. They are androgen-independent and express only low levels of AR [9, 10]. The basal epithelium is the most proliferative compartment and is made up in a hierarchical order (Figure 1-2) [4]. There

is a rare subset of stem cells (SCs) that ensures the regeneration of the prostate tissue [11, 12]. They are located within a supporting environment, the so-called "stem cell niche", which provides signals that are essential for their survival. Furthermore, in the niche the SCs are protected from signals that would result in their differentiation and apoptosis, that would otherwise result in an exhaustion of the SC pool [3, 13, 14].

To fuel the tissue with new cells, SCs give rise to basal, luminal and NEs, a process which is mediated by alternative differentiation pathways [3, 15]. During differentiation, the cells migrate through the basal layer to form terminally differentiated cells [3, 16]. The SCs give rise to transit amplifying cells (TAs) and these proceed to differentiate upon stimulation with androgens, stromal factors and signals from the extracellular matrix into committed basal cells (CBs), which develop into fully differentiated luminal cells [17-19]. The prostate epithelium is illustrated in Figure 1-2.

The NEs reside in the epithelium of the acini and ducts. They are terminally differentiated and androgen-independent [20]. NEs secrete a variety of hormones, such as serotonin, bombensin, neurotensin and calcitonin, which regulate the growth of the prostate [3, 21]. Underneath the epithelium there is the stromal compartment, which comprises different structures such as smooth muscle cells, fibroblasts, adipocytes, collagen and elastin [3]. The stromal compartment is critical for the maintenance of the prostate gland by the secretion of growth factors [22].

Prostate zones

a Central zone
b Fibromuscular zone
c Transitional zone
d Peripheral zone
e Periurethral gland region

Ejaculatory duct
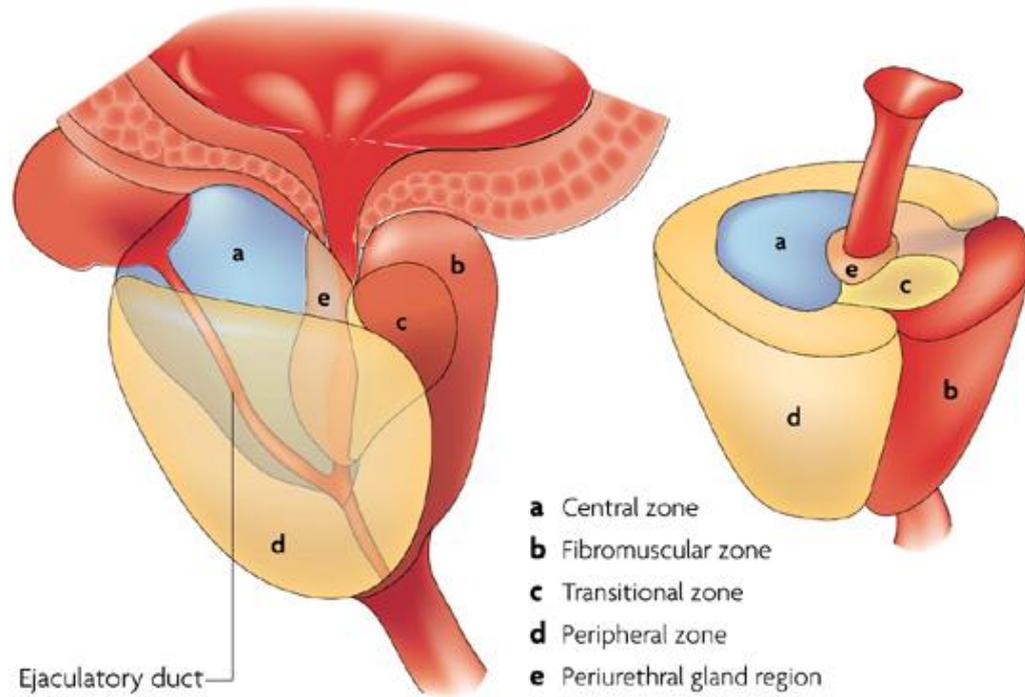
Figure 1-1 Zones of the prostate. Illustration of the prostate showing the central, anterior (fibromuscular), transitional and peripheral zone. Taken from [23].
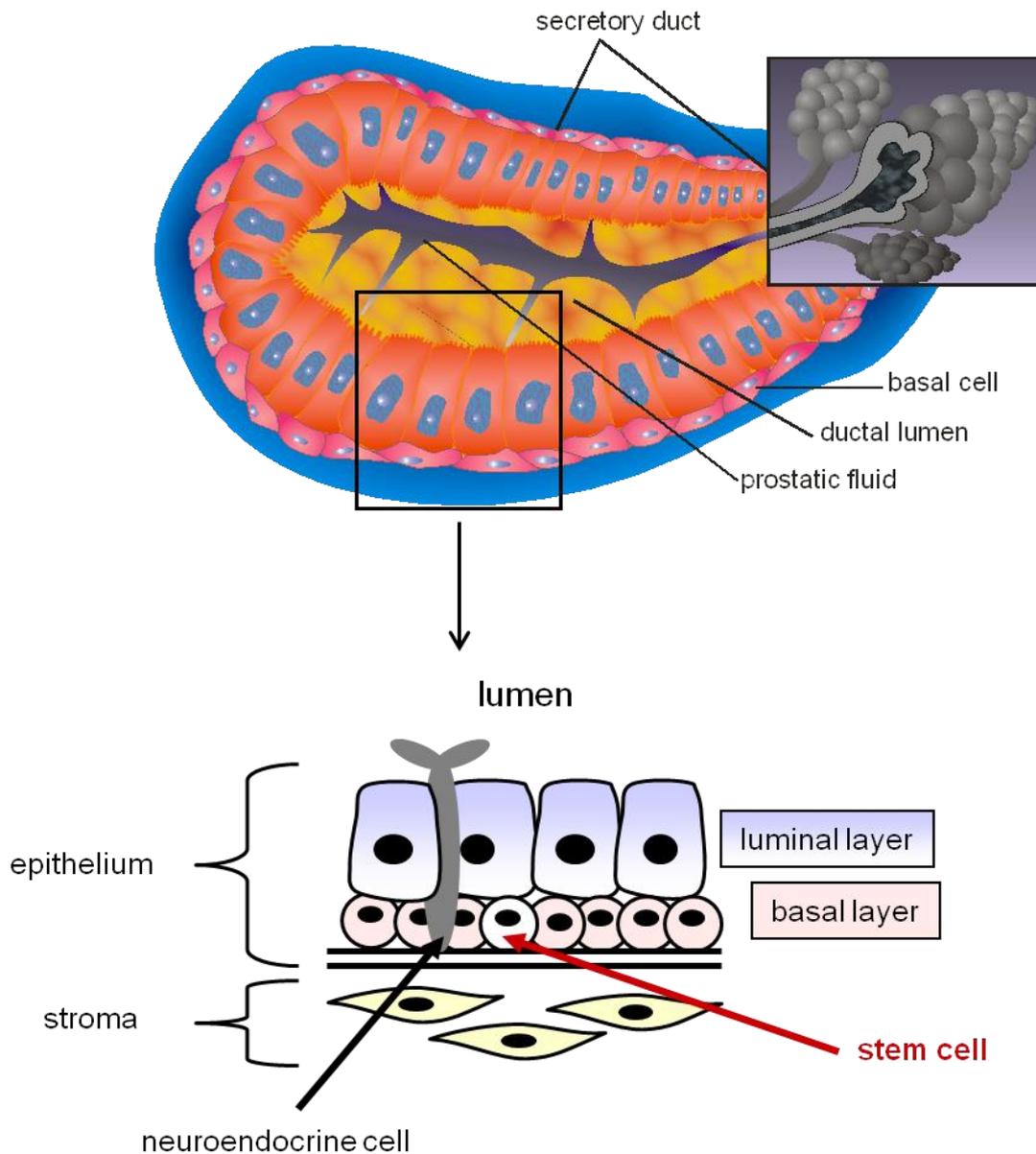
Figure 1-2 Anatomy of the prostate gland. The prostate gland consists of many fluid-filled ducts. The cellular structure within the ducts consists of an epithelium of undifferentiated basal cells (SCs, TAs, CBs; CD44/CK5/CK14+) and differentiated luminal cells (CD24/CK18/PSA/PAP/AR+) that have a secretory function. The neuroendocrine (ChrA+) cells are protruding through both layers. The basal layer also contains a small population of SCs (CD133+/$\alpha_2\beta_1^{high}$) that give rise to the differentiated cells within the epithelium. The prostate epithelium is separated from the stromal compartment by the basement membrane. The stromal fraction consists of fibroblasts and collagen. Modified and reproduced from [3, 4].

1.1.1 Non-malignant diseases of the prostate

1.1.1.2 BPH

BPH is a benign outgrowth of cells in the prostate that frequently occurs in ageing men. The disease is a result of a deregulated proliferation of the epithelial and stromal compartments [24, 25]. BPH is often treated with trans-urethral resections of the prostate (TURP) surgery to reduce a high frequency of urination owing to increased pressure on the bladder [3]. BPH is not thought to be involved in malignant transformation as it is localized in the transition zone of the prostate, whereas prostate cancer usually occurs in the peripheral zone [26].

1.1.1.3 Prostate intraepithelial neoplasia (PIN)

PIN is caused by an increased cell proliferation that causes, similar to prostate cancer, a degeneration of the basal-luminal cell stratification, even if the integrity of the basement membrane is maintained [3, 27]. High grade PIN (HGPIN) has been described as a pre-cancerous condition with progression to cancer after 5 years or more [3, 28-30].

1.2 Prostate cancer

1.2.1 Incidence and risk factors of prostate cancer

Cancer is one of the most common diseases leading to death in western countries. One of the most frequently diagnosed malignant disorders in men in the UK is the development of tumours in the prostate (Figure 1-3). According to Jemal et al. prostate cancer is the second leading cause of male cancer-related death in the USA and UK (12% of all male cancer related deaths) [31, 32]. Despite its strong geographical dependence, other risk factors include age, ethnic origin and diet [33]. Whereas prostate cancer is uncommon in young men, almost one-third of men around 50 years of age already have histologically identifiable prostate tumours and incidence rises

for men in their 80s [33-35]. Concerning the ethnic origin, the highest incidence is found in African Americans [33, 36]. Also diet has been extensively researched due to the variation in prostate cancer incidence between different countries. Calcium from dietary or supplemental sources has been associated with an increased prostate cancer risk, whereas lycopene and selenium were linked with a decreased risk in some studies [37].
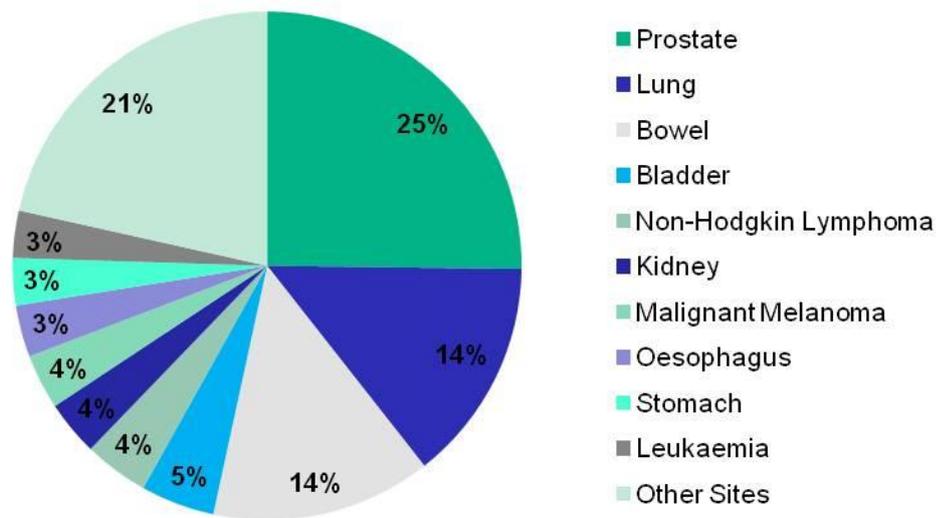
Figure 1-3 The 10 most commonly diagnosed cancers in men (excluding non-melanoma skin cancer) in the UK. Reproduced from CRUK statistics, 2009.

1.2.2 Diagnosis of prostate cancer

The diagnosis of prostate cancer relies on the determination of serum levels of the protein PSA that is secreted by prostate luminal cells. Elevated levels of PSA are linked to malignancy [3, 38]. However, in some cases the PSA test fails. Even though the PSA test is a commonly used method, it cannot distinguish aggressive from non-aggressive cancers [33]. As a consequence, false positive results can result in patients undergoing unnecessary surgery [33]. There is a 5% rate of false-positive and 2% rate of false negative results [3, 39]. PSA is not exclusively secreted by the prostate and can also be expressed by other tissues such as the lung [33, 40]. Furthermore, high PSA levels are not necessarily linked to malignancy and may be a result of PIN, inflammation or infection [3, 41, 42]. In regard to false-negative results, a study revealed that even some individuals with normal PSA levels had prostate tumours [43].

However, the next step after the detection of high PSA levels (>4 ng/ml) is the preparation of a biopsy for histological analysis to confirm the presence of the tumour and its grade of malignancy [3]. The tissue is examined according to the Gleason grading system, which was established in the sixties and remains the most important clinical prognostic factor (Figure 1-4), [33, 44]. Two areas of the tissue with the most common and second most common tumour pattern are scored with the values 1-5. A normal cellular structure would be assigned with 1, whereas the value 5 would represent a highly malignant condition featured by loss of the common basal-luminal bilayer and integrity of the basement membrane. To determine the Gleason score both values are added. Hence, the lowest Gleason score can be 2 and the highest 10. Gleason scores over 7 are usually correlated with a poor clinical outcome [3, 45]. Other diagnostic methods which are particularly

used to assess the tumour progression are magnetic resonance imaging (MRI) or computer tomography (CT) scan [33].
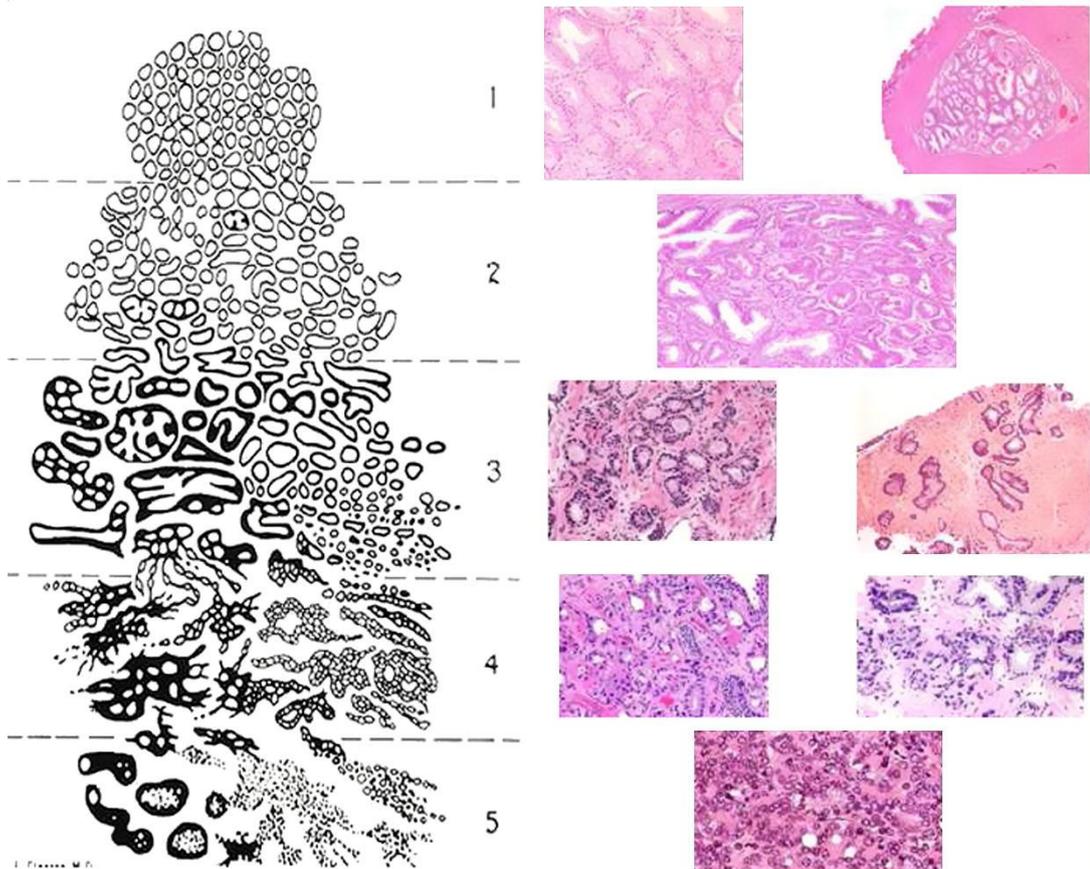
Figure 1-4 The Gleason grading system. Biopsies taken from prostate tissue are analyzed on the basis of their cellular morphology in order to identify disease related alterations. Pattern 1 represents healthy tissue consisting of small uniform glands. At pattern 2 there is more stroma between the tissue. Both, pattern 1 and pattern 2 are well differentiated. At pattern 3 there is a distinct infiltration from the cells at the margins of the gland and the cells are only moderately differentiated. At pattern 4 neoplastic cells arise and there are only very few glands. Pattern 5 is characterized by a lack of glands. Pattern 4 and 5 are poorly differentiated. Taken from [46].

1.2.3 Treatment of prostate cancer

The treatment modality depends on the progression/stage of the disease, which is for prostate cancer, assessed by the previously described diagnostic methods. Therapies for localized prostate cancer (tumours are contained within the prostate capsule) include watchful waiting, radical prostatectomy (surgical removal of the prostate) or radiotherapy which can be applied in form of external-beam radiation or brachytherapy (implantation of radioactive seeds into the prostate) [33, 47-49]. When metastases are found, these treatment options have only a limited efficacy with the result of a relapse of the disease.

A frequent therapy for advanced prostate cancer is androgen deprivation therapy (ADT). Owing to their importance in PSA production, cell survival, growth and proliferation, AR signalling pathways are a critical target for prostate cancer treatment [50, 51]. ADT can be conducted by chemical castration through substances designed to block AR signalling e.g. by gonodotropin-releasing hormone analogs or direct inhibition of the androgen receptor activity [33]. Furthermore it can also be achieved by surgical castration [33].

However, with ADT the patients´ life can be prolonged for rarely more than 2 years as tumours become castration resistant (CRPC) [33, 52]. Upon failure of ADT, the application of chemotherapeutic drugs, such as docetaxel or novel androgen ablation therapies, are used as a last line of treatment. These treatments typically only extend the patients´ life for up to 2 years and help to reduce the symptoms [53, 54].

Mitoxantrone was the first chemotherapeutic drug approved for the treatment of CRPC. Today it is typically given as a second-line treatment, where it can have palliative improvement for patients with cancer

progression after treatment with docetaxel [33]. New drugs such as abiraterone are used to decrease the testosterone levels, but they can only extend the mean life time expectancy of a patient with CRPC by a few months with little prospect of curing the disease [33, 55].

Research into new treatments against prostate cancer is crucial, as CRPC and also radiorecurrent prostate cancer present a serious issue with 30% of patients relapse [56-59]. There are a few new treatment strategies with success in clinical trials, including photodynamic therapy (PDT), high intensity focused ultrasound (HIFU), cryotherapy, gene therapy and immunotherapy, including vaccines [60-62]. HIFU, cryotherapy and PDT are focal therapies and target specific cancer areas, with minimum damage to normal tissue and reduced side effects [33, 63].

In conclusion, despite intensive research there are currently no therapies available that eliminate treatment-resistant secondary tumours and metastatic disease. Further research is required to find novel therapeutic targets and treatment strategies. Recent findings direct the origins of prostate cancer to cancer stem cells (CSCs) that might be a new therapeutic target.

1.2.4 Development of prostate cancer

1.2.4.1 The stages of prostate cancer

Prostate cancer development is defined by four basic stages. At stage 1 the tumour is small and localized inside the prostate gland [64]. At stage 2 the cancer is still located in the prostate gland, but is enlarged in comparison to stage 1 [64]. A hard lump might be felt during rectal examination [64]. At stage 3 the cancer has broken through the outer layer of the prostate gland to tissues such as the seminal vesicles [64]. In the most advanced condition,

stage 4, the cancer spreads to more distant locations such as the lymph nodes, bones, bladder, rectum, liver or lungs [64].

In advanced stages of prostate cancer, primary tumour cells acquire the ability to escape from the prostate capsule by expression of enzymes that inactivate substrate-anchoring proteins [3]. One example is the upregulation of heparanase that cleaves heparin-sulphate-modified proteoglycans in the extracellular matrix (ECM) [3, 65]. The malignant cells migrate to secondary locations through lymph node drainage or the vascular system [3]. There is also increasing evidence that aberrant stromal components play a role in tumour progression [3, 66].

1.2.4.2 Genetic changes in prostate cancer

Although no single tumour suppressor gene responsible for the onset of the disease has been identified yet, there are a number of candidate genes [67]. However, the loss of particular genes allows the progression of the disease at each stage (Figure 1-5) [67]: The loss of NKX3.1 is linked to the transformation of the normal prostate epithelium to PIN. PTEN and Rb loss allow the progression from PIN to the development of invasive carcinoma and loss of p53 function is often found at metastatic stages of the disease [67]. Also the AR gene plays a role in the malignant prostate and has been shown to have numerous sequence alterations in prostate cancer [68]. The AR binds to testosterone and is responsible for the transcription of genes that stimulate the growth of the normal prostate gland, but also of prostate cancer cells [68]. Furthermore, aberrant AR signalling is a main obstacle in androgen ablation therapy [68].

Genetic changes in the prostate can also occur at a gross level e.g. through chromosomal aberrations such as the TMPRSS2:ERG fusion, which was found

in 20% of HGPIN and 50-70% of patients with prostate cancer [3, 69, 70]. Also epigenetic mechanisms have been linked to prostate cancer [3]. For example a commonly inactivated gene through promoter hypermethylation is glutathiontransferase 1 (GSTP1) [71]. In prostate cancer GSTP1 expression is lost in almost 90% of tumours and 70% of PIN, making it to an early event in prostate carcinogenesis [71]. Another example is the inactivation of TIMP-2 through promoter hypermethylation [3, 72]. A normally functional TIMP-2 gene would prevent tumour invasion and metastasis [3, 73].
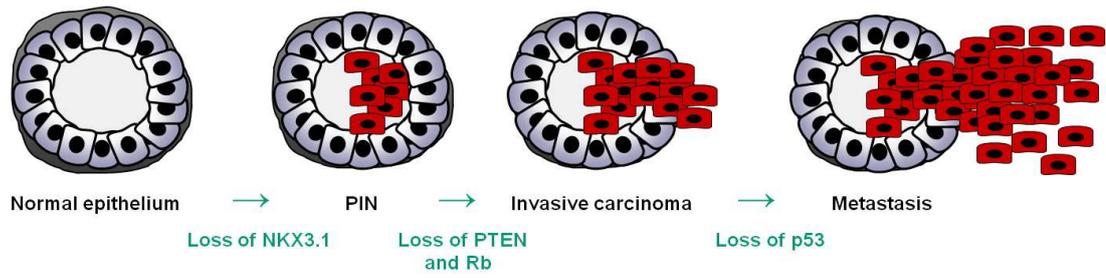
Figure 1-5 The progression of prostate cancer. Schematic presentation of the transformation of the normal prostate epithelium to prostate cancer and the loss of genes associated with each stage. Reproduced from [3, 67].

1.3 CSCs

Recent findings direct the origins of many cancers to CSCs rather than deregulated differentiated cells. Also prostate cancer was originally treated as a disease that developed from terminally differentiated luminal cells. When reconsidering the origin of prostate cancer it may be more logical to attribute the onset of the disease to oncogenic changes in basal cells and SCs [4]. The reason being, SCs persist during the life time of the host and the risk for the accumulation of mutations is therefore much higher than in progenitors or differentiated cells [4]. Also crucial pathways required for SC maintenance are correlated with carcinogenesis [74].

1.3.1 Normal SCs

SCs have the unique capacity for differentiation and self-renewal which distinguishes them from any other cell type. The self-renewal capacity ensures the maintenance of SCs during the life time of the host. It comprises **asymmetric** and **symmetric cell division.** Asymmetric cell division produces an identical daughter SC and a progenitor cell that can differentiate into a specific cell type of the tissue (Figure 1-6) [75]. A symmetric cell division generates two identical daughter SCs. Hence, asymmetric cell divisions maintain a constant number of SCs, whereas symmetric cell divisions increase the SC number. SCs can be mainly divided into **embryonic SCs** and **adult SCs**. Embryonic SCs are found in the inner cell mass of the blastocyst. They are defined as a population of undifferentiated pluripotent cells. Owing to their pluripotent character they are able to give rise to the three germ layers (mesoderm, ectoderm, endoderm) that later on develop into the specific tissues of the organism. Adult SCs or tissue specific SCs are derived from embryonic SCs. As embryonic SCs they form a reservoir of undifferentiated cells, but they can only develop into a limited number of

cell types to generate a specific tissue, a feature that is referred to as multipotency. The function of adult SCs is the replacement of dying cells (natural turnover e.g. the gut) and regeneration of damaged tissue (wound healing). Adult SCs have the capacity for self-renewal and are maintained during the life time of the host. During the last few decades various adult SC types have been identified. The first evidence for their existence was produced for SC originating from the bone marrow niche [76]. It was found that hematopoietic SCs were able to differentiate into any type of blood cell such as T cells, B cells, granulocytes, erythrocytes and mast cells when transplanted into irradiated mice [76]. The hematopoietic model was of great importance for the understanding of tissue development [77]. Subsequently, other types of adult SCs have been discovered in neuronal, epithelial, mesenchymal and epidermal tissues [11, 78, 79].

Various pathways are essential for the regulation of the self-renewal and differentiation capacity of SCs. A role for Notch signalling has been shown in neural SCs as well as in mouse prostate development [80, 81]. Das et al. 2008 and Kalani et al. 2008 demonstrated that Wnt signalling was critical in retinal and neural SCs [82, 83]. Hedgehog and transcription factor B lymphoma Mo-MLV insertion region 1 (Bmi-1) have been shown to play a role in regulating the normal mammary gland [84]. During normal organogenesis these processes are strictly regulated. Importantly, the deregulation of self-renewal may be one of the key events leading to carcinogenesis [84].
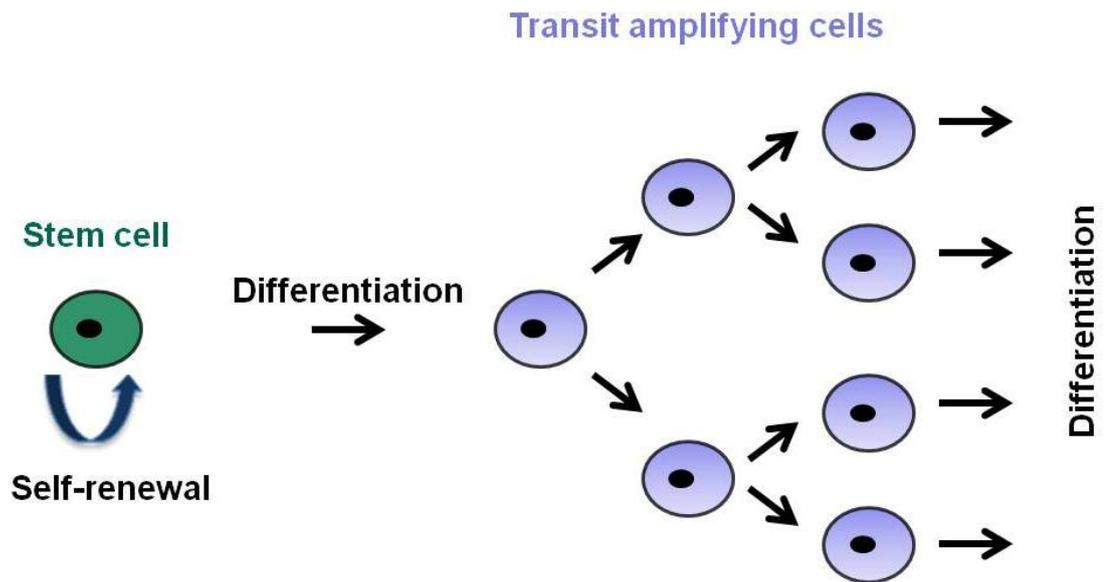
Figure 1-6 Asymmetric cell division in SCs. SCs have the capability for self-renewal and differentiation. Upon division they create an identical daughter cell and a TA that undergoes differentiation. Reproduced from [75].

1.3.2 The CSC model

There are two main models for carcinogenesis. The **stochastic model** proposes that the tumour mass is **homogenous**. According to this theory every cell in the tumour has the same tumour forming potential [4]. The **CSC model** suggests that the tumour consists of a **heterogeneous** mass of cells [4]. Here, only a small subset of cells, the CSCs, are capable of initiating tumourigenesis [4]. The CSCs might develop from a deregulation in normal SCs that reside in the tissue e.g. prostate SCs.

Like normal SCs replenish their specific tissue, CSCs might form a reservoir that reconstitutes the tumour mass [4, 85]. They divide and expand the CSC pool and develop into heterogeneous cancer cells [85]. The main criteria that define CSCs are the capacity for self-renewal, differentiation, invasion, extensive proliferation and tumour initiating capacity [86-88]. The CSC model for the development of prostate cancer is presented in Figure 1-7.

1.3.3 CSC types

A relationship between SCs and carcinogenesis was first shown in 1997 in acute myeloid lymphoma (AML) [88]. A population of cells expressing the markers $CD34^{++}CD38^{-}$ initiated AML in NOD/SCID mice, whereas committed progenitor cells failed to engraft [88]. These cells showed major features of SCs, such as capacity for self-renewal, differentiation and high proliferative potential [88]. In the following years, CSCs were also identified in many solid tumours in the breast, lung, head and neck, pancreas, liver, kidney, colon, ovarian, brain bladder, endometrial and prostate [87, 89-103].

1.3.4 Characterization of prostate CSCs

Normal human prostate SCs were first identified by experiments in a rat model that showed the regression of the prostate gland upon castration [4, 12, 104]. The prostate could then be restored by hormone induction [4, 12,

105]. The observation that this cycle could be repeated multiple times led to the conclusion that a surviving castration-resistant SC population must exist [4]. Subsequently, normal human prostate epithelial SCs were identified in the normal/benign prostate using gland regeneration experiments: a basal epithelial phenotype of cells positive for CD133 and expressing high levels of $\alpha_2\beta_1$integrin showed the highest clonogenic potential and gland regeneration in immuno-compromised mice [11, 106]. The same cellular phenotype was explored by Collins et al. 2005 to sub-fractionate epithelial cells from human prostate cancers [33, 87]. Prostate CSCs represented a very small fraction of the total tumour mass (approximately 0.1%) [4]. CD133 and $\alpha_2\beta_1$integrin^{high} cells isolated from primary cultures grown from prostate tumours had self-renewal, proliferative and differentiation properties in addition to invasiveness and an enhanced secondary colony forming efficiency, [33, 87]. The hierarchical and heterogeneous organization of the tumour mass suggests that CSCs give rise to the entire malignant tissue [107, 108].

In order to compare transcription patterns a microarray analysis was carried out on SCs (CD133$^+$/$\alpha_2\beta_1$integrin^{high}) and CBs (CD133$^-$/$\alpha_2\beta_1$integrin^{low}) from both benign and malignant prostate samples [33, 109]. A significantly different gene expression signature emerged in SCs compared to CBs [33, 109]. More crucially, gene expression differences were found when comparing benign SCs to SCs originating from malignant tissues [33, 109]. The profiles revealed that the expression of 581 genes was significantly different in SCs from malignant tissues relative to benign control cultures [33, 109]. A number of the genes identified in the CSC signature were linked to carcinogenic alterations, including promotion of an invasive phenotype in prostate and other cancers [33, 109]. By using Gene Ontology

and the KEGG pathway database, functional associations and the activation of signalling pathways were identified in CSC relative to benign tissues [33, 109]. For instance, malignant SCs expressed genes linked to inflammation such as IL-6 and NFκB activated genes [33, 109]. Furthermore, it showed that Wnt signalling, the JAK-STAT pathway and adhesion signalling pathways were upregulated in the CSCs [33, 109]. In prostate cancer Wnt signalling has been linked with both androgen-independence and bone metastasis [110-112].

There are further studies that aimed to define prostate CSC markers e.g. TRA-1-60/CD166/CD151 cells [33, 113]. Like CD133$^+$/$\alpha_2\beta_1$integrin^{high} cells, TRA-1-60/CD166/CD151 cells did not express markers associated with differentiated secretory luminal cells, AR or PSA [113]. They possessed major hallmarks of SCs such as multipotency as revealed by *in vitro* sphere-formation and tumour-initiation in the mouse model [33]. However, the authors did not directly correlate the expression of TRA-1-60/CD166/CD151 to CD133 expression [33]. Through analysis of microarray data from Birnie et al 2008 we know that the CD133$^+$/$\alpha_2\beta_1$integrin^{high} SC populations also expressed TRA-1-60/CD166/CD151 and constitute therefore potentially the same population [33]. Alternative or additional prostate SCs markers have been explored elsewhere [114].

1.3.5 CSCs as the origins of prostate cancer

Originally prostate cancer was thought to develop from luminal cells [124]. This conclusion was mainly based on the underlying ratio changes in prostate cancer [124]. The luminal: basal compartments change from ~1:1 in the normal prostate to a decrease of basal cells with the majority of cells having a luminal phenotype in malignant prostate tissue [33, 115, 116]. It

could be hypothesized that the luminal cells might have regained the function for self-renewal due to disruptions in cell signalling. For example a chromosomal translocation could generate a novel fusion protein, which reprogrammes a cell to express a self-renewal signature [117]. For instance, a mechanism that allows the transformation of a differentiated cell into a CSC has been identified in blast crisis chronic myelogenous leukaemia [85].

However, several findings propose that the cell of origin of prostate cancer resides in basal compartment and the likelihood of de-differentiation from luminal to basal cells is slim [16, 106, 118-122]. In particular SCs are a very likely candidate for tumour initiation. SCs are maintained during the lifetime of the host, hence the probability for the accumulation of genetic alterations in the SC population causative for tumour development should be higher than in short-lived terminally differentiated luminal cells [33]. Furthermore, pathways necessary for SC maintenance e.g. Notch, Sonic hedgehog and Wnt signalling are associated with carcinogenesis [33, 74]. Alternatively, prostate cancer might originate from differentiated progeny which revert into a SC-like cells [107, 114, 115, 123, 124].

However, support for a basal origin for prostate cancer has also been shown with mouse basal cells that developed into a tumour mass with a luminal phenotype after induction of ERG expression and activation of PI3K signalling [33, 118]. A similar result was seen with human benign prostate cells that were transduced with lentiviruses to introduce AKT, ERG transactivator and AR genes in luminal and basal cells [33, 119]. When transplanted into mice, only the basal cells were able to initiate tumour growth [33, 119]. Furthermore, the histological analysis of the tumour tissue revealed a reduced basal compartment, but an increased luminal compartment, which is a characteristic of human prostate tumours [33, 119].

CSCs might not only be the source of cancer development, but also play a role in therapy resistance and tumour relapse.
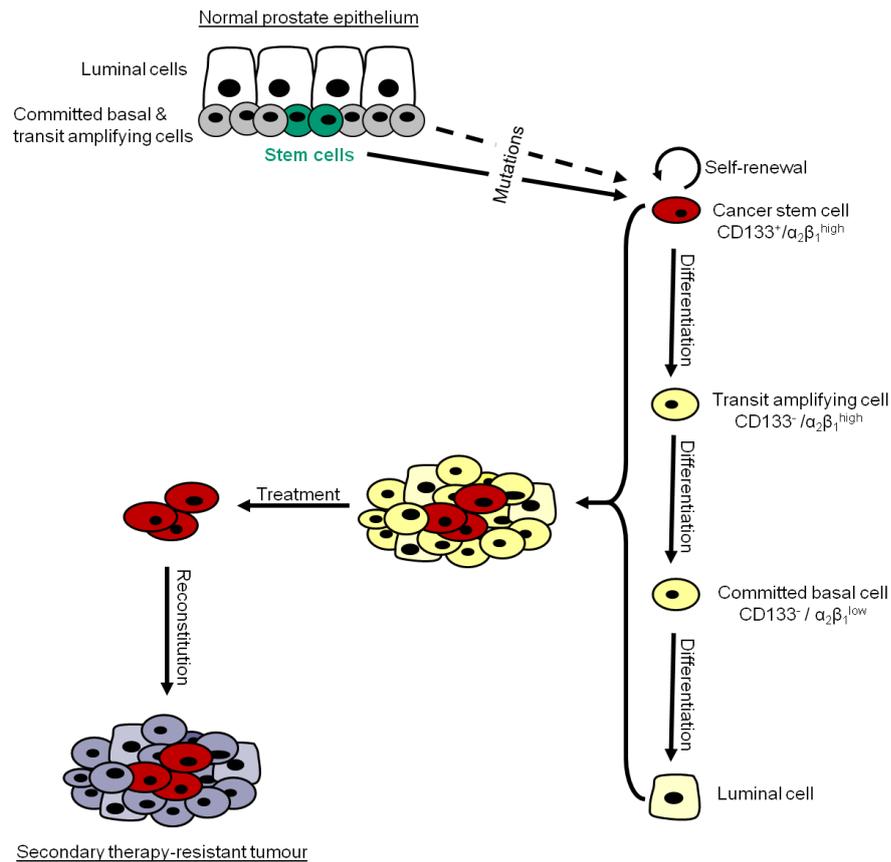
Figure 1-7 The prostate CSC theory. Normal prostate SCs (green) differentiate into TAs and CBs (grey) that develop finally into differentiated prostate cells (white). According to the prostate CSC theory mutations in prostate SCs or TAs might lead to their transformation into CSCs (red). These differentiate into TAs and CBs and make up a heterogeneous tumour mass (yellow). Contrary to their healthy counterparts, malignant cells fail to grow into structured layers. According to the CSC theory all of these different cell types (red, yellow) are present in a tumour and the CSCs form the reservoir of undifferentiated cells from which all other cell types arise. Reproduced from [33].

1.4 The DNA damage response

In view of constant DNA damaging influences the maintenance of genomic stability is a major concern in all cells and a coordinated response to DNA damage is necessary to ensure the survival of the host [125]. To maintain genomic integrity the cell devotes a wide range of mechanisms such as DNA damage checkpoints, DNA repair pathways, apoptosis, senescence and autophagy. The DNA damage response is predominantly controlled by the regulators Ataxia-telangiectasia mutated (ATM) and ATM and RAD3-related (ATR) proteins, which belong to the phosphoinositide-3-kinase (PI3K)-related protein kinases (PIKKs). The breakdown of these pathways is correlated with severe consequences for the host such as the development of cancer [125-128].

1.4.1 Sources of DNA damage

DNA damage can originate from **exogenous** and **endogenous** sources. **Endogenous DNA damage** can be a result of oxidative reactions with surrounding water molecules, oxygen and reactive oxygen species (ROS) generated by metabolic byproducts [125]. The induction of **exogenous damage** can be the consequence of mutagenic chemicals or viruses [125]. Radiation is another source of exogenous DNA damage, including non-ionizing radiation such as ultra-violet radiation (UV) and ionising radiation [125]. Ionising irradiation can arise from cosmic rays or earth bound sources [125]. The induction of exogenous DNA damage plays a critical role in chemo- and radiotherapy to kill cancer cells, even if ironically, exposure to DNA damaging conditions is linked to an increased cancer risk [125].

1.4.2 Introduction of DNA damage through chemicals for cancer therapy

For many cancers, surgery and radiotherapy are not sufficient to eradicate the malignant cells or may not be able to function optimally due to the location of the tumour. For this reason chemotherapeutic drugs are preferable to increase the probability of a long-lasting tumour regression. Many chemicals used against cancer are replication inhibitors. These specifically target rapidly proliferating cells, as many cancer cell types are, and thereby interfere with the normal progression of the cell cycle leading to DNA damage and ideally cell death. The following paragraph introduces six different replication inhibitors that are related to experiments carried out in this thesis. All of them, except excess thymidine, are of relevance in the clinic for cancer treatment.

The anti-cancer drug **etoposide** is a podophyllotoxin-derivative. Its mechanism relies on the production of strand breaks in DNA by inhibiting the enzyme topoisomerase II, which is important for unwinding DNA during replication [129]. The alkaloid **camptothecin** arrests the cell cycle by a similar mechanism as etoposide, but it inhibits topoisomerase I rather than topoisomerase II [130, 131]. **Carboplatin** is a derivate of cisplatin. Its exact mechanism of action is not known [132]. It causes platinium-DNA adducts leading to interstrand cross-link formation [132, 133]. **Doxorubicin** belongs to the group of anthracyclin-antibiotics. Its effect relies on two main mechanisms: firstly by intercalation into the DNA and thereby blocking transcription and secondly by directly blocking toposiomerase II [134, 135]. The taxane **docetaxel** inhibits cells during mitosis. It binds and stabilizes the microtubuli-apparatus thereby preventing progression through mitosis leading to cell cycle arrest [136]. **Thymidine** is not used for cancer therapy, but it is used for research purposes to trigger replication stress in cells.

Excess thymidine results in an increase of the intracellular dTTP pool and prevents supplement of dCTPs by allosteric regulation of ribonucleotide reductase [137, 138]. The resulting depletion of dCTP slows DNA synthesis and arrests cells in the S-phase [138].

1.4.3 DNA damage induced signalling

The DNA damage response is mediated through proteins of four main groups: **sensors** of DNA damage, **mediators** that enhance the signal generated through DNA damage and **transducers** that pass the signal to **effectors** which are responsible for the activation of cellular responses [125], (Figure 1-8).

A master regulator in the response to DSBs is the protein ATM, which belongs to the PIKKs [139]. The pathways downstream of ATM have been frequently described, but the mechanism of DNA damage sensing itself and the steps involved in ATM phosphorylation are mostly unknown [125]. It has been shown that the generation of DSBs results in the recruitment of the Meiotic recombination protein-11 (MRE11)-RAD50-Nijmegen breakage syndrome protein-1 (NBS1) (MRN) complex and the transformation of the inactivated ATM dimer into the monomeric, phoshorylated form of ATM (phATM) [140, 141]. Activated ATM binds to the MRN complex on the sites of DNA lesions and activates the C-terminal region of the histone variant H2A.X by phoshorylation [141]. γH2AX (the phophorylated form of H2A.X) is capable of binding Mediator of DNA Damage Checkpoint Protein-1 (MDC1) and recruits additional ATM-MRN complexes leading to further H2A.X phosphorylation [141]. The expression of γH2A.X is one of the early events measured after the introduction of DNA damage. It is crucial for the recruitment of repair factors such as RAD50, RAD51 and the product of the gene BRCA-1 [142]. Due to its central role in DNA damage signalling γH2A.X

is often used as a marker to detect DNA DBS, but also SSB. Furthermore, its appearance has been described as a genotoxic endpoint for the cell [143]. Upon its activation, ATM phoshorylates multiple substrates and thereby causes cell cycle arrest. The cell can re-enter the cell cycle following DNA damage repair or if the damage is not recoverable, the cell can activate apoptosis or senescence [144-146].

Another PIKK crucial in DNA damage signalling is ATR. The accumulation of single-stranded DNA (ssDNA) is the main trigger of the ATR-dependent checkpoint response [147]. It has been shown that in Xenopus egg extracts, the most developed model for this research, replication stress causes extended stretches of ssDNA [148, 149]. The generated ssDNA is then coated by RPA in an ATR-interacting protein (ATRIP) dependent manner [141, 150, 151]. ATRIP needs to be associated with the RAD9-RAD1-HUS complex that is able to detect and bind DNA ends adjacent to RPA-coated ssDNA [141, 152]. The RAD9-RAD1-HUS-Complex recruits topoisomerase-binding protein-1 (TOPBP1) to sites of DNA lesions leading to an activation of ATR [141, 153, 154]. Activated ATR then phoshorylates checkpoint kinase Chk-1 on ser-345 and ser-317 [141, 155-157]. After dissociation of activated Chk-1 from the chromatin it phosphorylates a wide range of downstream targets [141]. Recently, ATR has also been shown to respond to DSB breaks [158].
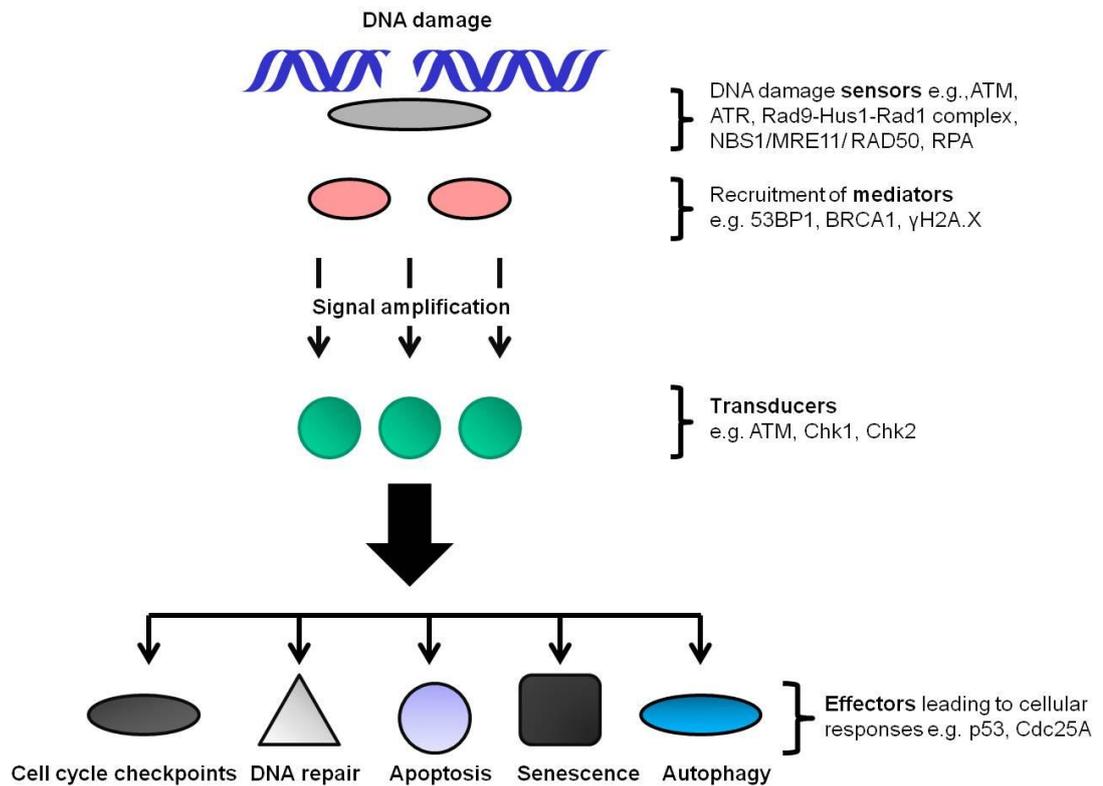
Figure 1-8 The recruitment of proteins as response to DNA damage. The DNA damage response is coordinated by sensors, mediators, transducers and effectors, which lead to different cellular responses. Reproduced from [125, 159].

1.4.4 DNA repair

Evolution has equipped the cell with several repair mechanisms that are capable of recognising and repairing distinct types of DNA damage [125]. From a simplified point of view DNA repair comprises three main processes: (i) recognition of DNA damage, (ii) excision or removal of the DNA damage and (iii) restoration of the DNA [125]. Depending on the type of DNA damage, cells initiate different types of repair mechanisms. Single nucleotide errors resulting from DNA damage or errors in DNA replication are repaired by base excision repair (BER), nucleotide excision repair (NER) or mismatch repair (MR) [125, 160]. BER is also used for the repair of SSBs. The more severe DSBs are repaired by non-homologous end-joining (NHEJ) or homologous recombination (HR) [125, 161, 162].

1.4.4.1 BER/ SSB repair

The BER pathway serves to eliminate fragmented or modified bases in DNA. BER is also used to repair SSBs, which can be generated endogenously by ROS or IR and the abortive activity of topoisomerase I and II [163-166]. There are two different variants of BER: the predominant short patch mechanism and the long patch mechanism (Figure 1-9). The first step in short patch BER is the removal of the base by a DNA Glycosylase, a process that leads to the generation of an Apurinic/apyrimidinic site (AP site) [125]. The APE1 endonuclease then incises the DNA strand (leading to a SSB) [167]. The detection of SSBs is predominantly via PARP1 [167]. PARP1 is responsible for the recruitment of XRCC1 to the sites of DNA damage [168]. XRCC1 is essential for the recruitment of factors that mediate end processing, gap filling (DNA polymerase β) and finally ligation (DNA ligase IIIα) [169, 168]. Long patch BER also requires the APE1 to cleave the DNA strand but depends on the factors PCNA, RFC and DNA polymerase δ or ε

and DNA Ligase I for further processing [170]. Whereas in short patch repair only one nucleotide is "flapped" away from the strand in long patch repair a "flap" of 2-8 nucleotides is produced, which is excised by the flap endonuclease 1 (FEN1), [125, 170].
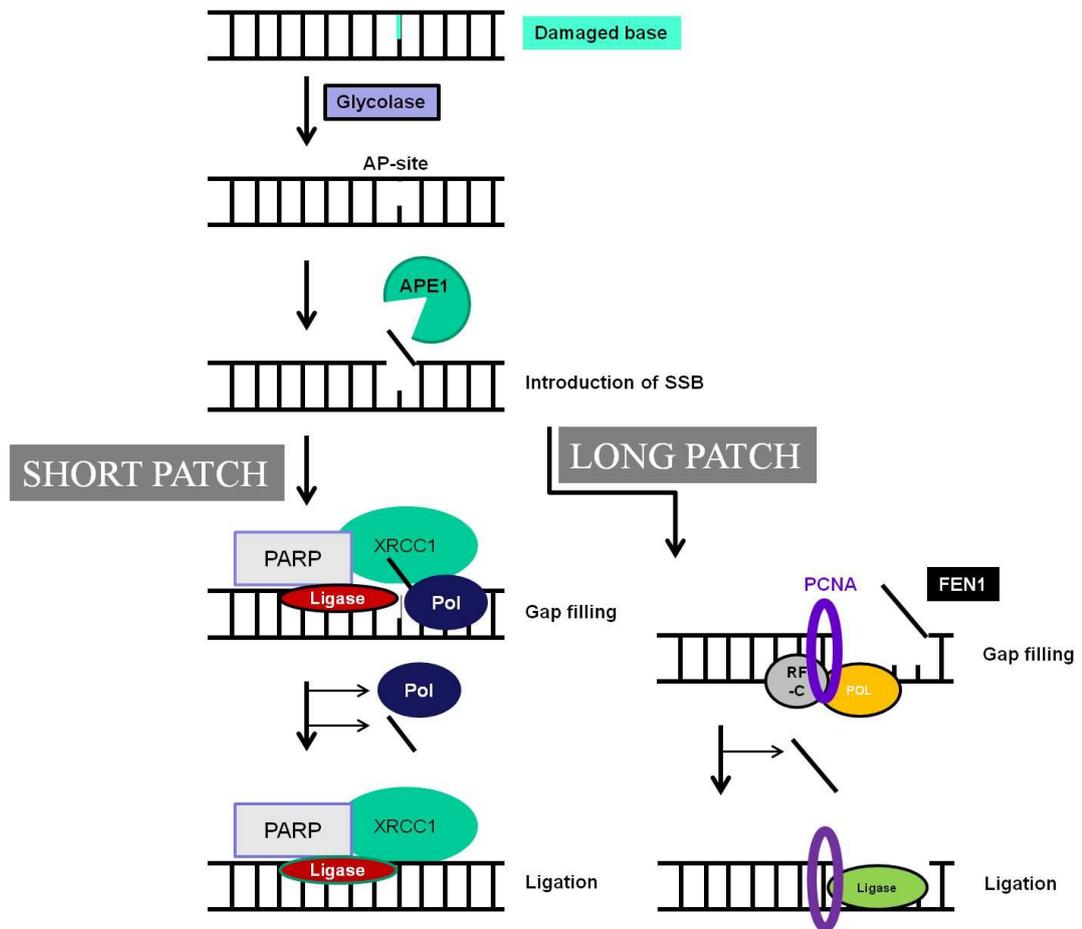
Figure 1-9 The mechanisms of BER repair. BER consists of a short patch and a long patch pathway. Both processes initiate with the generation of an AP site, but are then mediated by different types of proteins. Reproduced from [125, 170].

1.4.4.2 DSB repair

DSBs are the most severe form of DNA damage as they can lead to the loss of genetic information [125]. DSBs can be generated by oxidative stress, IR and topoisomerase inhibitors [166, 171, 172]. DSBs can be repaired through NHEJ and HR. The main difference between the two pathways is that HR requires sequences of homologous DNA for the alignment of the broken ends, whereas NHEJ re-joins them without using homologous regions. The first step of NHEJ in mammals is the recognition and coating of broken DNA ends by the Ku70/80 heterodimer to prevent degradation [125, 173]. Ku70/80 is required for the recruitment of DNA-PK$_{cs}$ to the site of the lesion [174]. Potential overhangs are processed by Artemis and Polynucleotide Kinase (PNK) [125, 175, 176]. The strand gaps are then filled by DNA Polymerase ß [177]. DNA-PK (=DNA-PK$_{cs}$ associated with Ku70/80) recruits the XRCC4-DNA ligase IV which is essential for resealing the DNA [178]. A schematic presentation of NHEJ is shown in Figure 1-10. HR uses homologous DNA as a template to repair of DSBs. The mechanism is particularly associated with the S-Phase when sister chromatids are available. The first step of HR involves a 5´-3´resection of the DSB end which generates a 3´single stranded overhang [125, 179]. This produces ssDNA, which is coated by Rad51that is required for strand invasion [180, 181]. The invasion leads to a displacement of the homologous DNA region and the subsequent generation of a D-Loop (D=displacement). This event creates an X-shaped structure known as Holliday junction [182]. DNA synthesis is then carried out using the homologous template by DNA polymerase Ɛ followed by a ligation step [125, 183]. A schematic presentation of HR is shown in Figure 1-11.
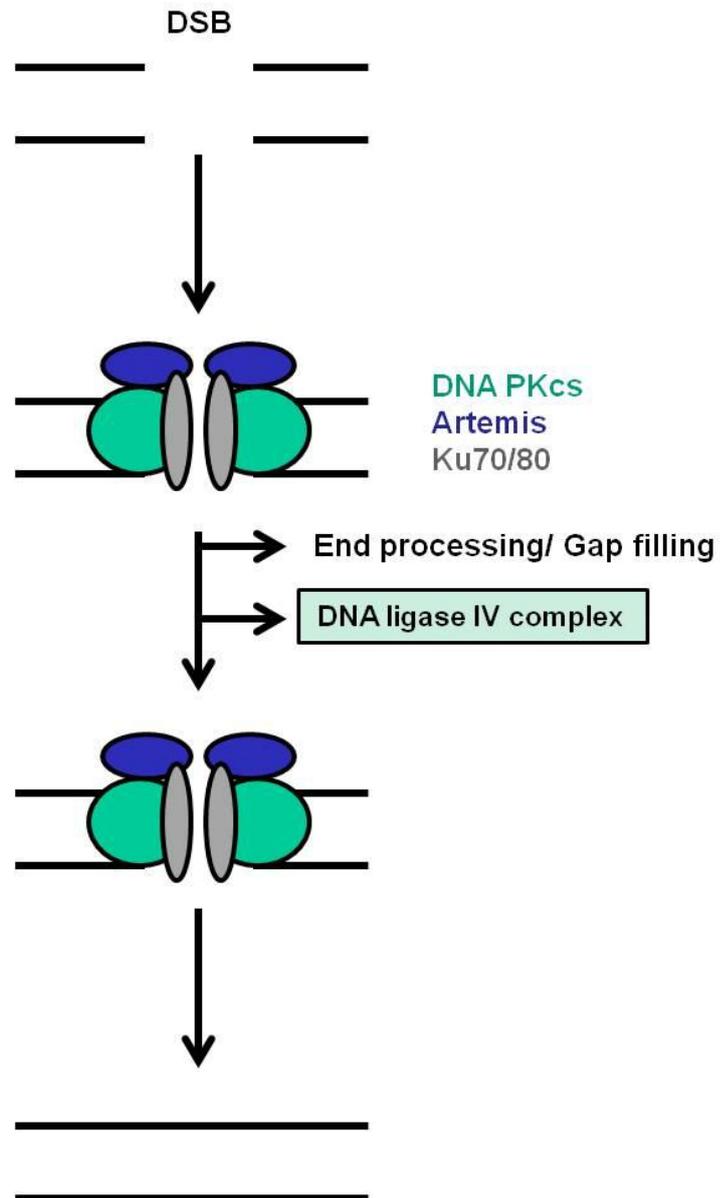
Figure 1-10 The mechanism of NHEJ. DSBs are repaired by NHEJ. DNA-PKcs, Artemis and Ku70/80 locate to the site of the lesion for end processing and gap filling. DNA ligase IV is required for the ligation. Reproduced from [125, 170].
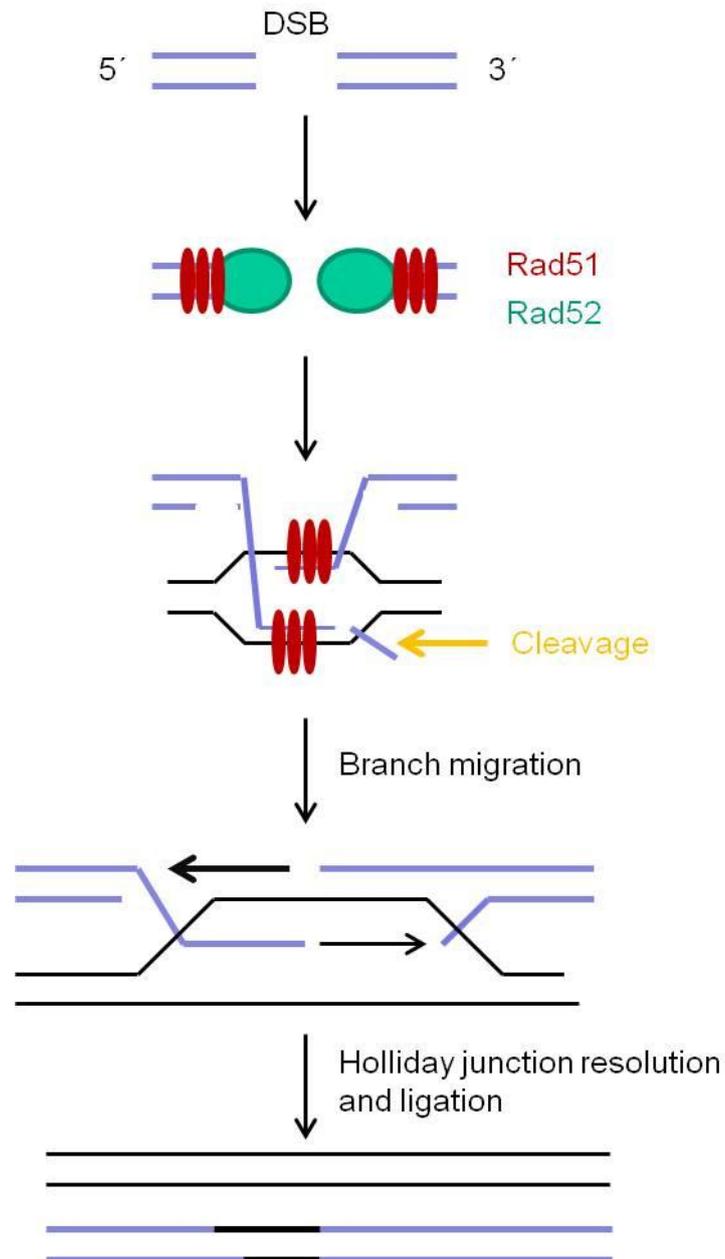
Figure 1-11 The mechanism of HR. HR starts with a strand resection that creates a 3' overhang. The next step is coating by Rad51 (required for strand invasion) and Rad52 (function unknown). The strand invasion displaces a strand from the homologous region by the formation of a D-loop structure and a Holliday junction. The lost DNA sequences on both strands are restored and the resolution of the Holliday junction is then carried out by enzymes (resolvases) that produce nicks. Modified from [125, 170].

1.4.4.3 Regulation of DNA repair

ATM is critical in the NHEJ pathway as it phosphorylates Artemis. ATM activates DNA- PKcs by phosphorylation on threonine-residue-2609, which is a stimulator for Artemis nuclease activity. ATM also functions in the HR pathway by phosphorylating many factors like BRCA1, c-ABl, Bloom Syndrome Protein, H2A.X, and NBS1[184]. Also, ATR signalling is critical for regulating the repair of various DNA lesions. It targets a wide range of proteins linked to recombination (BRCA1, Werner syndrome ATP-dependent helicase, Bloom syndrome protein) [185-188]. ATR and BRAC-1 play a role in the regulation of BER [189].

1.4.5 Cell cycle checkpoints

The cell cycle of an eukaryotic cell can be divided into four stages: the Gap phase 1 (G1), synthesis of sister chromatid phase (S), Gap phase 2 (G2) and Mitosis (M). Cells that are out of cell cycle are in G0 and referred to as quiescent or dormant. The cell cycle is strictly regulated by cyclins and cell cycle checkpoints which control the order of these processes in cycling cells to ensure that a distinct event happens only after completion of a previous event [125, 190-193]. This is crucial, as for example cells need to be prevented from entering S-Phase when only an insufficient amount of nutrients are available or proceeding to mitosis before the complete duplication of the genome and other components (e.g. organelles) has occurred [125, 191-193]. In the presence of DNA damage, the induction of cell cycle checkpoints is a critical step as they allow time for cellular responses such as DNA repair or apoptosis [125]. The cell cycle checkpoints can be classified as **G1/S**, **S**, and **G2/M** (Figure 1-12) [194]. In the presence of DNA damage the G1/S checkpoint serves to prevent the cell from entering S-phase by inhibiting initiation of replication to ensure genomic

stability [170, 194]. The intra-S-phase checkpoint is initiated by DNA damage that occurs during S-phase or by unrepaired lesions that passed the G1/S checkpoint [170, 195]. The intra-S-phase checkpoint it not capable of halting the DNA replication, but is able to slow the S-Phase by suppression of origin firing [195, 196]. The G2/M checkpoint serves to avoid mitotic entry of damaged cells [196]. Although these checkpoints are distinct, the DNA damage sensors responsible for their activation seem to be shared by all three pathways [170]. ATM and ATR play a central role in the regulation of checkpoints [170]. In the G1/S checkpoint ATM phosphorylates p53 and Chk2 [170]. These phosphorylations lead to the activation of two main pathways: one to initiate and one to maintain G1/S [170, 197]. The initiation is mediated by phosophorylation of Chk2, which phosphorylates Cdc25A phosphatase leading to its inactivation and proteolytic degradation leading to G1 arrest [170, 198, 199]. Alternatively to the ATM-Chk2-Cdc25A pathway (activated through IR) the initial arrest can also be caused by the ATR-Chk1-Cdc25A pathway (activated by UV light) [170]. P53 plays a role in mediating the maintenance of the G1/S arrest [197].

During the ATM-regulated intra-S-phase checkpoint, in response to DSBs, ATM triggers two parallel pathways. ATM phosphorylates Chk2 using MDC1, H2A.X and 53BP1 as mediators, which leads to the degradation of Cdc25A [170]. ATM can also initiate a second pathway by phosphorylating the proteins NBS1, SMC1, BRCA1 and FANCD2 [170]. Both pathways lead to a block of replication [170]. Furthermore, in response to SSBs there is a ATR-Chk1-Cdc25A mediated pathway [170].

For the G2/M checkpoint the ATM-Chk2-Cdc25A or ATR-Chk1-Cdc25A pathway can be activated depending on the type of DNA damage [157, 200, 201]. The proteins MDC1, 53BP1 and BRAC1 mediate the signal generated

through DNA damage to Chk2 and Chk1 and these regulate Cdc25A (Chk1, Chk2) and Wee1 (Chk1) leading to G2 arrest [170].
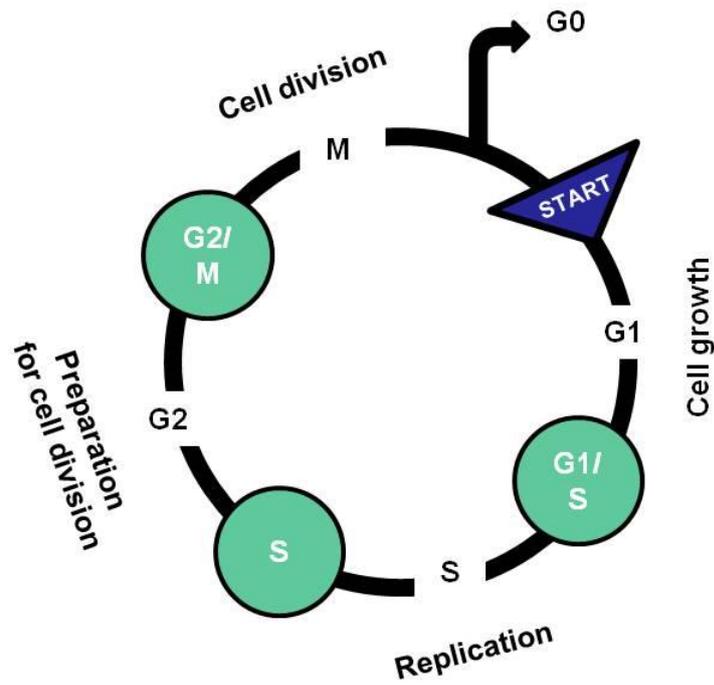
Figure 1-12 The cell cycle including its checkpoints. The cell cycle can be divided into four stages: G1, S-phase (synthesis of sister chromatids), G2 and M-Phase (mitosis). Dormant or quiescent cells are in G0. Before the transition into the next stage of the cell cycle the cell passes cell cycle checkpoints (G1/S, S, G2/M).

1.4.6 Apoptosis

In contrast to necrosis, a consequence of tissue injury, apoptosis is a programmed death induced by the cell to ensure the survival of the host. Apoptosis is an energy-dependent mechanism and is characterized by distinct morphological changes [202]. It plays a role in the normal cell turn-over, development and function of the immune system, embryonic development and chemical-induced cell death [202]. Inappropriate control of apoptosis is causative for various human disorders including many types of cancer [202]. There are two major apoptotic signalling pathways: the **extrinsic** pathway that is mediated through the death receptor and the **intrinsic** mitochondrial pathway. The important apoptotic mechanism to eliminate DNA damaged cells is intrinsic apoptosis.

The intrinsic pathway is initiated by signals such as the absence of growth factors, radiation, toxins, hypoxia and free radicals [202]. These conditions lead to changes in the inner mitochondrial membrane resulting in the opening of the mitochondrial permeability transition pore, the loss of the mitochondrial transmembrane potential and the release of pro-apoptotic proteins, such as cytochrome c, from the intermembrane space into the cytoplasm [202, 203]. Cytochrome c release can be initiated via the tumour suppressor p53 [202, 204]. Cytochrome c binds and activates Apaf-1 and procaspase 9, which is referred to as the apoptosome [202, 205, 206]. This triggers a caspase-cascade leading finally to programmed cell death to clear the host of defective cells [202, 204].

The control and regulation of intrinsic apoptosis occurs through members of the Bcl-2 family of proteins [207]. To regulate apoptosis, ATM targets p53, the E3 ubiquitin ligase MDM2, Chk1and Chk2, H2AX and BRCA1 [208-211]. P53 is known to play a critical role in the regulation of the Bcl-2 family, even

if the mechanisms are not fully understood [212]. It is believed that the members of the Bcl-2 family are paramount for the regulation of cytochrome c release through modification of mitochondrial membrane permeability [202].

1.4.7 Autophagy

Autophagy is a cellular stress response. Following autophagy cells can undergo apoptosis, or use it as a survival mechanism. Similar to apoptosis, autophagy could play an important role in human disease [202]. Autophagy is characterized by the sequestration of the cytoplasm and its organelles in membrane vesicles (autophagosomes) and subsequent transport to the lysosomes for degradation [202, 213]. In contrast to apoptosis, autophagy is a caspase-independent process [214]. A main trigger for autophagy are starvation conditions, where autophagy serves as a survival mechanism [215, 216]. Additionally, it can be caused by a range of chemotherapeutic agents [217]. It has been demonstrated that its induction is an escape mechanism, which prevents the cell from inducing apoptosis [218-220].

1.4.7.1 The mechanism of autophagy

The first regulatory process of autophagy involves the de-repression of the mTOR Ser/Thr kinase, which inhibits autophagy by phosphorylation of Autophagosome-autophagy-related gene (AP-Atg) 13 [221]. AP-Atg 13 has been identified in yeast, but a mammalian homologue is not known at this time [221]. In mammalian cells the endoplastmic reticulum has been proposed as the source of the autophagosomal membrane [222, 223]. The autophagosome arises initially from a structure referred to as "phagophore", where the cytoplasm or organelles are wrapped by a double membrane [215, 216]. The AP-Atg proteins, which are located in the membrane of the vesicles, play a major role in autophagosome formation [216]. In yeast the

AP-Atg proteins have been extensively studied and it has been demonstrated that they fulfil tasks in scaffolding the pre-autophagosomal structures and phagophore elongation [216, 224]. The autophagy gene Beclin 1 has been identified as an important factor that modulates the function of AP-Atg proteins [216]. In addition the membranous protein LC3-II plays an important role in autophagosome formation [224]. The membranes enclose their contents in an non-specific fashion [216]. Upon sequestration, autophagosomes fuse with lysosomes to form autolysosomes and the cytoplasm derived materials are degraded by hydrolases [216]. Through this process macromolecules are degraded into monomeric units such as amino acids and are then transported to the cytoplasm for reuse [216]. The process of autophagosome formation is illustrated in Figure 1-13.
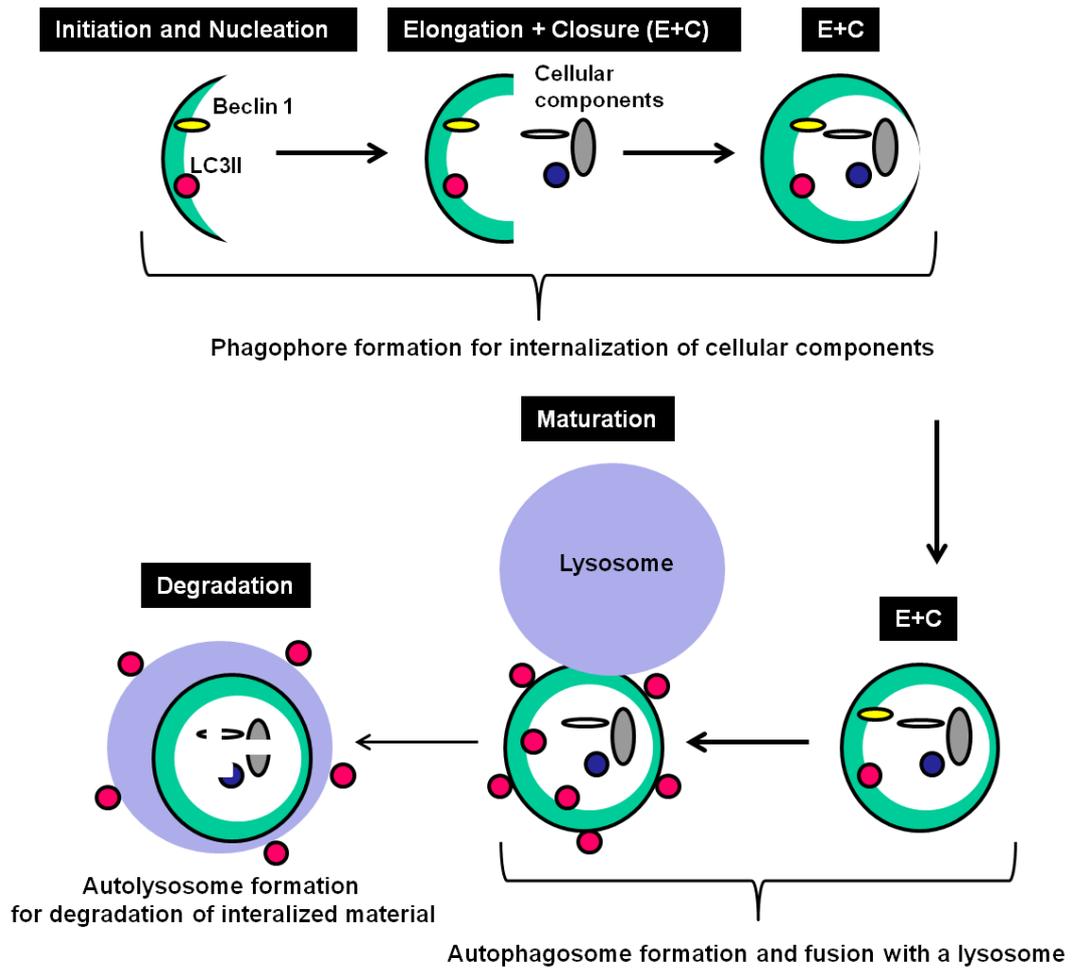
Figure 1-13 The process of autophagy in mammalian cells. In the first step cytoplasm and organelles are included from the phagophore which closes to form an autophagosome. The autophagosome fuses with a lysosome to form an autolysosome that degrades the internal material for reuse. Modified from [216, 225].

1.4.8 Senescence

Cellular senescence is an irreversible cell cycle arrest that acts as a safeguard programme of the cell to reduce its proliferative capacity after the exposure to stress signals [226]. Hence, like apoptosis, cellular senescence has a tumour suppressor function [226]. A growing line of evidence suggests senescence as a critical mechanism in response to chemotherapeutic agents [226]. Whereas the "replicative senescence" is related to cellular aging and was found to be induced through DNA damage signals from eroded telomeres that shorten with each cell division, "premature senescence" is an acutely inducible form of senescence [226-228]. Both mechanisms are biochemically and morphologically highly related [226]. The cellular insults that cause "premature senescence" may include ROS, unresolved DNA damage, γ-irradiation, and chemotherapeutic drugs [226, 229-234]. Agents that cause an acute senescence in tumour cells are considered as an option to force a terminal rest programme [226]. However, in some experimental set ups this form of senescence has been shown to be reversible, therefore raising issues about its therapeutic effect in the long term [235, 236].

1.5 Therapy resistance of CSCs

There are several factors that hamper a successful (prostate) cancer therapy. Among these are hypoxia, anti-apoptotic mechanisms, aberrant androgen-receptor signalling, increased drug efflux through the expression of ABC-transporters, detoxifying enzymes and cellular quiescence [33]. Recent findings link CSCs to therapy-resistance, in particular in relation to some of the mentioned resistance mechanisms (Figure 1-14). It is proposed that the CSCs are a therapy resistant fraction within the tumour that does not respond to conventional treatments and might therefore be responsible for

the recurrence of secondary therapy-resistant tumours [33, 100, 114, 237–239]. Normal SCs harbour better protective and repair mechanisms against DNA damage [240–243]. This is essential for a cell type that maintains during the life time of an organism, and is, due to this time factor, more likely to accumulate genetic alterations [242]. The more effective shielding against DNA damage is crucial to fulfil their tasks in tissue regeneration properly without passing alterations to the daughter cells. It is likely that CSCs "hijack" these features and are therefore less responsive to DNA damage introduced by cancer therapy [237, 244, 245]. This raises the issue of how CSCs are better protected against treatment than more differentiated tumour cells.

1.5.1 Mechanisms of therapy resistance in CSCs

A variety of mechanisms causal for treatment resistance in the CSC population have been proposed. For instance, CSCs are believed to have an **enhanced resistance to DNA damage**. Normal SCs exhibit efficient DNA mutation defence systems. When mutations occur that transform SCs into CSCs these defence systems are thought to protect CSCs against chemotherapy and irradiation [246]. Two candidates responsible for the mediation of therapy-resistance in CSCs might be Chk1 and Chk2 that become activated after genotoxic stress and arrest the cell cycle to enable repair [246]. Chk1 and Chk2 have higher activities in SC compared to normal cells [247]. In regard to CSCs, inhibitors against Chk1 and Chk2 partially reverse the resistance to irradiation in glioblastoma CSCs [247, 248].

Quiescence in cells is a critical mediator of treatment resistance, as most therapeutic strategies are designed to target rapidly proliferating cells. Indeed, many cancer treatments work initially for the majority of rapidly

proliferating primary tumour cells, but fail to eradicate quiescent populations. In particular, adult CSCs were shown to be in G0, a feature they might have inherited from their healthy counterparts [242]. Some studies already demonstrated that quiescent CSC populations e.g. from the colon, breast, ovaries, and pancreas harboured both *in vitro* and *in vivo* abilities to resist therapies that killed the main bulk of tumour cells [242, 249-251]. Hence, unsurprisingly the type of cell leading to initiation of secondary tumours must be the surviving CSC pool that re-enters cell cycle to re-populate the tumour by giving rise to extensively proliferating TAs [242].

Another factor correlated to therapy-survival of CSCs are **ROS defence enzymes**. ROS such as superoxide, hydrogen peroxide, hydroxylradical and nitrous oxide are produced *in vivo* as a result of normal metabolism [252]. They have influence on carcinogenesis, cardiovascular disease and ageing as they cause oxidative damage to proteins, lipids and DNA [252]. Peroxiredoxins are highly conserved enzymes that function to scavenge ROS. Their loss is associated with a tumour prone phenotype due to accumulation of damaged DNA [253]. Peroxiredoxins are thought to be key players in radio- and chemoresistance of cancer cells, as ROS are mediators of these therapeutic strategies. In a work of Diehn et a. 2009 CSCs derived from the breast were demonstrated to express higher levels of ROS defence enzymes in comparison to their more differentiated counterparts which were correlated with radioresistance [254]. Lower ROS levels have also recently been reported for central nervous system SCs and haematopoietic SCs as well as their early progenitors [255-261].

The **family of ATP-binding cassette transporters (ABC-transporters)** transport a large variety of substrates through the membrane, including metabolic byproducts, lipids, sterols and drugs. One of their main functions

is to expel toxins from the liver, kidneys and gastrointestinal tract. Due to their capability to excrete undesired substances, ABC-transporters are thought to play a critical role in chemotherapeutic agent resistance. Three types are mainly correlated with drug resistance: P-gp (ABCB1/multi-drug resistance (MDR) 1), MDR-associated protein (MRP1/ABCC1) and breast cancer resistance protein (BCRP/ABCG2). Their expression in different types of tumours has been correlated with a poor clinical outcome [262]. One frequently observed characteristic of CSCs is a high expression of ABC-transporter proteins in comparison to more differentiated cells, which led to the definition of the so-called "side population" (SP). There are various studies that link the expression of ABC-transporters to enhanced resistance properties of CSCs e.g. in the brain, lung, breast and prostate [263-267].

The aim of many anti-cancer therapies is to trigger apoptosis. CSCs seem to be **less sensitive to the induction of apoptosis** by cytotoxic agents and radiation therapy compared with more differentiated tumour cells [244, 268]. This might be due to Akt pathway activation and the overamplification of anti-apoptotic proteins such as those of the Bcl-2 family [246, 269]. Another important inhibitor of apoptosis in CSCs and promising target for cancer therapies is the transcription factor NFκB [246]. In neural SCs it has been demonstrated that they are protected from undergoing apoptosis due to the absence of caspase-8 and overexpression of PED (Phosophoprotein Enriched in Diabetes over-expression) [270]. Also the expression of the cytokine IL-4 seems to be paramount for mediating drug resistance by inhibition of apoptosis [271, 272].

Furthermore, it has been reported that the **reactivation of (developmental) signaling cascades** including EGF/EGFR, SCF, Sonic hedgehog, Notch and/or Wnt/β-catenin seems to play a major role [244, 268, 273].

Finally, CSCs are not only believed to escape many therapeutic approaches, it is even thought that they may enrich after the induction of therapy by selecting for resistant CSC subpopulations within a heterogeneous CSC pool [246]. Evidence for radiation-induced enrichment has already been shown for both brain and breast CSCs [246]. Due to these findings, specific targeting of CSCs must be considered for improving current anti-cancer strategies with the aim of sensitizing tumours toward conventional therapies and effectively abrogating tumourigenesis. So far only very little is known about therapy-resistance of SCs derived from prostate cancer tissue. A more profound knowledge about their nature might be the key for the development of new treatment strategies to eradicate prostate tumours on the long-term. The elucidation of these mechanisms is paramount for our understanding of treatment resistance.
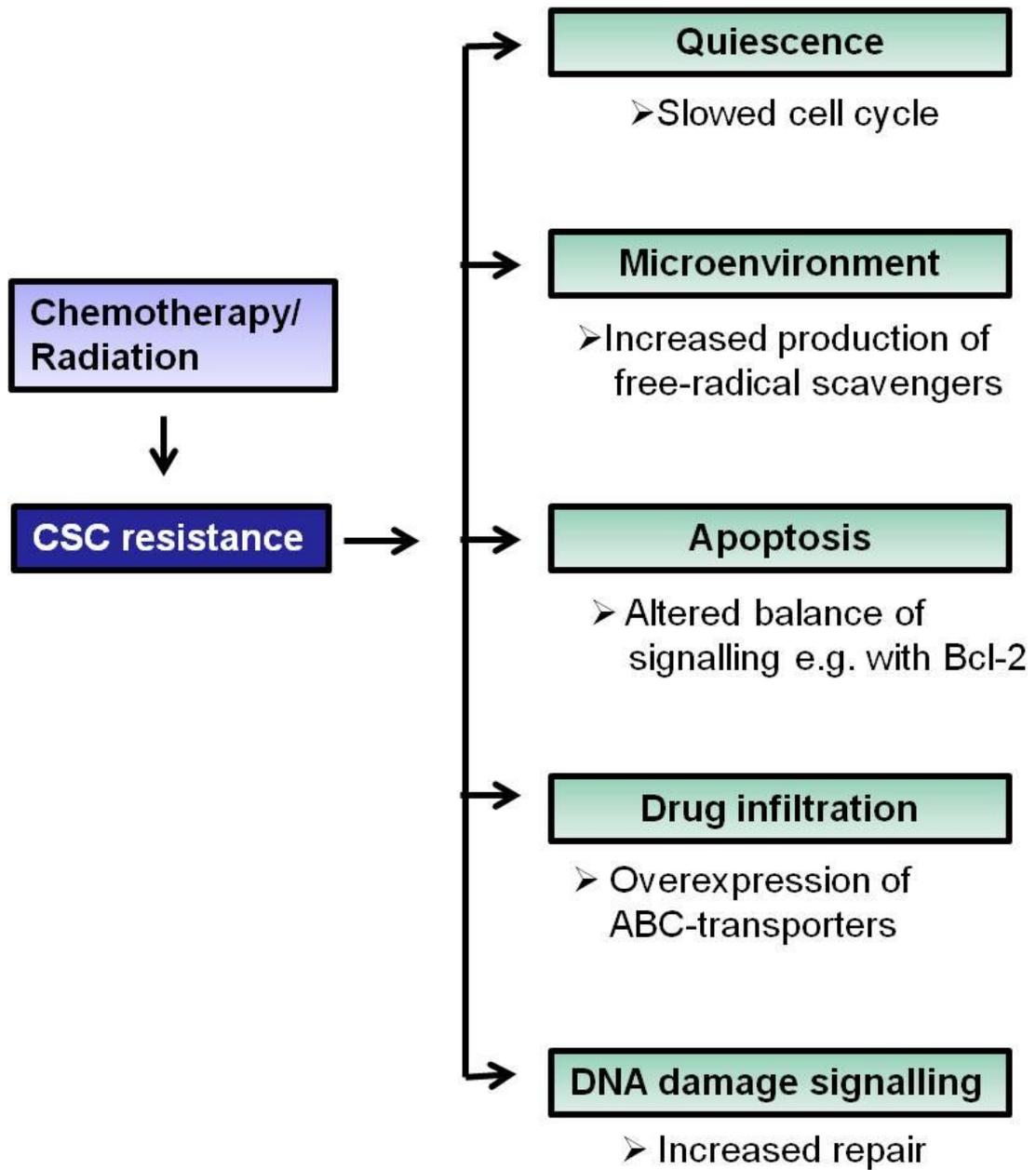
Figure 1-14 Mechanisms leading to therapy-resistance in CSCs. Note that the expression of ABC-transporters applies only to chemoresistance. Modified from [246].

Aim and strategy of the study

It was the aim of this study to investigate the therapy-resistance potential of CD133+ $\alpha_2\beta_1$/ integrin^{high} SCs derived from malignant and benign prostate tissues in comparison to CD133– $\alpha_2\beta_1$/ integrin^{high} TAs and CD133– $\alpha_2\beta_1$/integrin^{low} CBs originating from the same tissue. For this purpose epithelial cells were isolated from prostate tissues and expanded in culture to enrich subsequently for the above mentioned cell populations. The project aimed to answer two main questions:

Are SCs more resistant to the induction of DNA damage than TAs and CBs?

- The **extent of DNA damage** was assessed after treatment of the different populations with the "model drug" etoposide. We used alkaline comet assays as a direct measurement of DNA damage and staining for the repair factor γH2A.X as an indirect measurement, both of were analysed by immunofluorecence microscopy.

- The recovery of selected populations after etoposide treatment was examined by clonogenic assays.

What might be the mechanisms of potential therapy-resistance in SCs?

- The expression of **ABC-transporters** is a frequently reported therapy-resistance mechanism of cancer cells. In particular CSCs were demonstrated to be highly capable of expelling undesired substances. We re-analysed a microarray data set for the expression of ABC-transporters at mRNA level in our prostate epithelial cell model. To conduct a functional analysis we incubated the cells with the fluorescent substance calcein and measured the change of calcein

levels by the plate reader to compare the effectiveness of the ABC-transporters.

- Another likely mechanism of resistance to treatment is **cellular dormancy or quiescence**, as chemotherapeutic drugs are mainly designed to target rapidly proliferating cells. Cellular dormancy was assessed by staining for the protein Ki67 and subsequent assessment by immunofluorescence microscopy.

- The **failure of apoptotic mechanisms** is a common problem in cancer cells. Hence, we assessed apoptotic cell death following etoposide treatment by staining for activated caspases and examination by flow cytometry. Furthermore, we stained for LC3B to elucidate **autophagy** as an alternative cellular response. We assessed cell viability in prostate cancer cells following drug treatment using MTS.

Chapter II

MATERIALS AND METHODS

2. MATERIALS AND METHODS

2.1 General Methods

2.1.1 Human prostate tissue processing and culture

Prostate tissue was taken with approval from York and Hull Research Ethics Committee from patients undergoing transurethral resection of the prostate (TURP) and open or laparoscopic radical prostatectomy operations (ORP and LRP respectively). Diagnosis, age and treatment of the individual patients are listed in Table 2-1 and 2-2. Epithelial cells were isolated as described by [11]. Briefly, prostate tissue was washed with PBS, chopped and digested in collagenase for 12 h at 37°C on a shaker to release epithelial structures (acini and ducts). Epithelial cells were separated from stromal cells by repeated gravity centrifugation at 100 g, RT, 1 min. The material was resuspended in trypsin and left for 30 min at 37°C on a shaker. Epithelial cells were transferred to 10 mm BioCoat TM Collagen I plates and co-cultured with a confluent layer of irradiated STO feeder cells in stem cell media (SCM) at 37°C.

2.1.2 Maintenance of primary cell cultures

 Prostate epithelial cells were grown in co-culture with irradiated STO feeder cells in SCM on 10 mm BioCoat TM Collagen I plates at 37°C. Culture media was replenished every second day. For subculture, cell cultures were trypsinized as explained in 2.1.3 and pelleted at 200 g, RT, 5 min. Cells were resuspended in SCM and transferred to BioCoat TM Collagen I cellware and grown at 37°C. Cells were subcultured at a ratio of 1:2, 1:3 or 1:4 depending on their growth.

2.1.3 Harvesting of primary cells and cell lines

When epithelial cells reached approximately 80% confluency, culture medium was removed and cells were washed once with PBS and treated with 1 ml trypsin for 1 min. Trypsin was blocked with R10. The procedure was repeated to remove the entire population from the plates.

2.1.4 Cryopreservation

For storage in liquid nitrogen, cells were trypsinized as explained in 2.1.3, pelleted at 200 g, RT, 5 min and resuspended in cold freezing media (FM) at a concentration of $1 - 2 \times 10^6$ cells/ ml. Cells were aliquoted in cryovials and stored at – 80°C for at least 24 h prior to transfer into liquid nitrogen. To culture from frozen stocks cells after freezing, cells were plated with irradiated STO feeder cells in 10 ml SCM. The media was replenished after 24 h to remove the DMSO-containing freezing media from the culture.

2.1.5 Preparation of STO feeder cells

STO fibroblasts were grown on T175 plastic flasks. When they reached approximately 80–90% confluency they were trypsinized and pelleted at 200 g, RT, 5 min. Cells were washed with PBS and resuspended in 10 ml SCM per 100 cm^2 of culture surface. Cells were transferred into universal tubes and treated with an γ-irradiation dose of 60 Gy to inactivate mitosis. Cells were stored at 4°C and used within 4 days.

2.1.6 Selection of SCs, TAs and CBs from primary cell cultures

Human prostate epithelial cells were harvested as described in 2.1.3. Cells were washed once in MACS buffer at 200 g, RT, 5 min and resuspended in 5 ml SCM. To separate $\alpha_2\beta_1^{low}$ cells (CBs) from the $\alpha_2\beta_1^{high}$ population (SCs and TAs) 10 mm BioCoat TM Collagen I plates were blocked with blocking solution at 37°C for 1 h. The blocking solution was removed and plates were washed once with PBS. Cells were incubated on the blocked plates at 37°C

for 20 min. $\alpha_2\beta_1^{low}$ cells do not adhere within the indicated incubation time and can be collected easily from the plate afterwards. The plates were washed once with PBS. The $\alpha_2\beta_1^{high}$ population was released from the plates by repeated trypsinization as described in 2.1.3. CD133$^+$/$\alpha_2\beta_1^{high}$ SCs and CD133$^-$/ $\alpha_2\beta_1^{high}$ TAs were separated by a CD133 Cell Isolation Kit. Up to 10^8 cells were resuspended in 300 µl MACS buffer, 100 µl FcR blocking reagent and 100 µl CD133 antibody microbeads. Sorting using MACS MS columns was then carried out in accordance with the manufacturers' instructions. Briefly, each magnetic column was used for approximately 6 x 10^6 cells. After elution of the cells from the first column up to 4 ml of the CD133$^+$ elute was passed through a second column to increase the purity of the population.

2.2 Single cell analysis

2.2.1 Immunocytochemistry for γH2A.X foci and Ki67

The different cell subpopulations were selected as described in 2.1.6 (or used unselected depending on the type of experiment). Cells were plated on collagen I-coated 8-well chamber slides (10 000 for CBs and TAs; for SCs a lower number depending on the yield). For the γH2A.X staining, cells were incubated with 30 µM etoposide for 30 min or 45 min to induce DNA damage. Additional time points with etoposide were carried out to assess repair by removing the drug, washing once with PBS and leaving the cells at 37°C for additional 24 h in SCM. A small set of samples were treated with 2 mM thymidine at 37°C for 24 h to induce replication stress. For the Ki67 staining cells were left untreated.

The following volumes were applied per 8-well chamber slide: After removal of the medium, cells were washed with 1 ml PBS and fixed in 1.6 ml Fixation-Permablization buffer at RT for 15 min. Cells were washed with 1

ml PBS. Cells were washed with 1.6 ml 0.5 % Nonidet-P40 (NP40) in PBS at RT for 20 min to remove cytoplasmic proteins and subsequently washed with PBS. The primary antibody anti-human γH2A.X was diluted 1: 1000 in 0.5% BSA in PBS and cells were incubated in 1.6 ml at 4°C o/n. After removal and washing three times with PBS, 1.6 ml of the secondary antibody goat anti-mouse Alexa Green 488 was added in a 1:1000 dilution in 0.5% BSA in PBS and incubated at RT for 45 min in the dark. The chambers were removed from the chamber slides and DNA was labelled with DAPI. A coverslip was mounted on the slides and fixed in place with nail polish. γH2A.X was detected by immunofluorescence microscopy. For analysis ~100 cells (but at least 50 cells) were counted per well and the % of γH2A.X positive cells was determined. For the Ki67 staining the same procedure was applied. In this case a goat anti-rabbit Alexa Red 568 served as a secondary antibody.

2.2.2 LC3B staining

Primary cells were harvested as described in 2.1.3 and plated on collagen I-coated 8-well chamber slides. After incubation with 60 µM etoposide for 60 h, cells were washed once with PBS and incubated in fixation buffer for 15 min. The cells were washed three times with PBS and permeablized in 0.25% Triton-100 in PBS for 10 min. Cells were washed three times with PBS and blocked with IF-blocking buffer for 1 h. The LC3B antibody was diluted in 0.1% Tween 20/ 0.1% BSA in PBS and left on the cells for 1 h. Cells were washed three times with PBS and incubated for 45 min with a 1: 1000 dilution of goat-anti-rabbit Alexa 488 in 1% BSA in PBS. Cells were washed three times with PBS and mounted with DAPI for final assessment by immunofluorescence microscopy.

2.2.3 Alkaline Comet Assay

Primary cells were harvested according to 2.1.3. Cells were selected according to 2.1.6 (or left unselected depending on the type of experiment). 30 000 cells (for SCs less depending on the yield) were treated per tube in 1 ml etoposide in suspension while rotating on a MACS spinner at 37°C. The etoposide concentrations ranged from 30 μM to 250 μM and the incubation times from 30 min to 3 h. After treatment, cells were pelleted at 200 g, RT, 5 min and resuspended in 25 μl PBS. The following steps were carried out in the dark: Tubes were placed in a waterbath at 37°C and 225 μl low melting agarose was added per tube. Samples were dropped onto agarose-coated slides and covered with coverslips. Slides were cooled for 15 min at 4°C. Coverslips were removed and immersed in lysis buffer o/n. The following day, samples were placed into alkaline electrophoresis buffer and incubated for 40 min at 4°C. Slides were run in a gel tank apparatus in alkaline electrophoresis buffer at 24 V (300 mAmps) for 40 min and drained afterwards. Samples were placed in neutralizing buffer for three times for 10 min. To stain the samples SYBR-Gold was diluted 1:10 000 in TE buffer pH 7.5 and 300 μl was added to each slide and covered with a coverslip. Samples were assessed by immmnofluorescence microscopy and images of ~ 100 cells per sample were taken to be analyzed with the comet analysis software TriTek – CometScore Version 1.5.

2.2.4 Neutral Comet Assay

Cells were harvested according to 2.1.3. Unselected populations were used or cells were selected according to 2.1.6. 30 000 cells per tube (for SCs less depending on the yield) were treated in 1ml etoposide in suspension while rotating on a MACS spinner at 37°C. The etoposide concentrations ranged from 30 μM to 1mM and the incubation times from 30 min to 3 h. After

treatment cells were pelleted at 200 g, RT, 5 min and resuspended in 25 μl PBS. The following steps were carried out in the dark: Tubes were placed in a waterbath at 37°C and 225 μl low melting agarose was added per tube. Samples were dropped onto agarose-coated slides and covered with coverslips. Slides were cooled for 15 min at 4°C. Coverslips were removed and immersed in lysis buffer o/n. The following day samples were placed into TBE electrophoresis buffer for 10 min. Slides were run in a gel tank apparatus in TBE electrophoresis buffer at 24 V for 20 min and drained afterwards. To stain the samples, SYBR Gold was diluted 1:10 000 in TE buffer pH 7.5 and 300 μl were added to each slide and covered with a coverslip. Samples were assessed by immunofluorescence microscopy and images of ~ 100 cells per sample were taken to be analyzed with the comet assay analysis programme TriTek – CometScore Version 1.5.

2.3 Caspase Assay

Cells were treated in culture with etoposide. The etoposide concentrations ranged from 15 μM to 125 μM and the incubation times from 12 h to 72 h. The supernatant was collected and cells were harvested according to 2.1.3. Cells were washed in 2 ml cold MACS per sample and centrifuged at 200 g, RT, 5 min. Cells were washed in 2 ml cold MACS buffer per tube and pelleted at 200 g, RT, 5 min. The CaspACE™ FITC-VAD-FMK In Situ Marker was diluted 1:500 in PBS and cells were resuspended in 100 μl per tube and incubated for 20 min at 37°C. Cells were washed in 2 ml PBS per tube and pelleted at 200 g, RT, 5 min. Cells were resuspended in 500 μl PBS. Caspase activity was assessed by a CyAn Flow Cytometer (Dako).

2.4 Plate reader experiments

2.4.1 Calcein efflux test

Epithelial cells were harvested according to 2.1.3 and selected according to 2.1.6 (or used unselected depending on the type of experiment). 1000–20 000 cells were plated on collagen I-coated 96-well plates and left to adhere for 2 h at 37°C in KSFM. CBs and TAs were seeded as triplicates whereas for SCs the yield was only sufficient for one well. KSFM was removed and 200 µl 1:5000 Calcein- AM Fluorescent Dye in KSFM was added per well and left for 15 min at 37°C. Calcein AM Fluorescent Dye was removed. The wells containing the plated cells were washed with once in PBS and 200 µl KSFM without Calcein AM Fluorescent Dye were added per well. The plates were measured in the plate reader immediately and kept at 37°C afterwards. After 1 h the KSFM (containing effluxed calcein) was taken from the cells and cells were washed with PBS. Fresh KSFM without Calcein Fluorescent Dye was added to the cells. This step was repeated after 2 h and 3 h. Plates were measured at all indicated timepoints.

2.4.2 Viability assay

Cells were harvested as described in 2.1.3 and transferred to collagen I-coated 96-well plates (5000 cells/ 100 µl SCM per well) After 24 h at 37°C media was removed and replaced by 100 µl fresh SCM containing a dilution series of replication inhibitors (see appendix). After four days, cells were measured by using the CellTiter96® A$_{queous}$ One Solution Cell Proliferation Assay. 20µl of solution was added and after 2 h incubation absorbance was measured.

2.5 Clonogenic recovery assay

TAs and SCs were selected as described in 2.1.3. 100 – 300 cells per well were seeded in triplicate on collagen I-coated 6-well plates in 2 ml SCM per

well and kept at 37°C. Cells were left for 2 h to adhere and washed once with PBS to remove floating cells. Fresh SCM was added to each well. The number of cells was then counted in every well. 500 µl irradiated feeder cells were added. Cells were treated for 45 min or 3 h with 30 µM etoposide or the appropriate dilution of DMSO at 37°C. Cells were washed twice with PBS and 3 ml SCM were added to each well. Cells were kept at 37°C and SCM was changed every second day. An appropriate amount of irradiated feeder cells was added to keep the plates confluent. After 8–14 days SCM was removed and cells were washed once with PBS. Cells were stained with 2 ml crystal violet solution per well for 20 min. Cells were washed twice with 3 ml PBS per well. The number of colonies was determined and related to the cells counted on the day of the selection. Different sizes of colonies were classified: colonies consisting of 2–4, 5–8, 9–16, 16–32 cells and > 32 cells.

2.6 Malignant and benign prostate tissue samples and cell lines

Sample (site)	Diagnosis	Age	Surgery	GS	PT
H020/09	Cancer	n/a	RP	3+4=7	–
H035/11 (LA)	Cancer T2c	n/a	RP	3+4 =7	–
H049/11 (LB)	Cancer/ side carcinoma T2c	n/a	RP (ORP)	3+3=6	–
PE665	Cancer	53	RP	3+4=7	–
PE531	Cancer	57	RP	4+5=9	–
H054/11 (RA)	Cancer	58	RP (LRP)	3+4=7	–
H018/09	Cancer HGPIN T2c	n/a	RP	1	–
H034/11	Cancer T3a		RP	3+4=7	–
H031/10	Cancer T2a	n/a	RP	3+4=7	–
H048/11 (LM)	Cancer	n/a	RP	3+3=6	–

H149/12	Cancer	78	TURP	N/A	Hormone therapy
Y018/11	Cancer	75	TURP	3+=6	Hormone therapy
H090/09	Cancer	80	TURP	4+5=9	Hormone therapy
H087/11 (LB)	Cancer	68	RP (ORP)	3+4=7	–
H131/11 (LA)	Cancer	70	RP (LRP)	3+4=7	–
H069/11 (RB)	Cancer	65	RP	4+3=7	–
Y062/11	Cancer	61	TURP	5+4=9	Hormone therapy

Table 2-1 Prostate carcinoma tissue

Abbreviations: **TURP** = Transurethral resection of the prostate; **GS** = Gleason score; **PT** = Previous treatment; **RP** = Radical prostatectomy; **LRP** = Laparoscopic radical prostectomy; **ORP** = Open radical prostatectomy; **HGPIN** = High grade prostate intraepithelial neoplasia; **Tumour stages: T2a** = tumour in half or less than half of the 2 lobes, **T2c** = tumour in both lobes; **T3a** = tumour has spread through the capsule; **Sites the cores were taken from**: RA, LA, LM, LB, RB → R = Right, L = Left, A = Apex, M = Mid, B = Base

Sample	Age	Surgery	GS	PT
Y004/09	77	TURP	–	–
Y031/08	83	TURP	–	–
Y024/08	72	TURP	–	–
Y040/09	67	TURP	–	–
Y025/09	84	TURP	–	–
Y010/11	61	TURP	–	–
Y031/11	80	TURP	–	–
Y052/10	72	TURP	–	–
Y040/10	67	TURP	–	–
H053/11	n/a	TURP	–	–
Y025/11	75	TURP	–	–
Y030/11	88	TURP	–	–
H053/11	N/A	TURP	–	–

Y023/09	88	TURP	–	–
Y075/11	80	TURP	–	–

Table 2-2 BPH Tissue samples

Abbreviations: **TURP** = Transurethral resection of the prostate; **GS**=Gleason score; **PT** = Previous treatment

Cell line	Origin	Media	Dilution upon subculture
RC165N/hTERT [274]	Benign prostate derived cell line	R-Media	1:5
RC92a/hTERT [274]	Malignant prostate derived cell line	R-Media	1:5
PNT1a	Normal prostate epithelial cell line	R10	1:5
LNCaP	Human prostatic adenocarcinoma metastatic site in supraclavicular lymphnode	R10	1:5
BPH-1	Benign prostate derived cell line	R5	1:10
PC3	Human prostatic adenocarcinoma metastasis site in the bone	H7	1:5
STO	Mouse embryonic fibroblasts	D10	1:10

Table 2-3 Mammalian cell lines

2.7 Chemicals

Drug	Company
Etoposide	Sigma cat. no. E1383
Carboplatin	Sigma cat. no. C2538
Docetaxel	Fluka cat. no. 01885-25MG-F
Doxorubicin	Fluka cat. no. D1515-10MG
Camptothecin	Sigma cat. no. 365637
Thymidine	Sigma cat. no. T9250

Table 2-4 Chemotherapeutic drugs

Kit/ Reagent	Dilution	Company
BD ™Calcein AM Fluorescent Dye	1:5000	BD Bioscience cat. no. 354216
CaspACE™ FITC–VAD–FMK In Situ Marker	1:500	Promega cat. no. G7461
Mounting Medium with DAPI	–	Vectashield Laboratories cat. no. H–1200
NuSieve® GTG® Agarose	–	Cambrex cat. no. 50080
SYBR–Gold nucleid acid gel stain	1:10 000	Invitrogen cat. no. S11494
CD133 Microbead Kit	–	Miltenyi Biotec Ltd cat. no. 130–050–801
Collagenase Type I	–	Worthington cat. no. MX1H12791
FCR blocking reagent	–	Miltenyi Biotec Ltd cat. no. 130–059–901
DMSO	–	Sigma–Aldrich cat. no. D8418
CellTiter96® A$_{queous}$ One Solution Cell Proliferation Assay	–	Promega cat. no. G3582
Trypsin–EDTA	–	Gibco cat. no. 15400–054
FCS	–	PAA cat. no. A15–041
Goat serum	–	Sigma Cat. No R4505
Rabbit serum	–	Sigma Cat. No G6767

Table 2–5 Kits and reagents

Antibody	Host	Reactivity	Dilution	Company
γH2A.X	mouse	anti–human	1:1000	Millipore cat. no. 05–636
Ki67	rabbit	anti–human	1:1000	Abcam cat. no. ab15580
CD133/2 (293C3)–APC	mouse	anti–human	1:11	Miltenyi Biotec cat. no. 130–090–854
Alexa 568	goat	anti–rabbit	1:1000	Invitrogen cat. no. A11036

| Alexa 488 | goat | anti-mouse | 1:1000 | Invitrogen cat. no. A11029 |
| LC3B | rabbit | anti-human | 1:1000 | Abcam cat. no. ab51520 |

Table 2-6 Antibodies

Solution	Components
PBS	137 mM NaCl 2.7 mM KCl 4.3 mM Na_2HPO_4 1.47 mM KH_2PO_4 Adjust to a final pH of 7.4
Neutralizing Buffer	0.4 M Tris in dH_2O; adjusted to pH 7.5
MACS buffer	0.5% FCS 2 mM EDTA in PBS
Lysis buffer	2.5 M NaCl 1 mM EDTA 10 mM Tris 10% DMSO 1% Triton X-100 in dH_2O; adjusted to pH 10
Alkaline electrophoresis buffer	0.3 M NaOH 1 mM EDTA
TE buffer	1 M Tris – HCl 0.5 mM EDTA adjusted to pH 8
Fixation-Permablization buffer (for nuclear stainings)	2% PFA 0.2% Triton x-100 PBS adjusted to pH 8.2
Fixation buffer (for staining proteins in the cytoplasm)	3% PFA in PBS adjust to pH7
TBE electrophoresis buffer	89.15 mM TRIS 89.9 mM Boric Acid 3.98 mM EDTA
IF-Blocking Solution (LC3B staining)	5% goat serum 0.1% Tween 20 in PBS
Blocking solution (selection of epithelial cells)	0.3% BSA in PBS heat-inactivated at 80°C for 10 minutes
Crystal violet solution	PBS

| | 1% crystal violet | |
| | 10% ethanol | 84 |

Table 2-7 Solutions

2.8 Media and plastic ware

Media	Components	Origin
RPMI 1640	---	Gibco, cat. no. 31870-074
DMEM	----	Gibco, cat. no. 41966-029
KSFM	---	Gibco, cat. no. 17005-075
Ham´s F-12	----	Lonza, BE12-615F
R5	RPMI 1640 5% FCS	as mentioned above as mentioned above
R10	RPMI 1640 10% FCS	as mentioned above as mentioned above
D10	DMEM 10% FSC	as mentioned above as mentioned above
H7	HAM´s F-12 7% FCS	as mentioned above as mentioned above
R-Media	500 ml KSFM 5ng/ml Epidermal growth factor 50µg/ml Bovine pituitary extract 2mM L-Gluatmine	as mentioned above as mentioned above as mentioned above as mentioned above
SCM	KSFM 5 ng/ml Epidermal growth factor 50 µg/ml Bovine pituitary extract 2 ng/ml LIF 2 ng/ml SCF 100 ng/ml Cholera toxin 1 ng/ml GM-CSF 2 mM L-Glutamine	as mentioned above Gibco, cat. no. 10450-013 Gibco, cat. no. 13028-014 Millipore, cat. no. LIF 2010 First link, cat. no. 62-64-206 Sigma, cat. no. C8052-1MG Miltenyi, cat. no. 130-093-8865 Gibco, cat. no. 25030-024
FM	RPMI 1640 20 % FCS 10 % DMSO	as mentioned above as mentioned above as mentioned above

Table 2-8 Mammalian cell line culture media

Plastic ware	Company
20 x 10 mm BioCoat TM Collagen I	BD Biosciences cat. no. 356450
Collagen coated 6-well plates	BD Biosciences cat. no. 354400
Collagen coated 8-well chamber slides	BD Biosciences cat. no. 354630
Collagen coated 96-well plates	BD Biosciences cat. no. 356407
T75 flasks	Corning Incorporated cat. no. 430641
MS columns	Miltenyi Biotec Ltd cat. no. 130-042-201

Table 2-9 Plastic ware

2.9 Statistical Analysis

The statistical analysis was conducted by Sigma plot 11.0. For paired t-test or Wilcoxon rank sum test, values were considered to be significant when $p < 0.05$.

Chapter III

RESULTS

3. RESULTS

3.1 Assessment of DNA damage in primary prostate epithelial cells using comet and γH2A.X assays

The extent of DNA damage in cancer cells after their exposure to therapy is an important indicator to elucidate their treatment susceptibility. We used etoposide – a drug that also has clinical relevance for the treatment of many cancers – as a "model drug" for our studies. In order to compare levels of DNA damage in selected malignant and benign prostate populations, we treated cells with etoposide and employed comet and γH2A.X assays.

3.1.1 Assessment of the DNA damage after etoposide treatment by comet assays

3.1.1.1 Examination of the suitability of neutral and alkaline comet assays to detect etoposide-induced DNA damage

Comet assays rely on the separation of damaged DNA ("tail") from intact DNA ("head") by gel electrophoresis, imaging of "comets" by immunofluorescence microscopy and the subsequent quantification of DNA damage e.g. by the parameter % of DNA in tail (Figure 3-1). Both neutral and alkaline comet assays were performed to examine which technique was most suitable for detecting etoposide-induced DNA damage. In general, neutral comet assays are more specific for the detection of DSBs, but less sensitive than alkaline comet assays, which allow the quantification of DSBs, SSBs and alkali-labile sites [275]. Use of comet assays to assess etoposide-induced DNA damage has been carried out before [166, 275]. However, the effect on primary prostate epithelial cells has not been measured. This was clearly of relevance in these studies. In order to verify whether neutral comet assays were suitable, we treated PNT1A cells and selected primary cells (H020/09), with several etoposide concentrations for different time points (Figure 3-2). In both assays only a slight increase of the parameter % DNA in

tail was detected. This result suggested that neutral comet assays were not suitable to detect etoposide-induced DNA damage. Alkaline comet assays were then carried out using RC92a/hTERT cells and two primary samples (Y004/09 and Y025/09), (Figure 3-3). In RC92a/hTERT cells the levels of DNA damage increased strikingly and revealed more than 90% DNA in tail for all treated samples (Figure 3-3 A). In primary samples the response appeared to be weaker than in RC92a/hTERT cells, but still stronger than with neutral comet assays (Figure 3-3 B and C). Comparative images presenting the observed amounts of DNA damage, revealed by either neutral or alkaline comet assays, emphasize the suitability of the alkaline comet assay to detect DNA damage in our system (Figure 3- 4). We concluded that the high pH in the alkaline version encouraged the unwinding and release of DNA better than in neutral comet assays and was furthermore able to detect several types of DNA damage induced by etoposide.
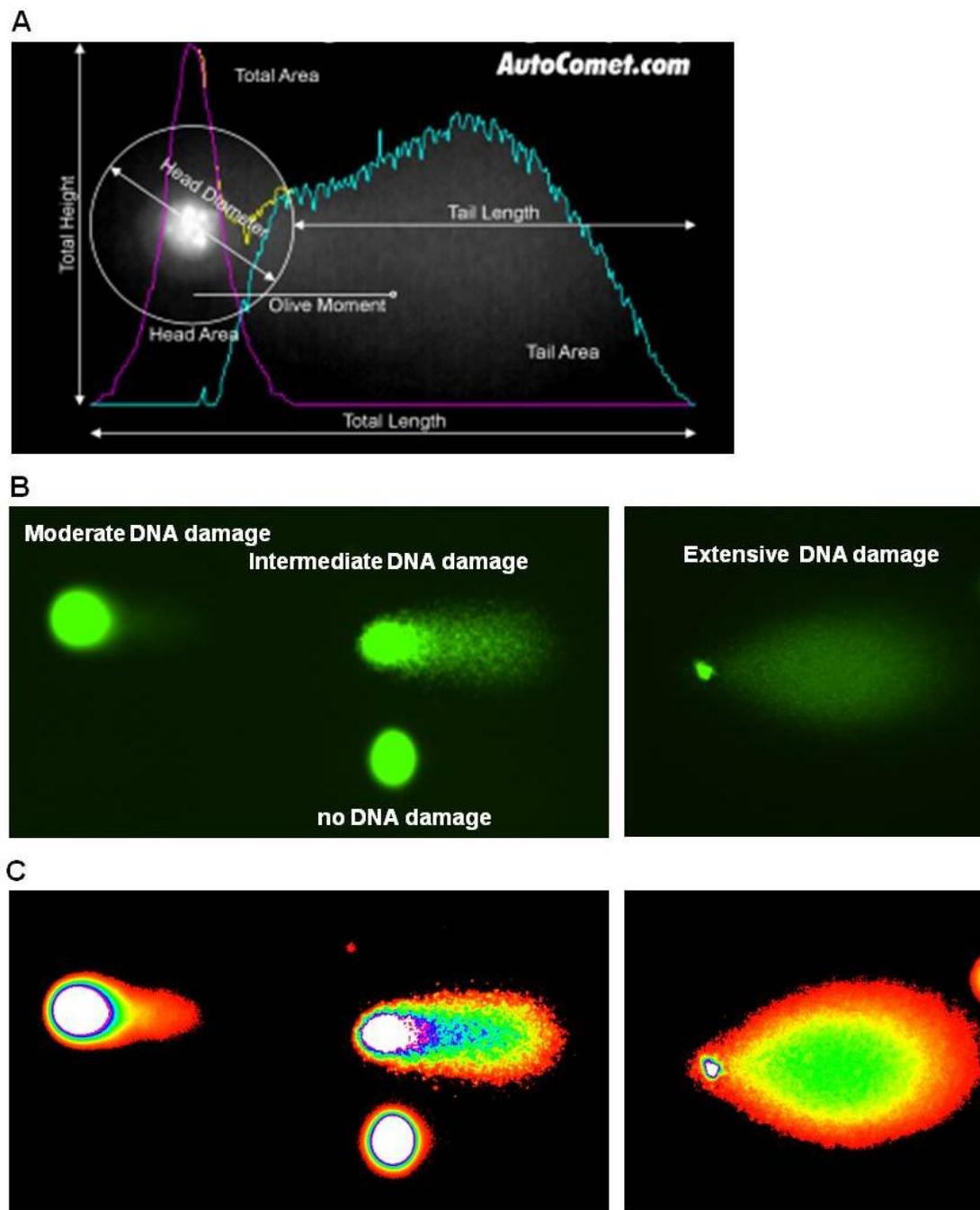
Figure 3-1 Assessment of DNA damage using comet assays. Cells were subjected to gel electrophoresis and stained with SYBR Gold for subsequent visualization by immunofluorescence microscopy. (A) The "head" of a comet represents undamaged DNA, whereas the "tail" represents damaged DNA. Image shows measurements made by AutoComet TriTek software. (B) Examples for cells with and without DNA damage from an alkaline comet assay. (C) Images as shown in B were analysed by TriTek comet score software.
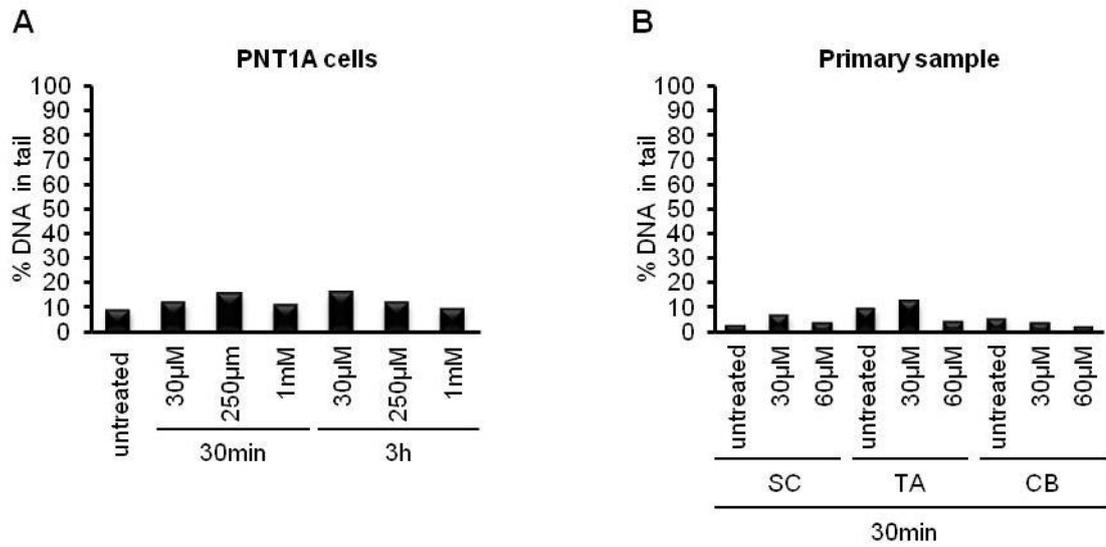
Figure 3-2 Determination of suitability of neutral comet assays to detect etoposide-induced DNA damage. (A) PNT1A cells and (B) selected primary cells (H020/09) were treated with the indicated concentrations and time points with etoposide and % of DNA in tail was quantified by neutral comet assays. Bars represent median values of % DNA in tail. At least 50 cells were analyzed, but usually more than 100 depending on their availability.
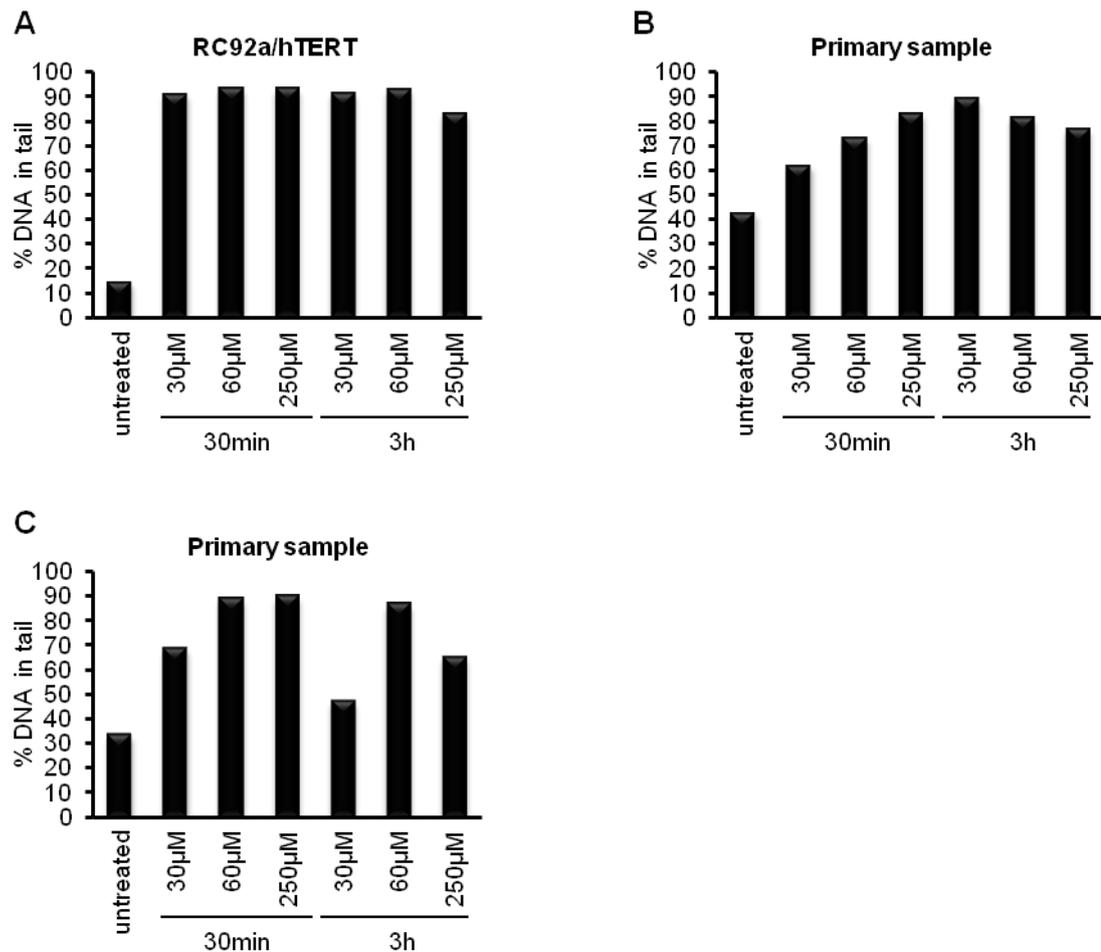
Figure 3-3 Determination of suitability of alkaline comet assays to detect etoposide-induced DNA damage. (A) RC92a/hTERT cells and (B, C) primary cells (Y004/09 and Y025/09 respectively) were treated with different concentrations of etoposide for the indicated times and % DNA in tail was assessed by alkaline comet assays. Bars represent median values of % DNA in tail. At least 50 cells were analyzed, but usually more than 100 depending on their availability.
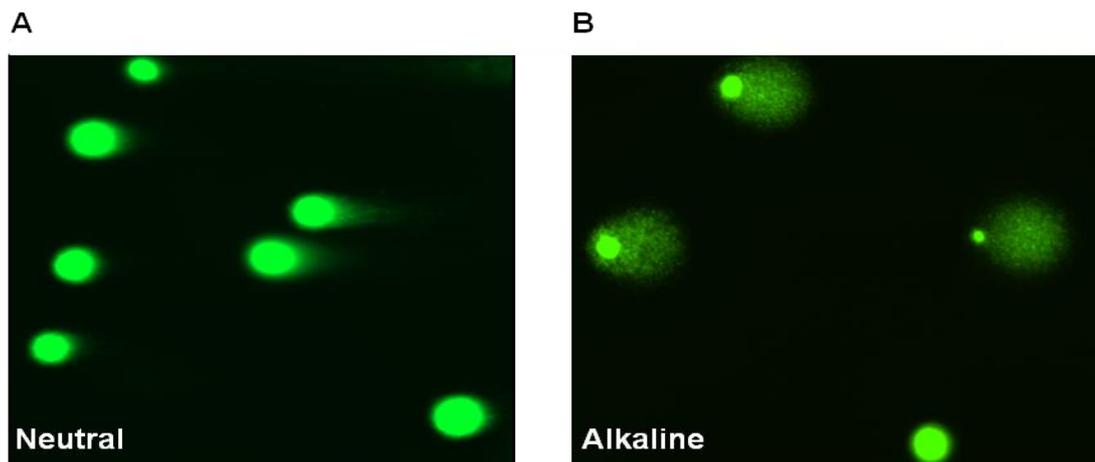
Figure 3-4 Alkaline comet assays are more suitable for detecting etoposide-induced DNA damage. The images are representative for the highest amounts of % DNA in tail observed in prostate primary cells by performing (A) a neutral comet assay and (B) an alkaline comet assay.

3.1.1.2 Comparative study of the levels of DNA damage using alkaline comet assays

In view of these findings we decided to proceed with alkaline comet assays for a comparative study of the DNA damage response in selected primary prostate malignant and benign populations. Initially, a number of alkaline comet assays with different etoposide concentrations and time points was conducted (Figure 3–5). With this assay SCs showed lower levels of DNA damage. There were significant differences between SCs vs. TAs (p = <0.001) and SC vs. CB (p= 0.007) at 30 µM etoposide for 45 min. When using more aggressive treatment conditions we observed a similar trend. Both malignant and benign SCs acquired less DNA damage than TAs and CBs. At an etoposide concentration of 250 µM for 45 min we found a significant difference in DNA damage between SCs and TAs (p=0.0029).

During the preparation of the previously described assays we found that the combination of 30 µM etoposide for 45 min was the most suitable. It was therefore applied to a higher number of samples (as already included in Figure 3–5). Treatment, which was too aggressive, might have resulted in (i) missing a potentially different response among the populations and (ii) creating an enormous DNA fragmentation below the detectable range of a comet assay. The % DNA in tail seemed to be reduced at aggressive treatment conditions relative to lower concentrations (Figure 3–5). This might have been due the obliteration of the DNA, which would make it undetectable. We analyzed the comet assays performed for our optimal treatment condition in more detail by separating malignant and benign samples and by enabling a correlation of SCs, TAs and CBs that originated from the same patient (Figure 3–6). When we compared the extent of DNA damage in malignant SCs to their corresponding TAs, we found a higher

susceptibility to etoposide in TAs (p= 0.008), (Figure 3-6 A). CBs from the same tissue were also seen to present with a higher amount of DNA damage than SCs, but in this case the difference was not significant. Interestingly, the amounts of DNA damage measured in malignant SCs were very low (median fold change of % of DNA in tail = 1.3), but an increased damage response was seen in SCs from the samples H018/11 and H090/09, which were both taken from patients that underwent hormone therapy. In selected populations of benign origin, we found a significant increase of % of DNA in tail in TAs after etoposide exposure when comparing them to SCs (p=0.008) (Figure 3-6 B). Benign CBs increased their levels of DNA damage post treatment, but we found no significant difference in comparison to SCs and TAs.

To visualize these differences between selected populations before and after treatment in regard to the % of DNA in tail, comparative example images were taken (Figure 3-7). As graphed in Figure 3- 6, SCs displayed less DNA damage following treatment (Figure 3-7 A, B) than TAs (Figure 3- 7 C, D) and CBs (Figure 3-7 E, F).

In conclusion, both malignant and benign prostate SCs were less sensitive to etoposide treatment than their differentiated counterparts. Their decreased susceptibility to the induction of DNA damage might therefore be correlated with a higher resistance to conventional treatments. A method to examine the DNA damage response further and even more detailed than with comet assays (direct measurement), is the use of the DNA damage marker γH2A.X, the phosphorylated form of a protein that is indicative of DNA lesions (indirect measurement).
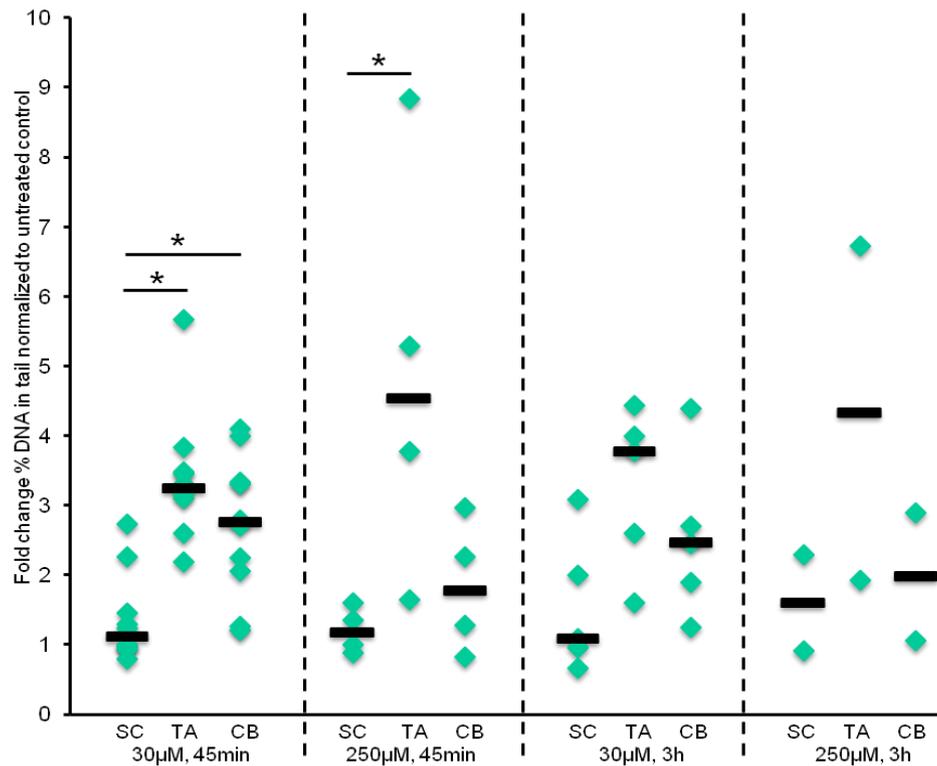
Figure 3-5 Prostate SCs from benign and malignant samples are more resistant to etoposide treatment than CBs and TAs. Malignant and benign SCs, TAs and CBs were selected from cultures grown from primary tissues. Cells were treated for the indicated time points in suspension and the % of DNA in tail was quantified by alkaline comet assays. Each symbol represents one patient. Black marks represent median values of % DNA in tail. At least 50 cells, but usually more than 100 were analyzed for the treatment condition 30 μM, 45 min depending on their availability. For the other treatment conditions occasionally less than 50 cells were available for analysis. These exceptions are listed in the appendix. Wilcoxon rank sum test for the 45 min, 30 μM: SC vs. CB: p= 0.007, SC vs. TA: p = <0.001; 45 min, 250 μM SC vs. TA: p = 0.0029. Non-significant p-values are listed in the appendix.

A

Cancer samples

B

Benign samples
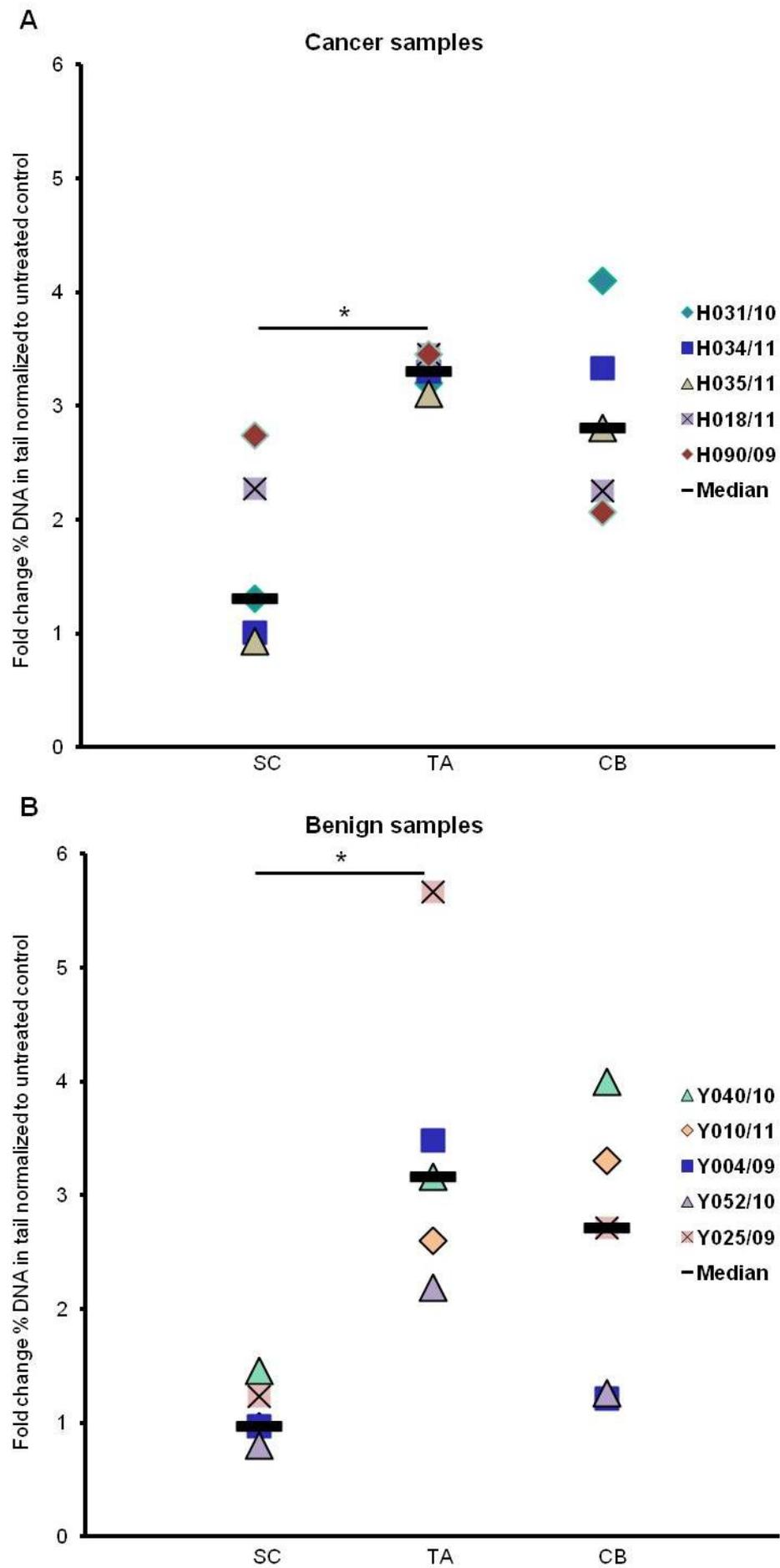
Figure 3-6 Primary malignant and benign SCs are more resistant to etoposide treatment than CBs and TAs. (A) Malignant and (B) benign SCs, TAs and CBs were selected from cultures grown from primary tissues. Cells were treated with 30 µM etoposide for 45 min in suspension and the % of DNA in tail was quantified by alkaline comet assays. Each symbol represents one patient. At least 50 cells were analyzed, but usually more than 100 depending on their availability. Wilcoxon rank sum test for malignant samples: SC vs. TA: p= 0.008; Wilcoxon rank sum test for benign samples: SC vs. TA: p= 0.008. Non- significant p-values are listed in the appendix.
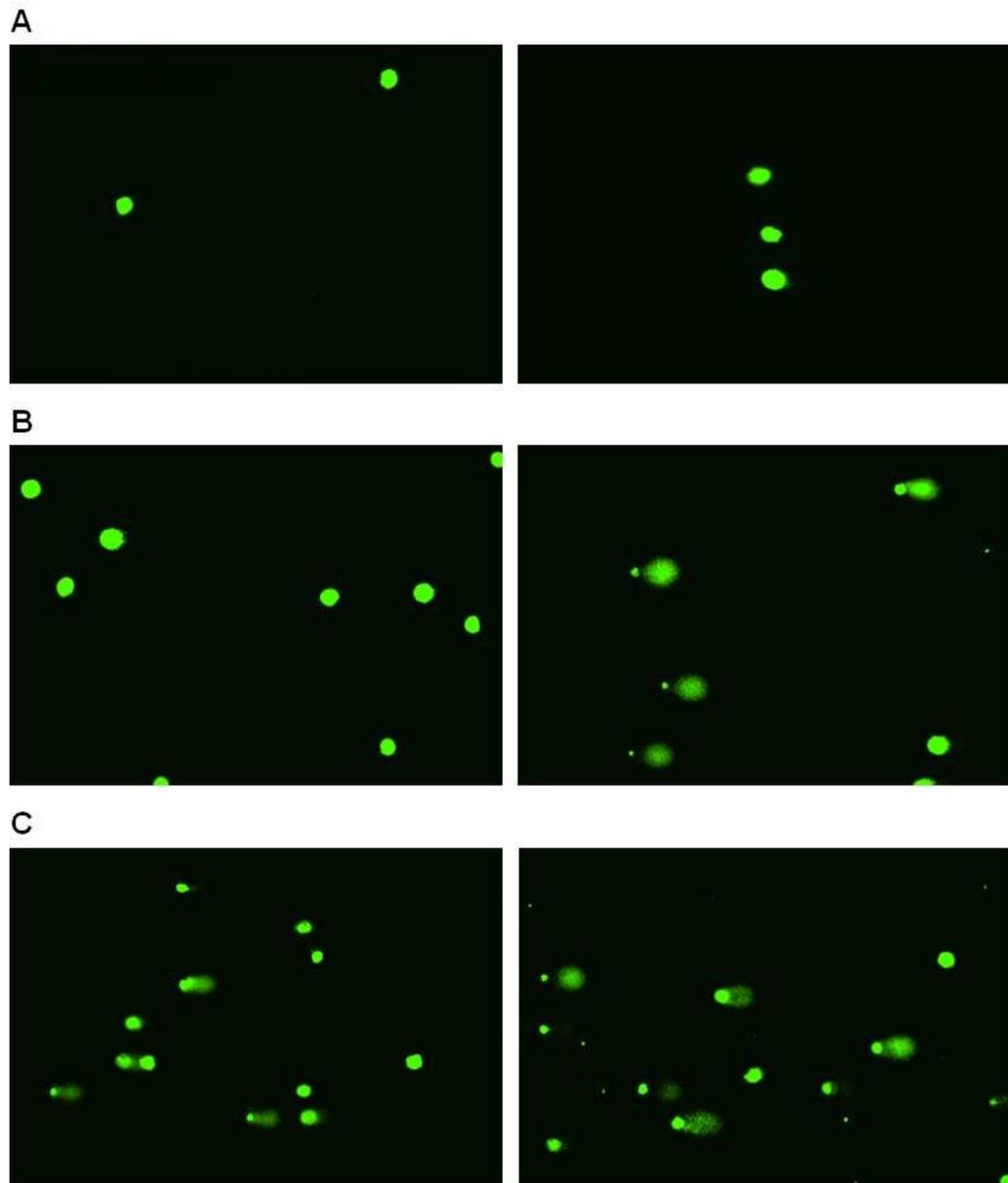
Figure 3-7 Comparative images of primary prostate populations following etoposide treatment. (A) SCs, (B) TAs and (C) CBs were selected from primary cultures and treated with 30 µM etoposide for 45 min. DNA damage was quantified by alkaline comet assays. Note the increasing % DNA in tail in (B) and (C) between the images on the left (before treatment) and images on the right (after treatment). The SCs could only be plated in a lower density, as SC yields are very low.

3.1.2 Assessment of the DNA damage after etoposide treatment by γH2A.X

3.1.2.1 Suitability of the DSB marker γH2A.X to assess DNA damage and repair

In order to detect DSBs in malignant and benign primary prostate SCs and TAs after exposure to etoposide, cells were stained for the DSB marker γH2A.X. The γH2A.X staining protocol was initially tested on unselected LNCaP, BPH-1 and primary cells (Figure 3-8). In both LNCaP and primary cells the number of γH2A.X positive cells increased strongly after treatment at different concentrations (Figure 3-8 A and E), whereas BPH-1 cells showed a weaker response (Figure 3-8 C). To assess whether or not γH2A.X was a suitable marker to examine repair in primary prostate cells, the drug was replaced by normal media after 45 min and cells were kept at 37°C for a further 24 h. In LNCaP and primary cells the γH2A.X foci were reduced ~50% in comparison to the levels observed directly after 30 min (Figure 3-8 B, F). In BPH-1 cells a slight repair was observed after 24 h when compared to the initial levels of γH2A.X at 30 min. (Figure 3-8 D).
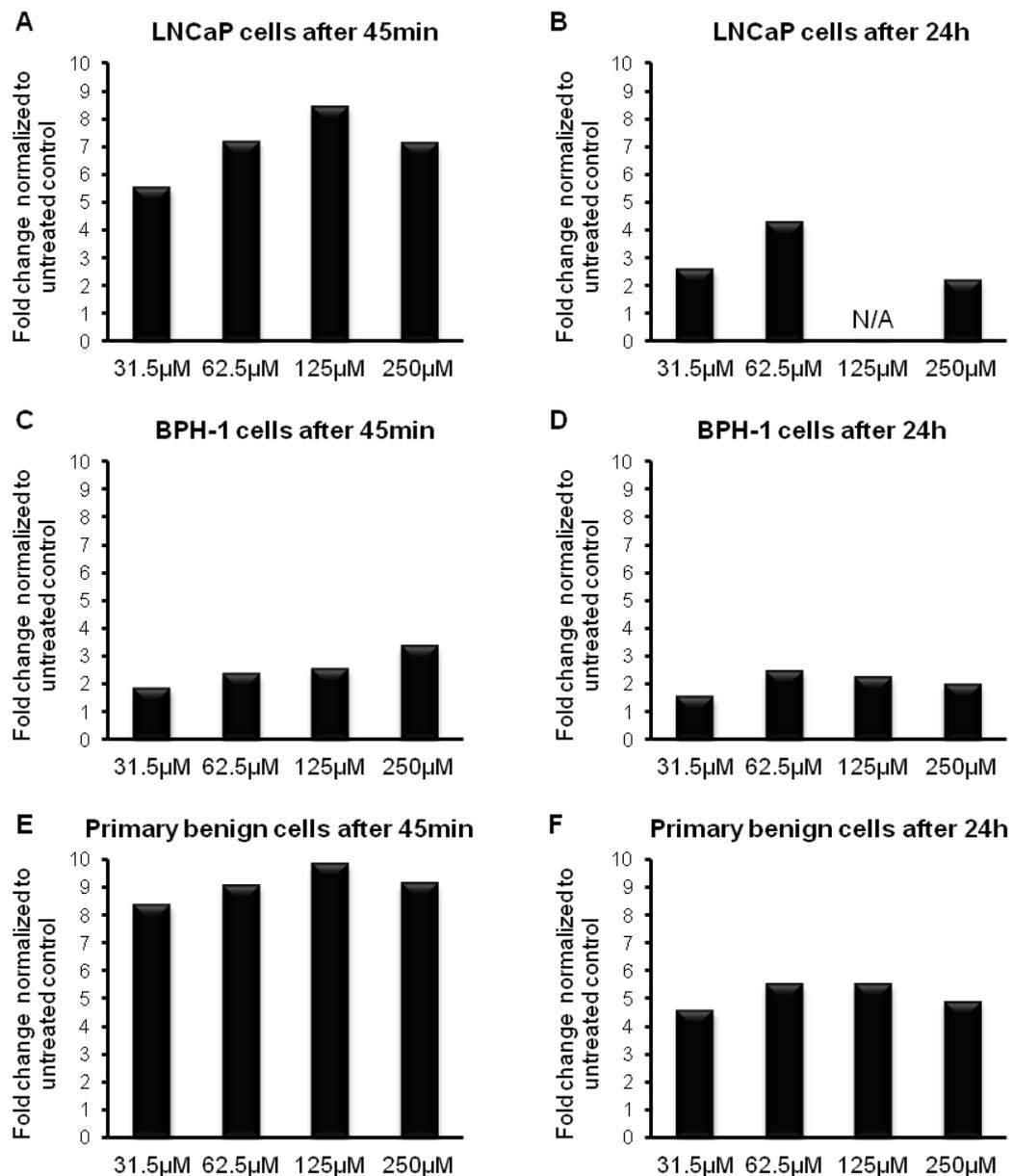
Figure 3-8 Determination of suitability of γH2A.X staining to assess etoposide induced DNA damage in cell lines and primary cells. (A, B) Unselected LNCaP cells, (C, D) unselected BPH-1 cells and (E, F) unselected primary cells (Y023/09) were plated on collagen I-coated 8-well chamber slides. (A, C, E) Cells were treated with the indicated concentrations of etoposide for 30 min, fixed, permeabilized and stained with a γH2A.X antibody. (B, D, F) The drug-containing media was replaced by normal media after 45 min and cells were kept for 24 h at 37°C to assess repair. The value for the concentration 125 μM in (B) is not applicable, likely due to a mistake during the preparation. At least 50 cells, but usually more than 100 were counted by immunofluorescence microscopy depending on their availability and the percentage of γH2A.X positive cells was determined.

3.1.2.2 Qualitative differences of γH2A.X positive cells in primary cells

When examining γH2A.X up-regulation in malignant and benign primary cells by immunofluorescence microscopy, qualitative differences regarding the γH2A.X pattern were observed. Mainly, γH2A.X positive cells with "classical" punctate foci and others with a diffuse staining throughout the nucleus (pan-nuclear staining). These two different types were further divided resulting in five different phenotypes (Figure 3-9 and 3-10):

➢ Punctate foci were divided into the types **"5-10 foci"** and **">10 foci"**

➢ The pan-nuclear γH2A.X distribution came with different intensities and was therefore divided into: **"pan-nuclear light" (PL)**, **"pan-nuclear intermediate" (PI)** and **"pan-nuclear strong" (PS)**.

This classification served later for a more detailed investigation of selected primary cells.
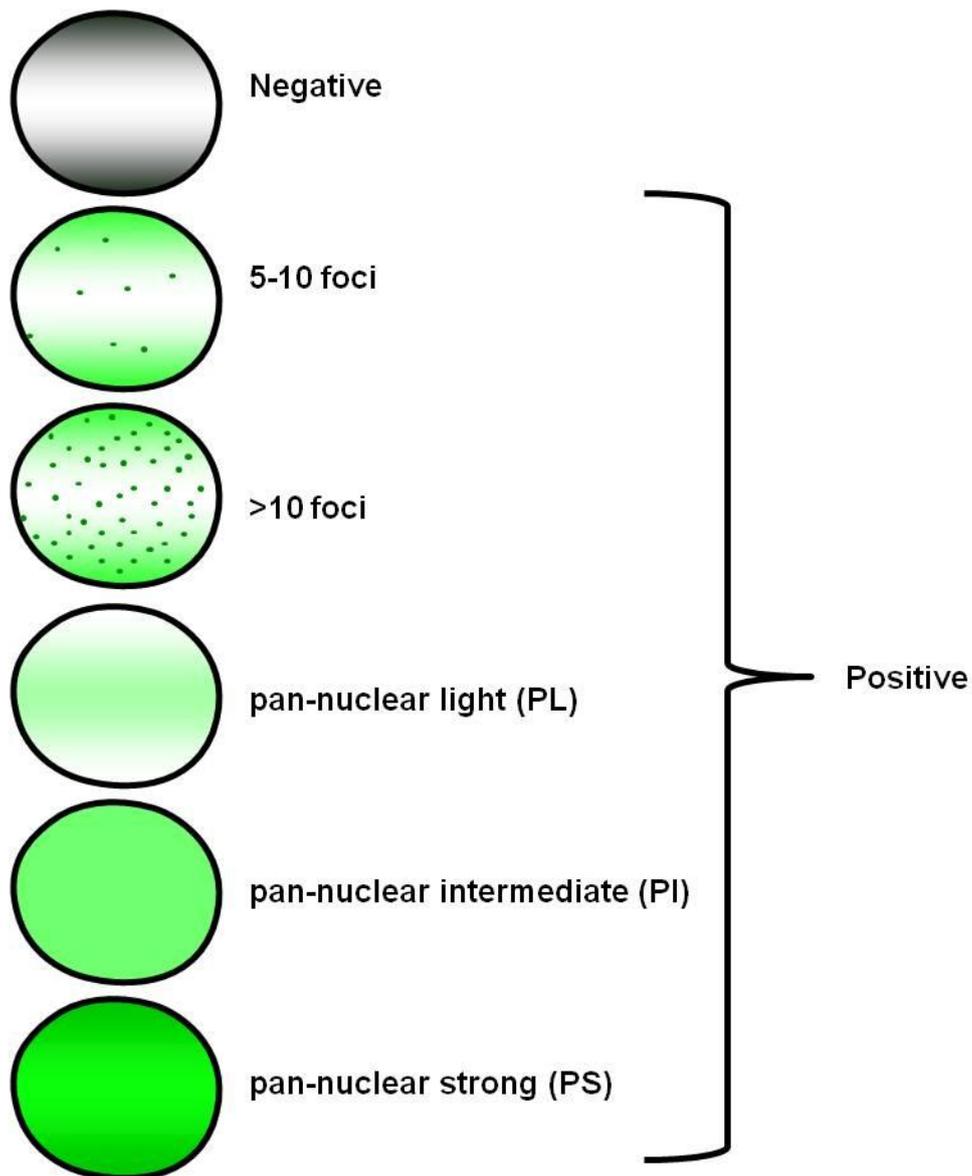
Figure 3-9 Schematic presentation of different γH2A.X phenotypes identified by immunofluorescence microscopy. Five different phenotypes of γH2A.X positive nuclei were found in malignant and benign primary prostate cells.

A

pan-nuclear strong (PS)

negative

pan-nuclear intermediate (PI)

B

negative

> 10 foci

C

5-10 foci

D

pan-nuclear intermediate (PI)

pan-nuclear light (PL)
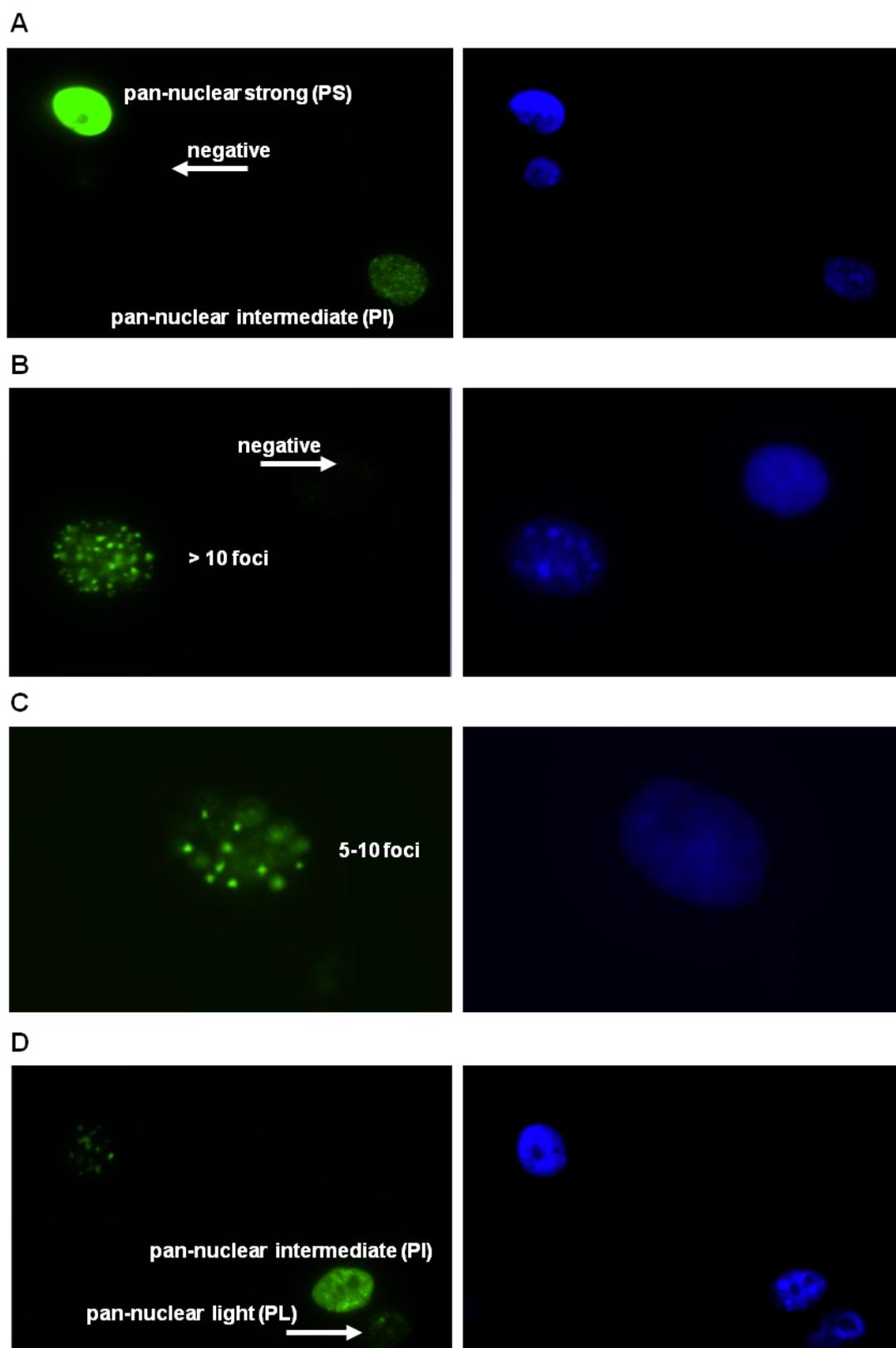
Figure 3-10 Different γH2A.X phenotypes in primary prostate cells identified by immunofluorescence microscopy. Primary prostate cells were plated on collagen I-coated 8-well chamber slides, fixed and permeabilized. Cells were stained with an antibody against γH2A.X (A, B, C, D; images on the left) and with DAPI (A, B, C, D; images on the right). Note that the PL signal appears significantly more intense through the eyepiece and intensity decreases when images are transferred for printing.

3.1.2.3 Quantification of γH2A.X positive cells in selected primary malignant and benign populations following etoposide treatment

Selected malignant and benign primary cells were incubated with etoposide for 45 min and stained for γH2A.X (Figure 3–11 and 3–12). The percentage of γH2A.X positive cells increased after treatment, which is presented as a fold change (Figure 3–11 A and 3–12 A). However, when comparing the median DNA damage levels of the two groups malignant SCs sustained significantly less damage in comparison to their corresponding TAs (p= 0.032), (Figure 3–11 A). When applying etoposide to SCs and TAs of benign origin, an increased γH2A.X expression was found in both populations. Benign-derived SCs also sustained less DNA damage than TAs, even though the difference was not statistically significant (Figure 3–12 A).

A second set of selected malignant and benign cells was subjected to etoposide for 45 min, replenished with normal media and left for 24 h at 37°C to allow repair (Figure 3–11 B and 3–12 B). In benign SCs and TAs a significant repair was observed when compared to the initial γH2A.X levels at 45 min (SCs 45 min vs. SCs 24 h: p=0.047; TAs 45 min vs. TAs 24 h: p=0.047; compare Figure 3–12 A to 3–12 B). However, it is difficult to compare the repair efficiencies of the two populations, as they sustained different amounts of DNA damage at 45 min. For SCs and TAs from malignant tissues no significant differences were revealed. In this case this is very likely due to the low number of malignant samples available for the statistical analysis (n=3). The assessments performed for Figures 3–11 and 3–12 take all of the five different types of γH2A.X phenotypes into account.

A

B
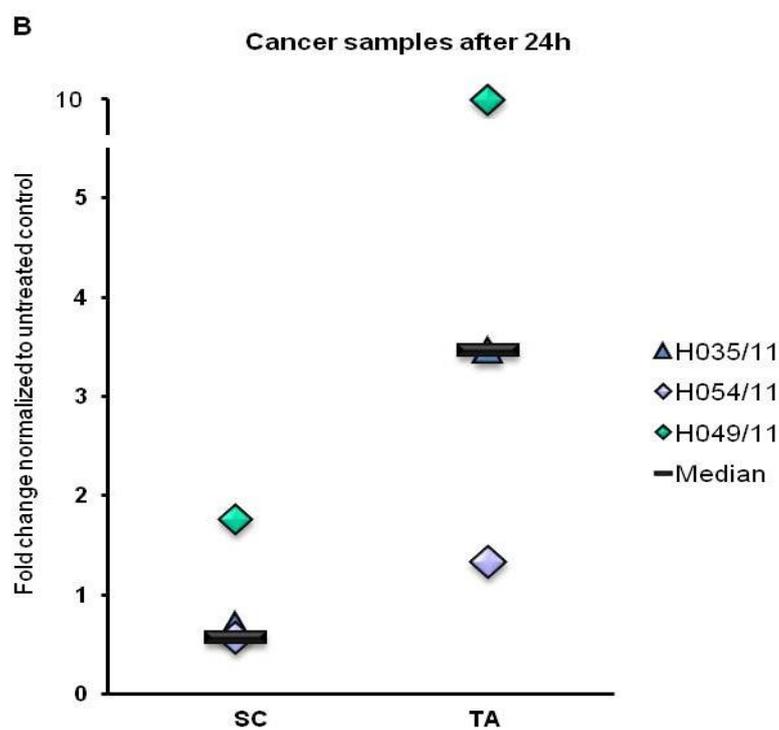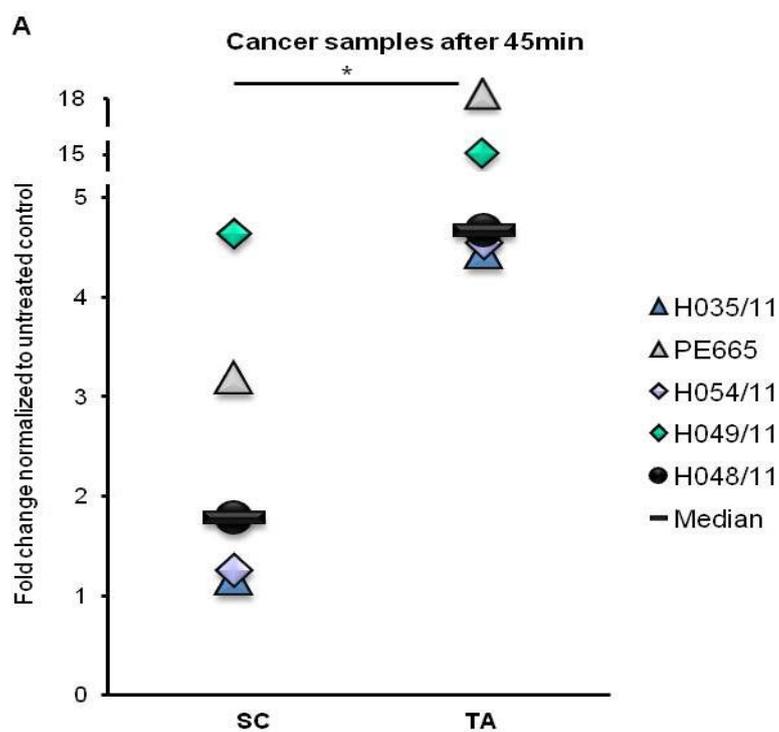
Figure 3-11 SCs from malignant tissues are more resistant to etoposide treatment than their corresponding TAs. (A) SCs and TAs were selected from cultures grown from malignant primary tissues and plated on collagen I-coated 8-well chamber slides. Cells were treated with 30 µM etoposide for 45 min, fixed, permeabilized and stained for γH2A.X. (B) The drug-containing media was removed after 45 min, replaced by normal media and cells were kept for 24 h at 37°C to allow repair. The evaluation includes all different types of γH2A.X positive cells as explained in Figures 3-9 and 3-10. Each symbol represents one patient. At least 50 cells, but usually more than 100 were counted by immunofluorescence microscopy depending on their availability and the percentage of γH2A.X positive cells was determined. Wilcoxon rank sum test: TA vs. SC 45 min: p= 0.032. Non-significant p-values are listed in the appendix.

A

Benign samples after 45min

B

Benign samples after 24h
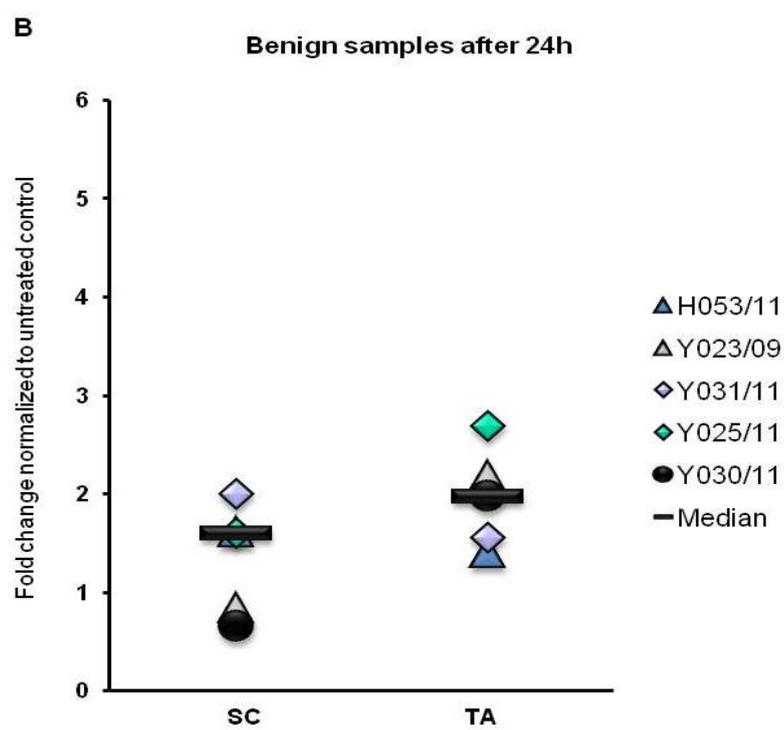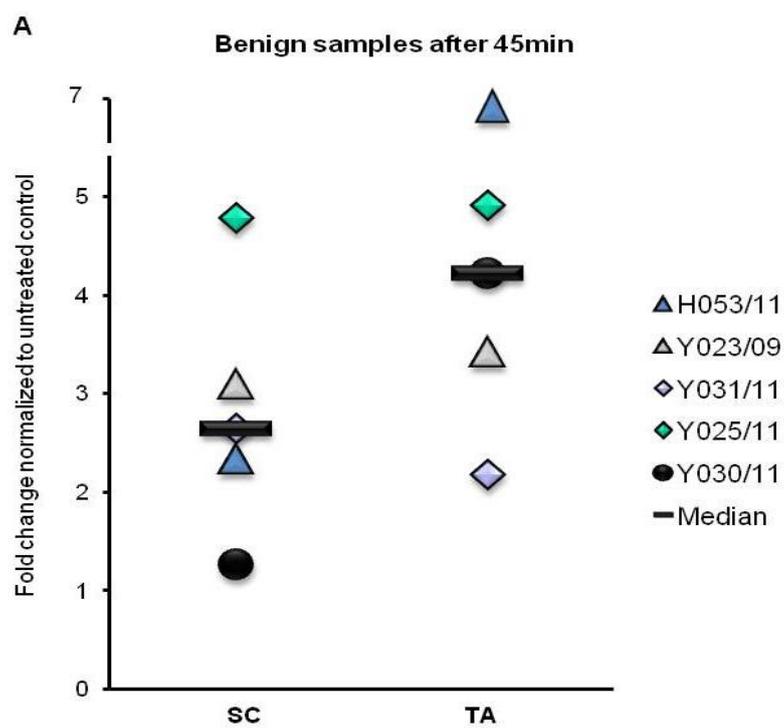
Figure 3–12 SCs from benign tissues are more resistant to etoposide treatment than their corresponding TAs. (A) SCs and TAs were selected from cultures grown from benign primary tissues and plated on collagen I–coated 8–well chamber slides. Cells were treated with 30 µM etoposide for 45 min, fixed, permeabilized and stained for γH2A.X. (B) The drug–containing media was removed after 45 min, replaced by normal media and cells were kept for 24 h at 37°C to allow repair. The evaluation includes all different types of γH2A.X positive cells as explained in Figures 3–9 and 3–10. Each symbol represents one patient. At least 50 cells, but usually more than 100 were counted by immunofluorescence microscopy depending on their availability and the percentage of γH2A.X positive cells was determined. The non–significant p–values are listed in the appendix.

3.1.2.4 Qualitative differences of γH2A.X in selected primary populations following etoposide treatment

To assess the frequency of the different γH2A.X phenotypes (as summarized in Figures 3-11 and 3-12), the patterns 5-10 foci, >10 foci, PL, PI and PS were quantified for each selected population (Figure 3-13). The different types of γH2A.X patterns were seen to increase after 45 min of treatment in all malignant populations (Figure 3-13 A), with SCs being affected less than TAs. The types >10 foci and PL were found to be particularly up-regulated when comparing malignant SCs to TAs. The phenotype >10 foci was significantly elevated in TAs when compared to SCs (p=0.032). After 24 h the number of γH2A.X positive cells dropped for most phenotypes in SCs and TAs, but increased for PL and PI in the TA population (Figure 3-13 B).

In benign samples the different γH2A.X phenotypes were found mostly at similar levels for TA and SCs, but the phenotype >10 foci was more strongly expressed in TAs (Figure 3-13 C). After 24 h, several γH2A.X phenotypes were present in comparable quantities in both benign SCs and TAs, but SCs had a higher fold-change of >5-10 foci and TAs in PI.

In conclusion, malignant and benign SCs and TAs both responded to etoposide exposure by increased DNA damage, with SCs being less susceptible than TAs. 24 h of repair diminished mostly the higher DNA damage in benign and malignant TAs, except for the patterns PL and PI in malignant TAs. Less is known about the meaning of different γH2A.X phenotypes, but the lower γH2A.X levels found in SCs after an initial dose of etoposide might be correlated with their resistance phenotype.
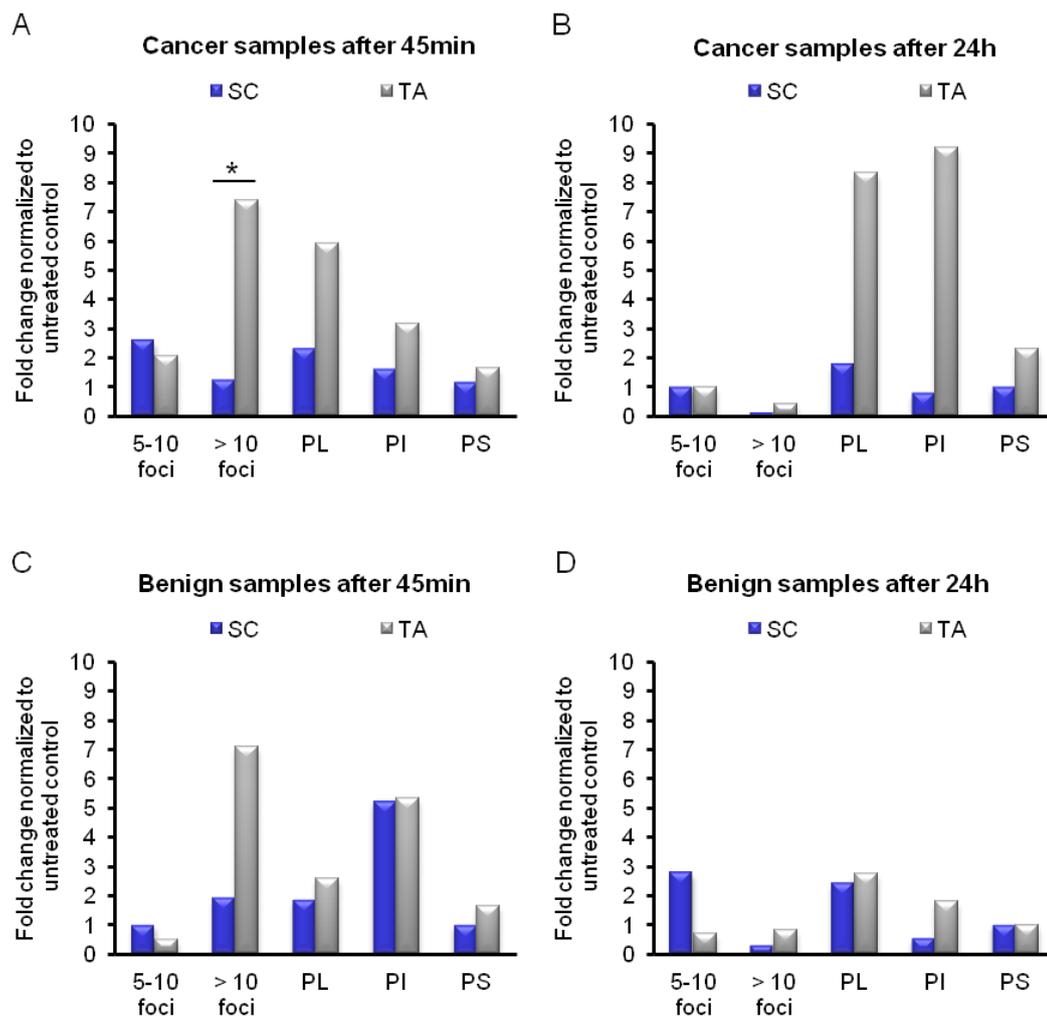
Figure 3-13 Quantification of the different γH2A.X patterns in SCs and TAs from malignant and benign primary samples. (A, C) Primary cells from malignant and benign samples were selected and plated on collagen I-coated 8-well chamber slides. Cells were treated with 30 µM etoposide for 45 min, fixed, permeabilized and stained for γH2A.X. (B, D) The drug-containing media was replaced by normal media after 45 min and cells were left for 24 h at 37°C to allow repair. At least 50 cells, but usually more than 100 were counted by immunofluorescence microscopy depending on their availability and the percentage of the different phenotypes of γH2A.X positive cells was determined. Bars represent median values of fold change of the different patient groups as shown in Figures 3-11 and 3-12. Wilcoxon rank sum test for cancer 45 min >10 foci SC vs. TA: p= 0.032. Non-significant p-values and the determination of the median fold changes are listed in the appendix.

3.1.2.5 Detection of γH2A.X after excess thymidine treatment

The DNA damage marker γH2A.X has been shown to respond to DSBs, but also to SSBs [166, 276, 277]. To assess whether this is the case in prostate primary cells we assessed γH2A.X expression in selected populations after 72 h treatment with excess thymidine. Excess thymidine is a trigger of replications stress that results in the formation of SSBs, but not DSBs. The cells increased γH2A.X expression which indicated that γH2A.X responds to SSBs in prostate primary cells (Figure 3–14).
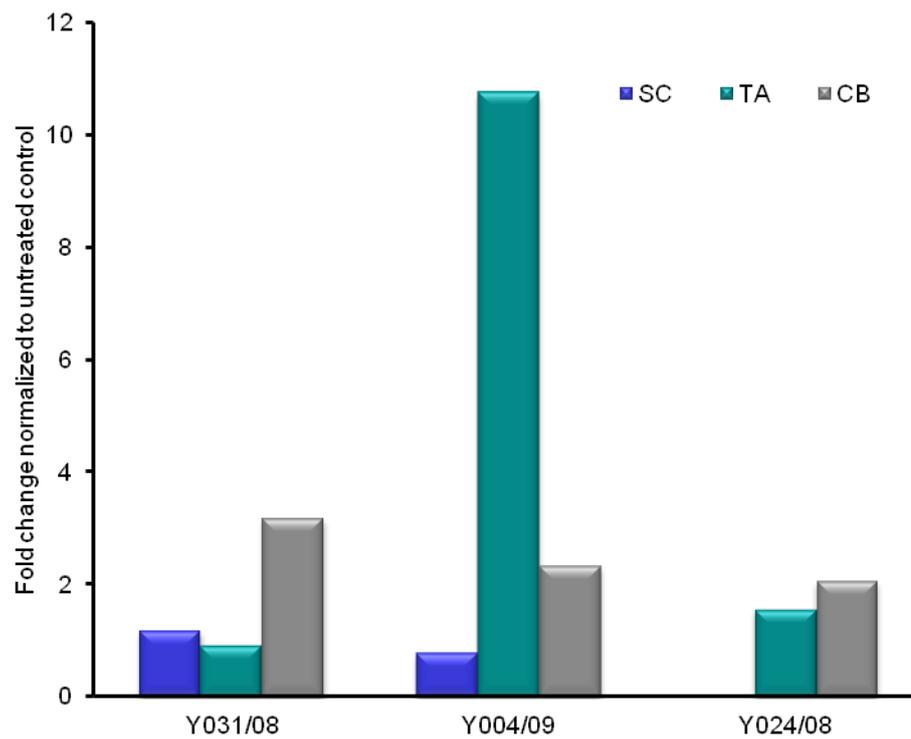
Figure 3-14 γH2A.X detects SSBs in primary prostate cells. Benign SCs, TAs and CBs were isolated from primary cultures, plated on collagen I-coated 8-well chamber slides and incubated for 72 h with 2 mM thymidine. Cells were fixed, permeabilized and stained for γH2A.X. At least 50 cells, but usually more than 100 were counted by immunofluorescence microscopy depending on their availability and the percentage of the different types of γH2A.X positive cells was determined.

3.2 Clonogenic recovery assays to determine the susceptibility of prostate epithelial cell populations to etoposide treatment

3.2.1 Optimization of the experimental set up for clonogenic recovery assays

Clonogenic recovery assays are an important method to investigate the drug resistance potential of cells. We seeded SCs and TAs originating from malignant and benign prostate tissues and assessed the influence of etoposide on their colony forming efficiency, which is defined *as number of colonies/cells plated÷100.* Reduction of colony forming efficiency by etoposide treatment indicates susceptibility to the drug. Colonies were classified into 2+, 4+, 8+, 16+ and 32+ cells, which equals 1, 2, 3, 4 and 5 population doublings, respectively. Example images for a clonogenic assay performed with primary prostate cells are shown in Figure 3–15. First, unselected primary cells were plated and treated with DMSO (vehicle) or 30 μM or 250 μM etoposide for 45 min and 3 h (Figure 3–16 A). Only at the combination 30 μM for 45 min did the cells form colonies, whereas all other combinations were found to be too aggressive and prevented the cells from any colony formation (0% colonies), (Figure 3–16 A). Hence, we decided to proceed with the concentration 30 μM etoposide for 45 min, as (i) we were able to find colonies at this concentration and (ii) the treatment conditions matched the treatment conditions used in the γH2A.X and comet assays, which enabled a better correlation of the results revealed from these different assays. To determine the appropriate time points for analyzing the number of colonies, the first two clonogenic recovery assays on selected populations were assessed at different time points (Figure 3–16 B and C). At day 4 (Figure 3–16 B) and day 3 (Figure 3–16 C) only a low number of colonies grew in the DMSO treated cells and the biggest colony size 32+ was only present in moderate quantities (as seen in 3–16 B). However, after

8 days (Figure 3–16 B) and 6 days (Figure 3–16 C) we found an increased colony number and increased colony sizes in SCs and TAs from both samples. Based on this assessment we decided that clonogenic recovery assays should be grown at least for one week prior to their assessment. However, the optimal time frame for growing a clonogenic recovery assay was later found to be strongly patient specific and in some cases longer times (up to 16 days) were required.
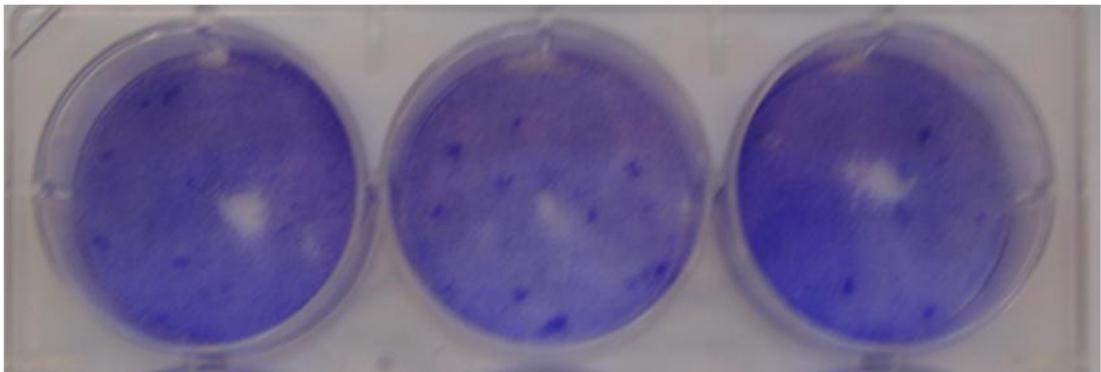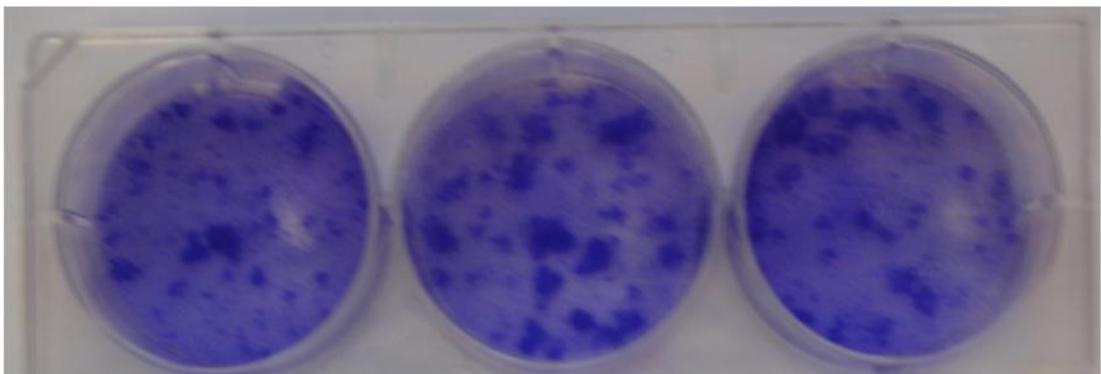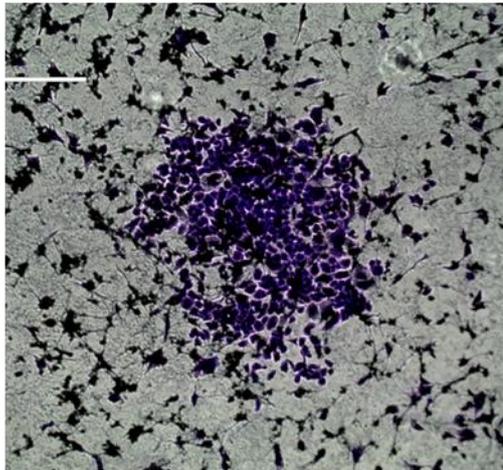
Figure 3-15 Examples for colonies observed in clonogenic recovery assays. (A) A crystal violet stained 32+ colony. (B) Crystal violet stained cells of a clonogenic recovery assay treated with DMSO (upper panel) or etoposide (lower panel).
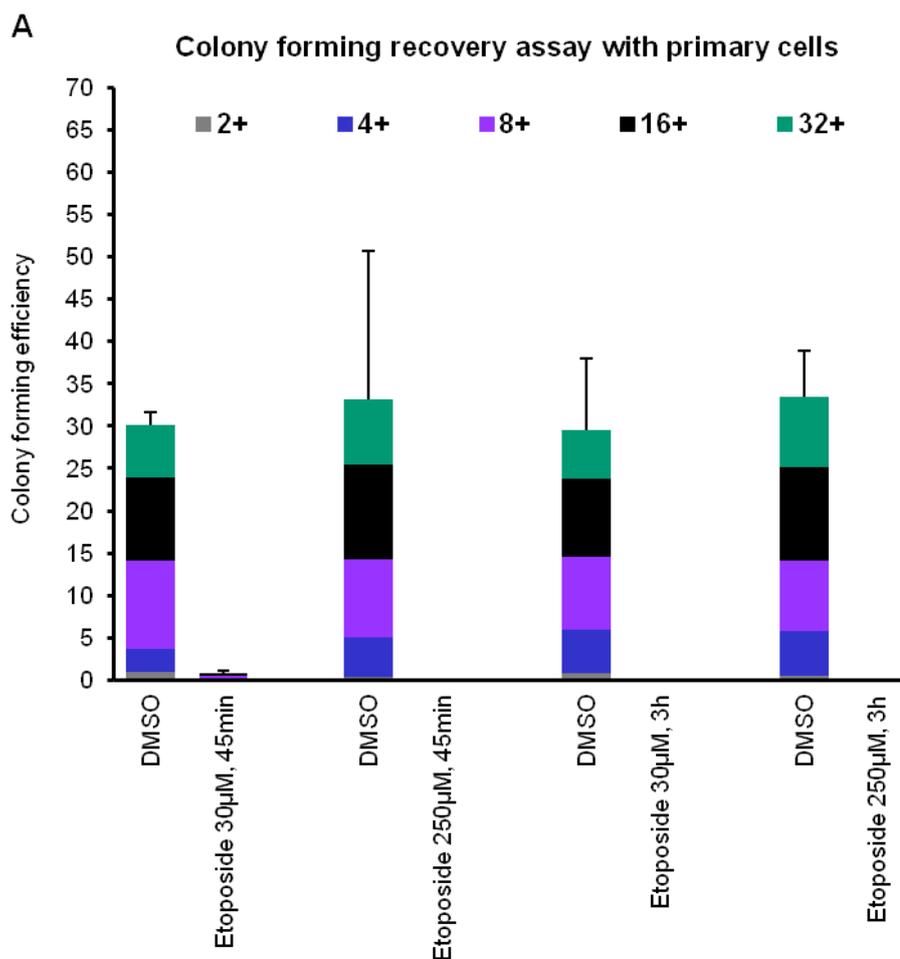
Figure 3-16 Suitability of clonogenic recovery assay to assess susceptibility of primary prostate cells to etoposide treatment. (A) Unselected benign primary cells (Y030/11) were seeded as triplicates on collagen I-coated 6-well plates with irradiated feeder cells. Cells were treated with etoposide for the indicated times and concentrations or with the appropriate dilution of DMSO and kept at 37°C. After one week different colony sizes (2+, 4+, 8+, 16+, 32+) were assessed. (B, C) Malignant primary cells (H035/11, PE531) were selected and seeded as triplicates on collagen I-coated 6-well plates with irradiated feeder cells. Cells were treated with 30 µM etoposide for 45 min or the appropriate dilution of DMSO and kept at 37°C. The different colony sizes (2+, 4+, 8+, 16+, 32+) were assessed after the indicated days. The colony forming efficiency was calculated by the formula *number of colonies/cells plated÷100.* Note that the error bars refer to the total number of colonies observed. Error bars for specific colony sizes are listed in the appendix.

B

Clonogenic recovery assay with primary cells

C

Clonogenic recovery assay with primary cells
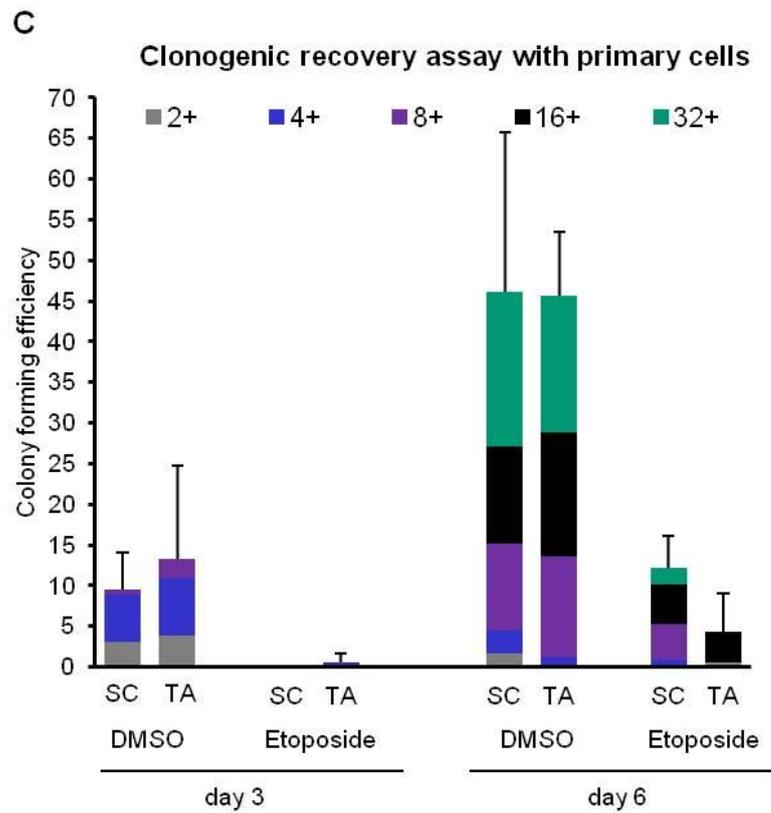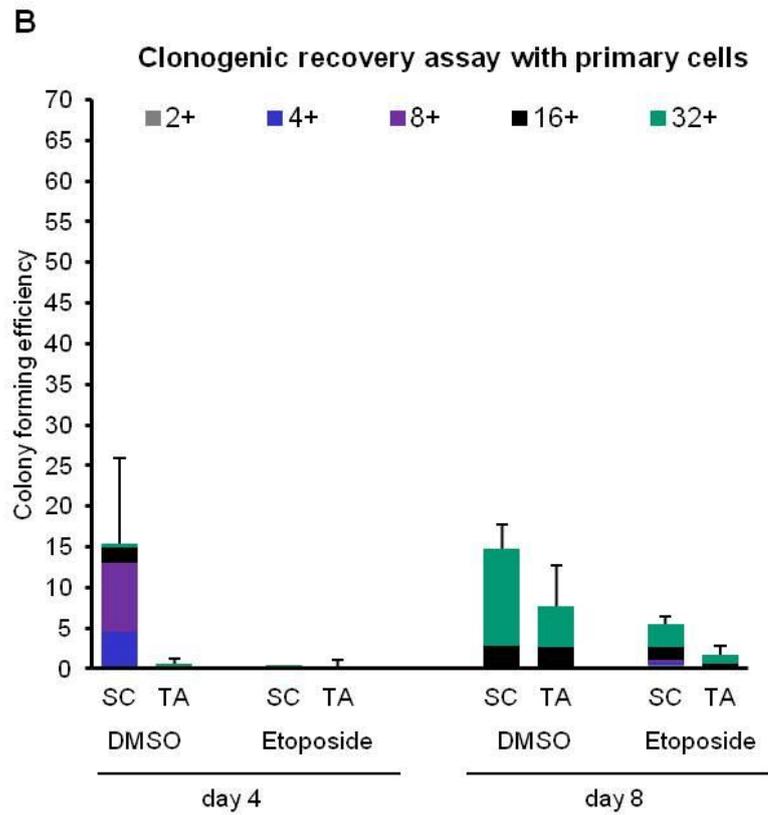
3.2.2 Comparison of the clonogenic recovery in SCs and TAs

A series of clonogenic recovery assays were conducted with SCs and TAs from malignant (n=7, Y062/11 = CRPC) and benign origin (n=2) to compare their therapy resistance potential (Figure 3–17 A and B). In the majority of cancer samples SCs showed a higher clonogenic recovery (except for H049/11). We found that benign samples usually failed to form any colonies (also when not treated with etoposide) and only Y031/11 and Y030/11 produced colonies. TAs from the sample Y031/11 showed a higher clonogenic recovery, whereas for Y030/11 SCs were more resistant. The bars as shown in Figure 3–17 A represent the entire five colony sizes observed in summary. A detailed analysis of the colony sizes is shown in Figure 3–17 B. The colony sizes 8+ and 16+ were found frequently and we assume that these would have developed into 32+ colonies, if allowed more time to continue. However, not all colonies grew with the same pace and faster growing ones would have started to merge and overgrow the plate. For this reason the clonogenic recovery assays had to be evaluated usually after 1–2 weeks. Please note that the risk of colonies merging can't be excluded for the samples YO30/11 and YO31/11 due to an enhanced growth in the DMSO control wells. In one case SCs and TAs from a malignant sample (H035/11) were treated with 30 µM and left for 3 h (Figure 3–17 C). TAs did not form any colonies under this condition, but a small number of SCs survived and formed colonies in the sizes 32+ and 16+. In conclusion, the clonogenic recovery assays revealed that in particular malignant SCs recovered better from etoposide treatment than malignant TAs, which might be another hint for their role in therapy resistance in prostate cancer.

A

Figure 3-17 Malignant SCs have a higher clonogenic recovery after etoposide treatment than TAs. Malignant and benign primary cells were selected and seeded as triplicates on collagen I-coated 6-well plates with irradiated feeder cells. Cells were treated with 30 μM etoposide for 45 min or the appropriate dilution of DMSO and kept at 37°C. (A) Summary of all colony sizes observed. (B) Detailed presentation of different colony sizes (2+, 4+, 8+, 16+, 32+) as shown in (A). (C) Selected cells of H035/11 were treated with 30 μM etoposide for 3 h. The percentage of the colonies grown was calculated by the formula *number of colonies/cells plated÷100*. Note that the error bars refer to the total number of colonies observed. Error bars for each specific colony size are listed in the appendix.

B

Colony sizes in clonogenic recovery assays with primary cells

■2+ ■4+ ■8+ ■16+ ■32+

C

Colony sizes in clonogenic recovery assays after 3h etoposide

■2+ ■4+ ■8+ ■16+ ■32+

3.3 Examination of the cell cycle status in primary prostate cells using Ki67

Since the cell cycle status plays a critical role in mediating therapy-resistance, selected primary cells originating from malignant and benign samples were selected and assessed for Ki67 expression. Ki67 is a nuclear protein strictly associated with proliferating cells [278]. It is present in all active stages of the cell cycle (G1, S, G2, and mitosis), but is absent from quiescent cells (G0) [278]. We investigated the presence of Ki67 by immunofluorescence microscopy (Figure 3-18 A and B). A significantly lower percentage of SCs from malignant tissues was found to be cycling (Ki67 positive) in comparison to malignant TAs (p=0.016) and CBs (p=0.008) (Figure 3-19 A). The assessment of selected benign samples revealed a similar trend (Figure 3-19 B). Benign SCs proliferated less in comparison to benign TAs and CBs. These data suggest that the cell cycle might play a role in the therapy-resistance of SCs derived from malignant prostate tissues.
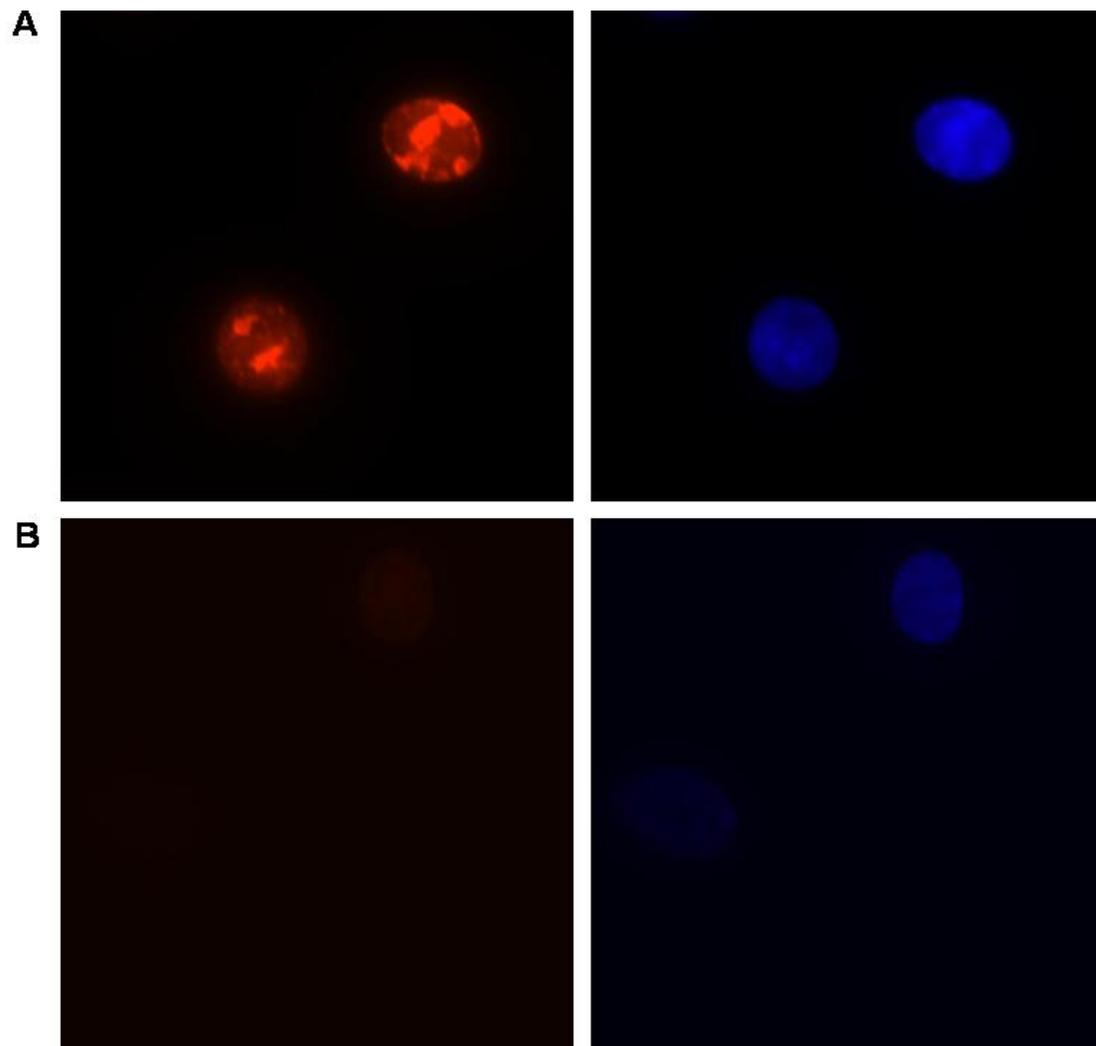
Figure 3-18 Example images for Ki67 staining in primary cells. Primary prostate cells were seeded on collagen I-coated 6-well plates, fixed, permeabilzed and stained for Ki67 and assessed by immunofluorescence microscopy. (A) Cells positive for Ki67 (left) and corresponding DAPI (right). (B) Cells negative for Ki67 (left) and corresponding DAPI (right).

A

B
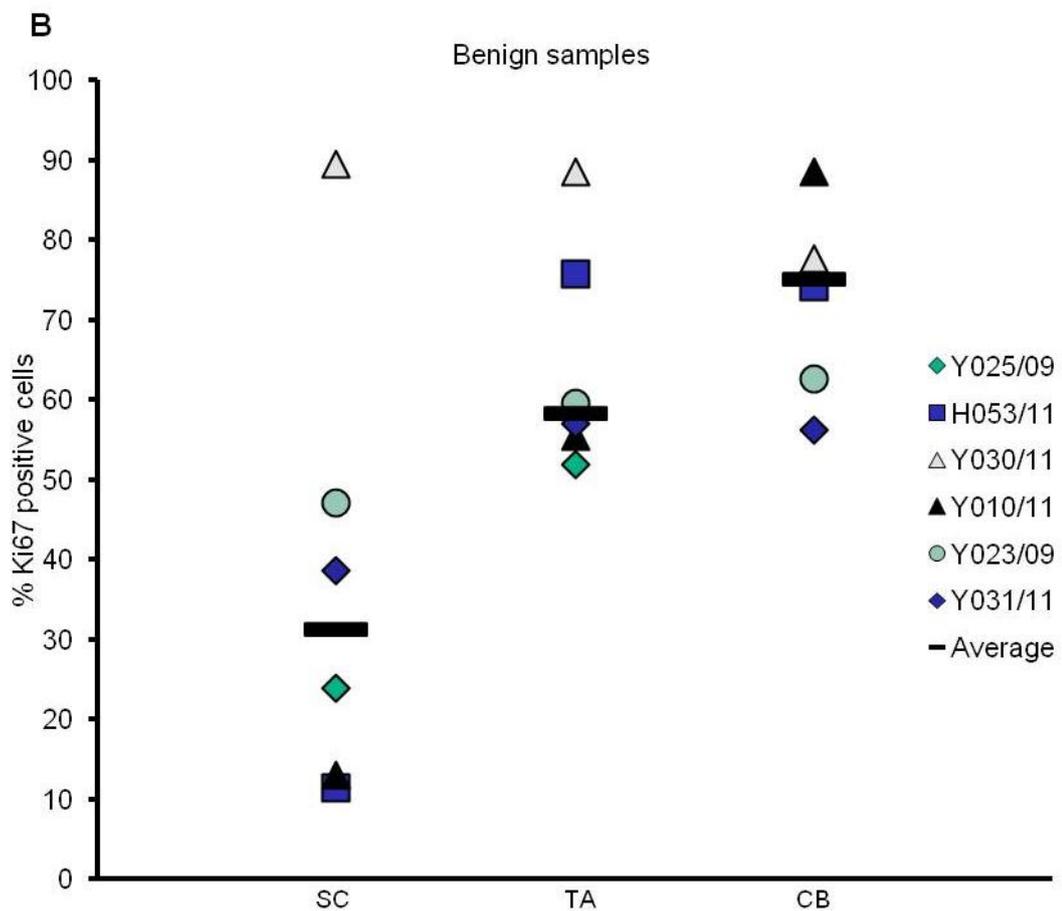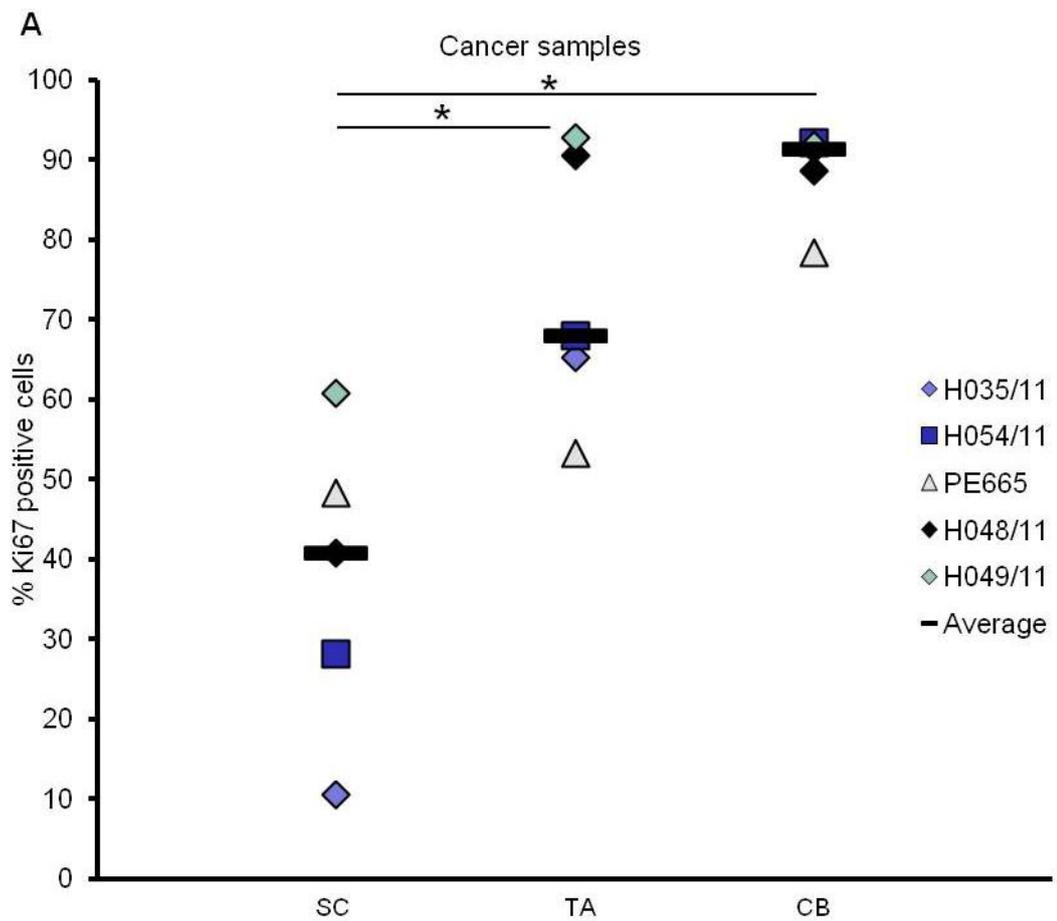
Figure 3-19 A lower percentage of SCs of malignant and benign primary prostate samples is in cell cycle in comparison to TAs and CBs. (A) Primary malignant and (B) benign prostate cells were selected and plated on collagen I-coated 8-well chamber slides. Cells were fixed and stained with an antibody against Ki67. At least 50 cells, but usually more than 100 were counted by immunofluorescence microscopy depending on their availability and the percentage of Ki67 positive cells was determined. One exception was made for SCs derived from cancer sample H048/11: a number of 32 cells had to be analysed. Wilcoxon rank sum test cancer samples SC vs. TA: p= 0.016; SC vs. CB: p= 0.008. Non-significant p-values are listed in the appendix.

3.4 Assessment of cell death in primary cells

One of the main obstacles in cancer therapy is resistance to apoptosis. In respect to prostate cancer cells our previous findings revealed that primary prostate cells reduced their colony forming efficiency through etoposide treatment (even if in TAs this effect was stronger than in SCs). This observation might have been a consequence of cell death through apoptosis. Alternatively, the cells could have remained viable, but suffered a loss of their colony forming potential. To address these questions further, we applied MTS assays to assess cell viability and apoptotic assays with an activated caspase in situ marker. Additionally, autophagy was tested as an alternative treatment response.

3.4.1 Viability assays to assess the effect of anti-cancer drugs on unselected primary cells

MTS assays on unselected primary prostate cells (PE665) served to elucidate the cell viability (Figure 3-20 A-F). The viability of cells decreased after 72 h incubation with the anti-cancer drugs etoposide (B), docetaxel (C), carboplatin (D), camptothecin (E) and doxorubicin (F).

A DMSO

B Etoposide

C Carboplatin

D Camptothecin

E Docetaxel

F Doxorubicin
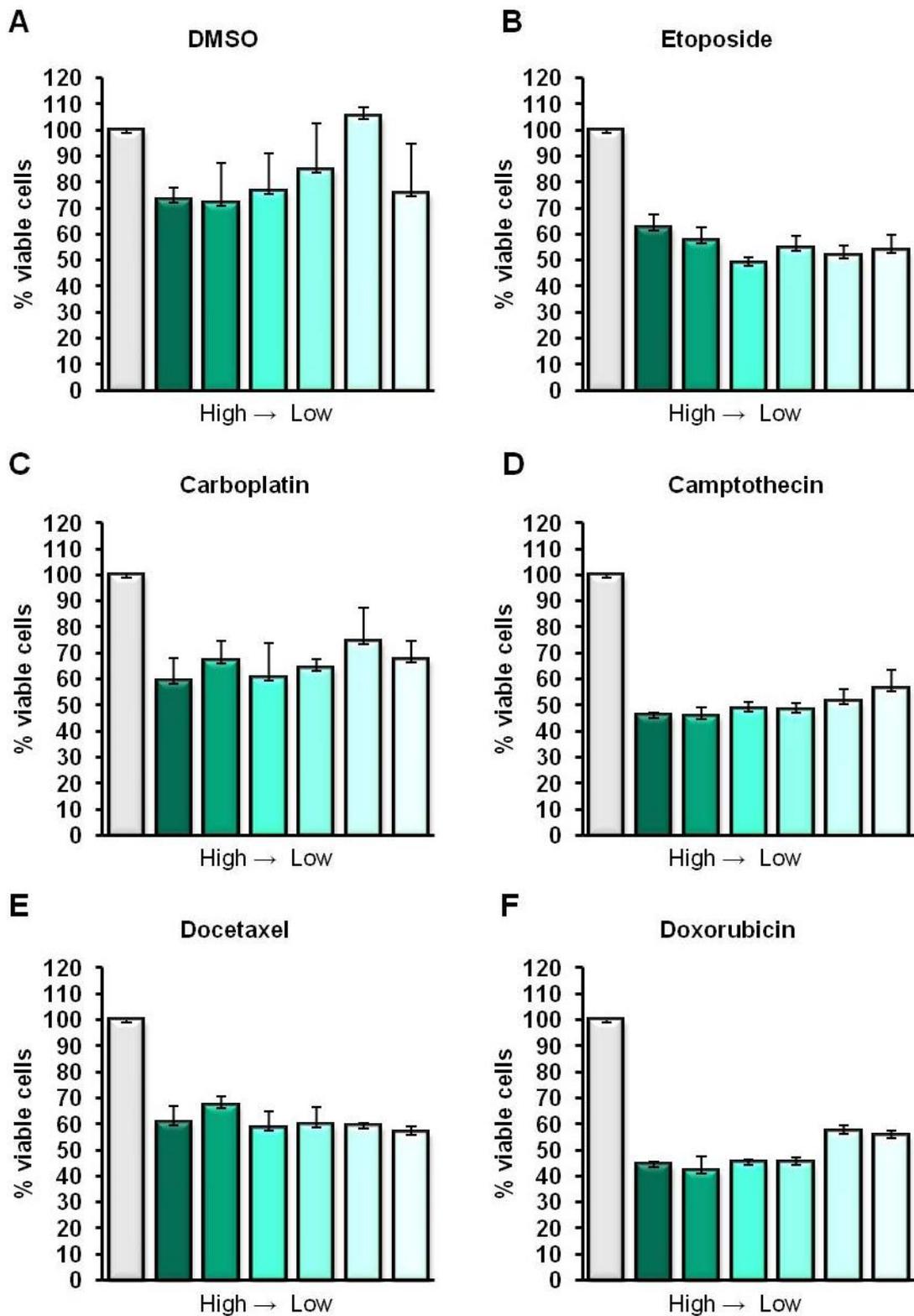
Figure 3-20 Unselected malignant primary cells reduce viability after treatment with anti-cancer drugs. Unselected malignant primary cells (PE665) were plated on collagen I-coated 96-well plates, incubated with different concentrations of etoposide, docetaxel, carboplatin, camptothecin and doxorubicin and left for 72 h at 37°C. Viability was assessed using MTS. Concentrations are shown from high to low (left to right) in each graph and listed in numbers in the appendix. The percentage of viable cells was determined by setting the DMSO control (first bar of each graph, grey) to 100% and calculating the values for the treated wells in percentile relation to that. Exception: The grey bar in the DMSO chart (upper panel, left) represents an untreated control.

3.4.2 Detection of active caspases for assessment of apoptosis

The previously described observations in clonogenic recovery assays and MTS assays raised the question of whether cells underwent apoptosis following treatment. For this reason we applied an activated caspase in situ marker for flow cytometry analysis to examine the apoptotic response to etoposide treatment using the described gating strategy (Figure 3-21). Initially, we examined the suitability of the caspase in situ marker as an indicator for apoptosis in the prostate cell lines RC165N/h-TERT and RC92a/h-TERT (Figure 3-22 A-C). The cells were incubated for 12 h, 24 h, 48 h and 72 h with 15 µM, 30 µM, 60 µM and 125 µM etoposide. We detected an increase of active caspases at 48 h and 72 h in a dose responsive manner in both cell lines. To exclude the possibility that etoposide interfered with the FITC-channel (where the caspase in situ marker was measured), cells were incubated with 60 µM etoposide for 48 h and compared to an unstained and untreated population of cells. Etoposide did not interfere with the FITC-channel. When cells were treated with etoposide the activated caspase positive population increased significantly, suggesting an apoptotic mechanism.

However, when the same caspase in situ marker was applied to primary samples, the outcome differed from that observed in cell lines (Figure 3-23). Cells originating from a patient who had failed hormone therapy (H149/11), a patient with a malignant disorder but without hormone therapy (H054/11) and cells from a BPH patient (Y030/11) were incubated with 125 µM etoposide for 24 h, 48 h and 72 h. The detected activated caspase levels for the three different samples were between 15 and 30% for the untreated and treated controls. None of the samples increased caspase activity significantly

at any treatment condition suggesting that apoptosis was blocked in these cells.
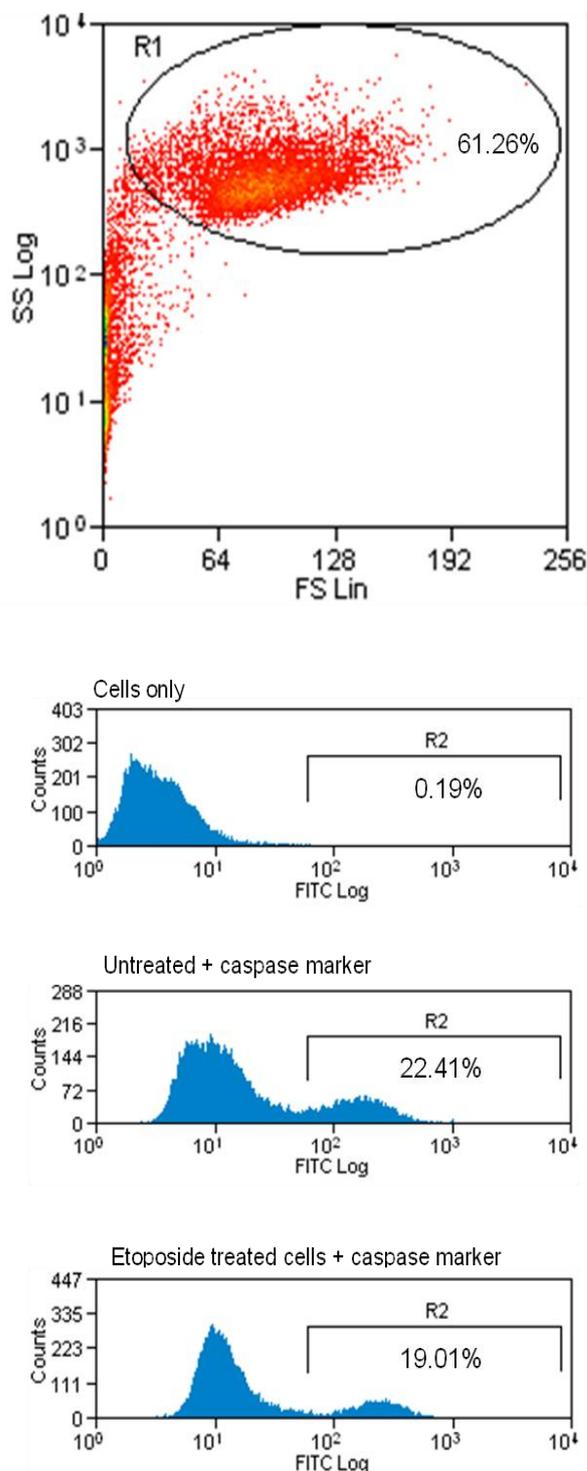
Figure 3–21 Gating strategy to detect apoptotic cells by flow cytometry. Debris was excluded by using the Forward/ Side Scatter. The cells in gate R1 were further analysed for binding to the caspase marker CaspACE™ FITC–VAD–FMK. The unstained control (cells only) was used to set the gates for the untreated and etoposide treated controls. Plots present the gating strategy by showing a primary sample (Y030/11). The same gating strategy was applied for cell lines (not shown). Note that there is no increase of apoptotic cells after 125 μM etoposide treatment, as apoptosis was found not to be activated in primary cells.

A

RC165N/ hTERT

B
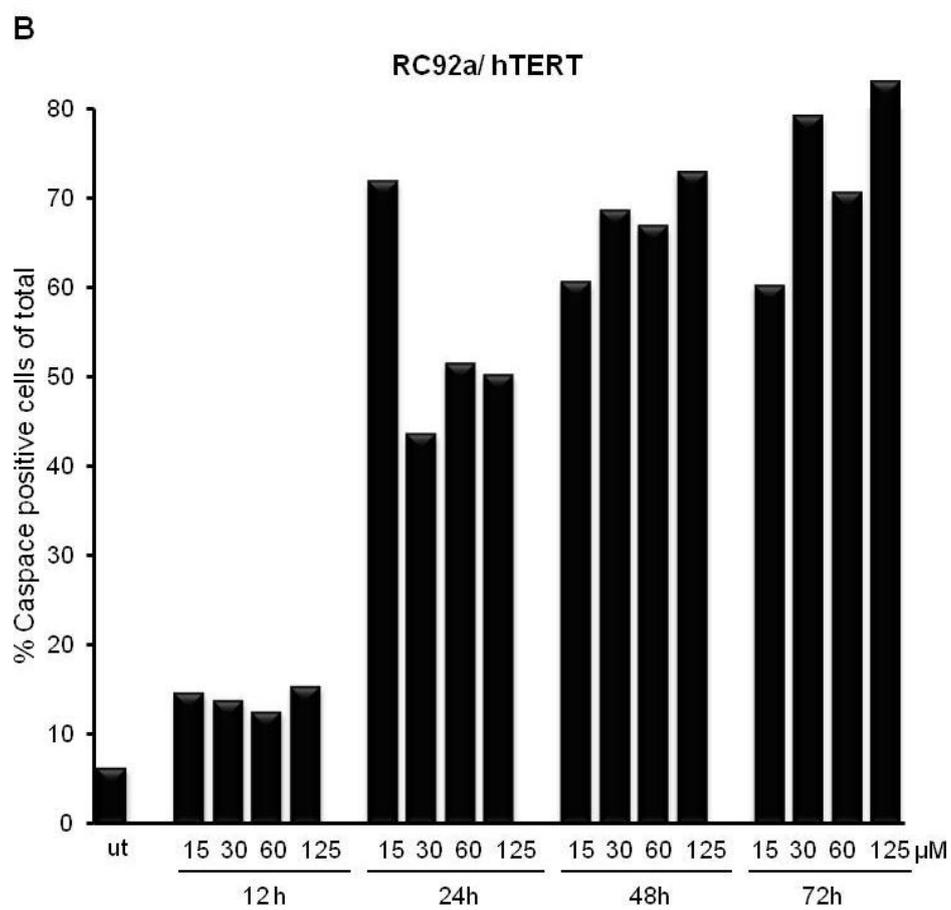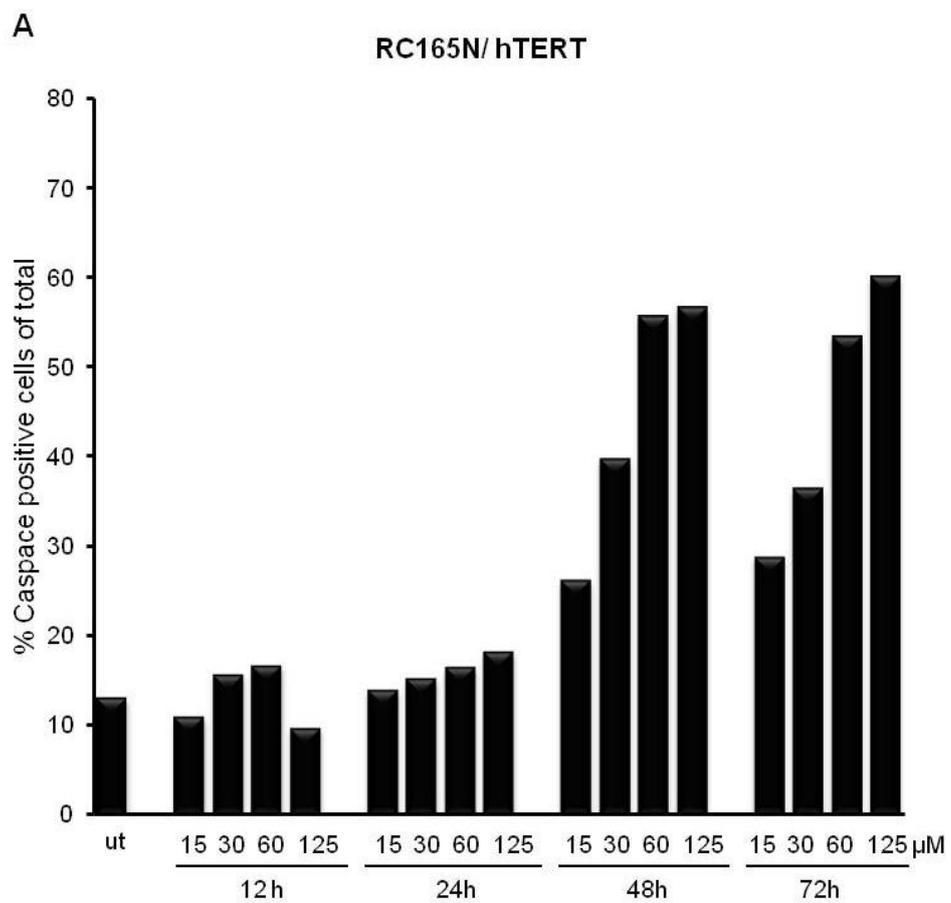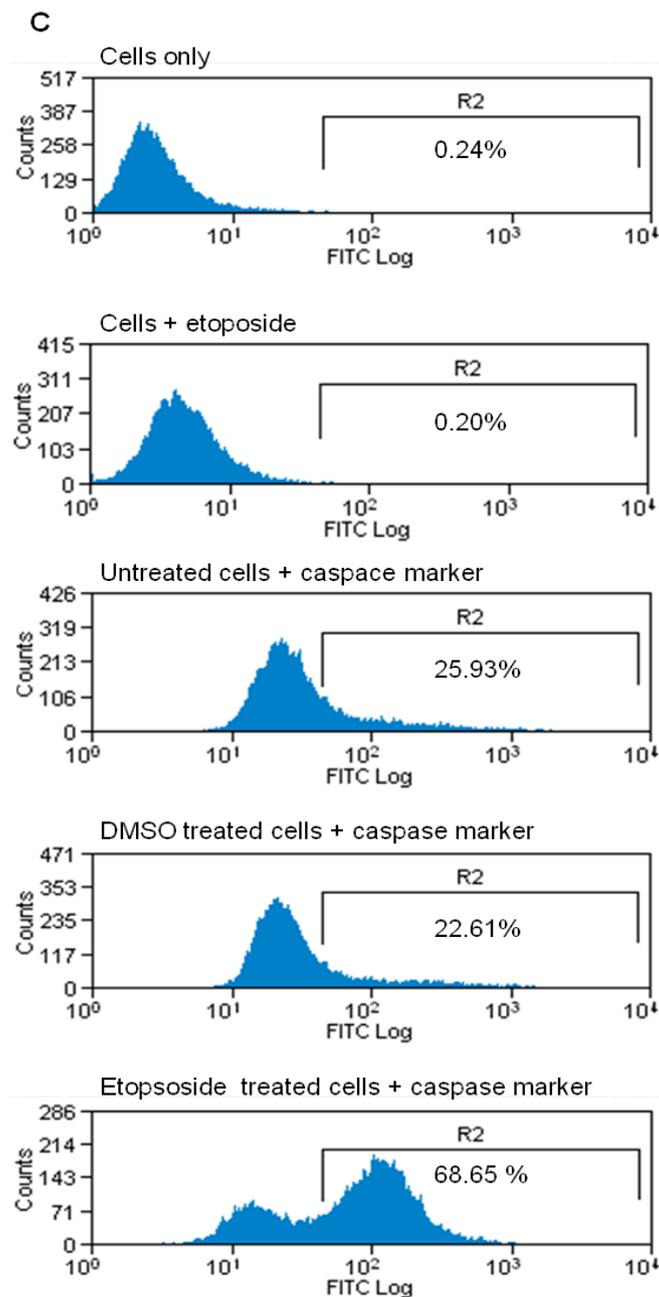
RC92a/ hTERT

Figure 3-22 RC165N/ h-TERT and RC92a/ h-TERT cells undergo apoptosis after exposure to etoposide. (A) RC165N/ h-TERT and (B) RC92a/ h-TERT cells were incubated for the indicated time points and concentrations (µM) with etoposide and kept at 37°C. Cells were stained with the caspase marker CaspACE™ FITC-VAD-FMK for flow cytometry. C demonstrates the relevant controls using the example of RC92a/h-TERT.
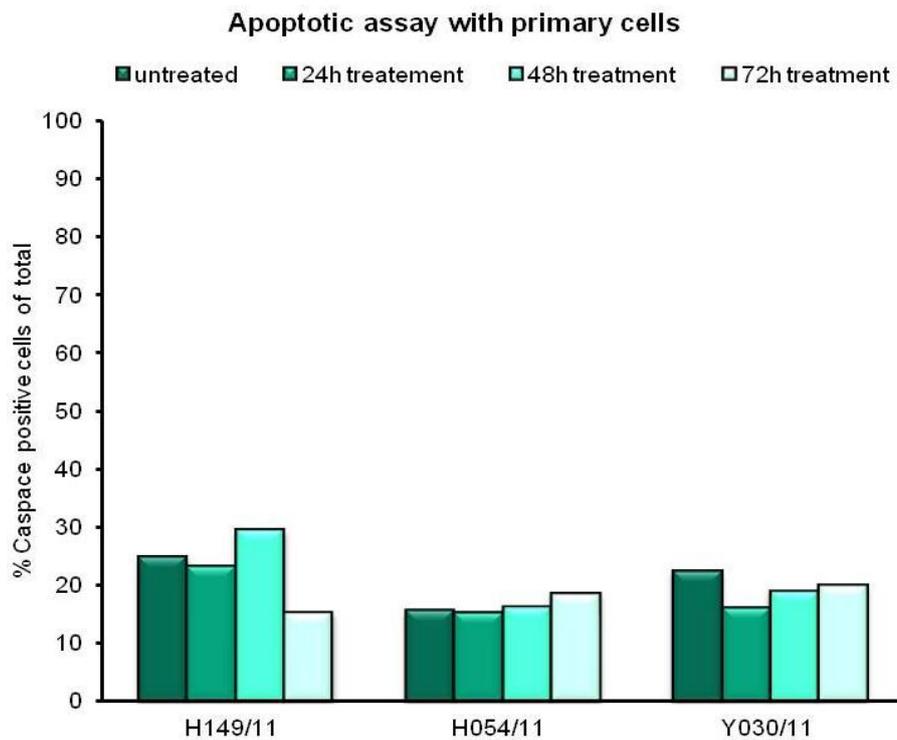
Figure 3–23 Unselected primary cells do not activate caspases following treatment with etoposide. Unselected primary cells (H149/11=CRPC; H054/11=cancer; Y30/11=BPH) were incubated for the indicated time points with 125 μM etoposide and kept at 37°C. Cells were stained with the caspase marker CaspACE™ FITC–VAD–FMK for flow cytometry.

3.5 Assessment of autophagy

Since we found no sign for apoptotic cell death in primary prostate cells we assessed autophagy as an alternative response with an antibody against LC3B (the protein is thought to be involved in formation of autophagosomal vacuoles), (Figure 3-24). Primary cells were left untreated (Figure 3-24, upper image) or in 60 µM etoposide for 60 h (Figure 3-24, lower image). When assessed by confocal microscopy, treated cells were found to be LC3B positive, suggesting autophagy. It would have been interesting to assess this phenomenon further for different cell populations of different samples, as it might have provided information about an alternative cell death. In conclusion, primary prostate cells were found to lose viability, but were at the same time resistant to apoptosis. Preliminary results point out that the cells might have undergone autophagy, a mechanism that can result in cell survival or cell death.
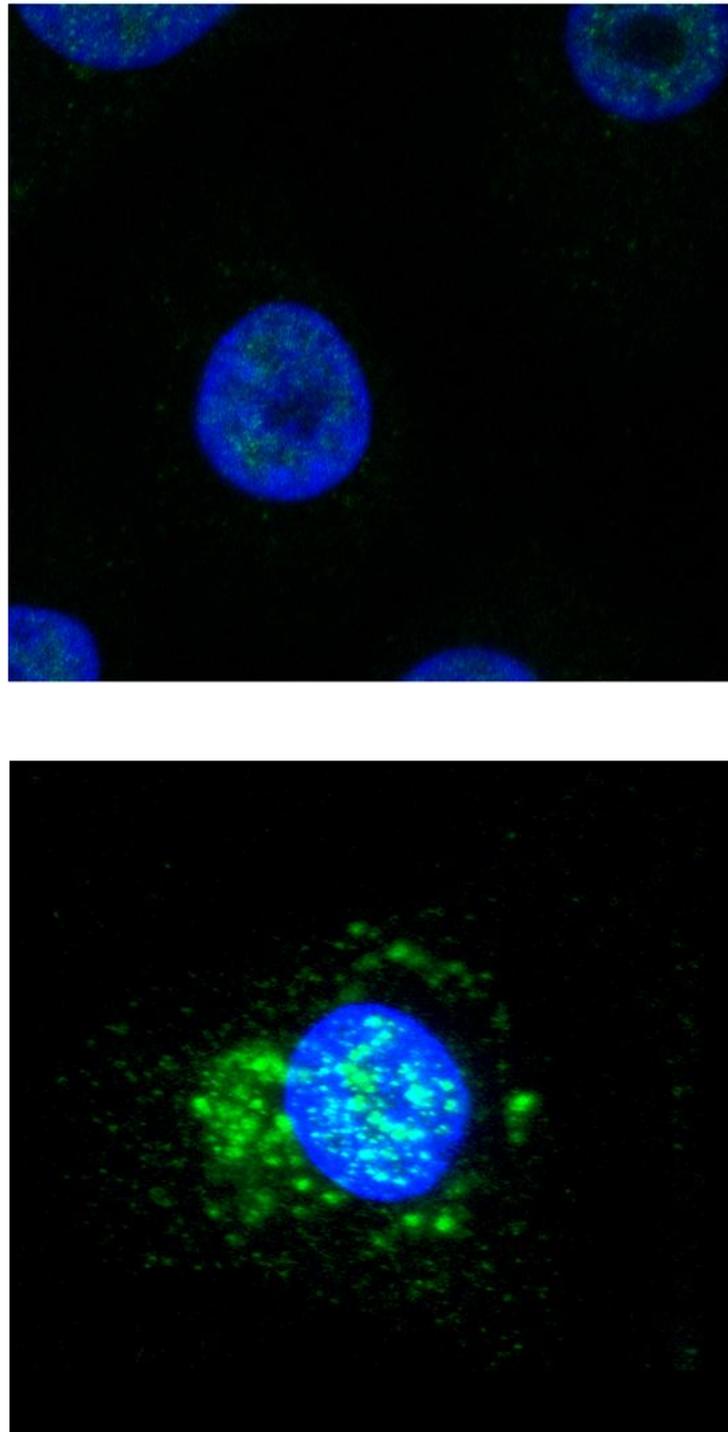
Figure 3-24 Primary cells display features of autophagy following etoposide treatment. Primary cells of a cancer sample (H131/11) were plated on collagen I-coated 8-well chamber slides and kept in absence (A) or presence (B) of etoposide (60 μM, 60 h) at 37°C. Cells were fixed and stained with an antibody against LC3B and assessed by confocal mircoscopy.

3.5 The role of ABC-transporters in mediating therapy-resistance in primary prostate populations

3.5.1 Gene expression analysis of ABC-transporters in primary prostate cells

ABC multidrug transporters are expressed in many human tumours and are thought to be a major source of chemoresistance. Hence, we studied ABC-transporters at the mRNA level by re-assessment of a microarray analysis prepared for a previous project [109]. SCs and CBs from malignant and benign primary prostate tissues revealed the presence of several ABC-transporters in both cell types (Figure 3-25). In particular ABCB1, ABCC1 and ABCG2 belong to the three major types of ABC-transporters correlated with drug resistance and were therefore of further interest. ABCB1 was present in about 50% of the tested samples, although its expression at the mRNA level was very low. ABCG2 was equally expressed in SCs and CBs. We found the etoposide-transporting protein ABCC1 [279] significantly higher expressed in SCs when compared to CBs (p= 0.002). ABCC5, which has not been shown to use etoposide as a substrate [279], was significantly higher expressed in CBs (p= 0.0016). According to these results, ABC-transporters might play a role in mediating therapy-resistance and explain some of the effects observed in this study. We decided therefore to proceed with functional assays.
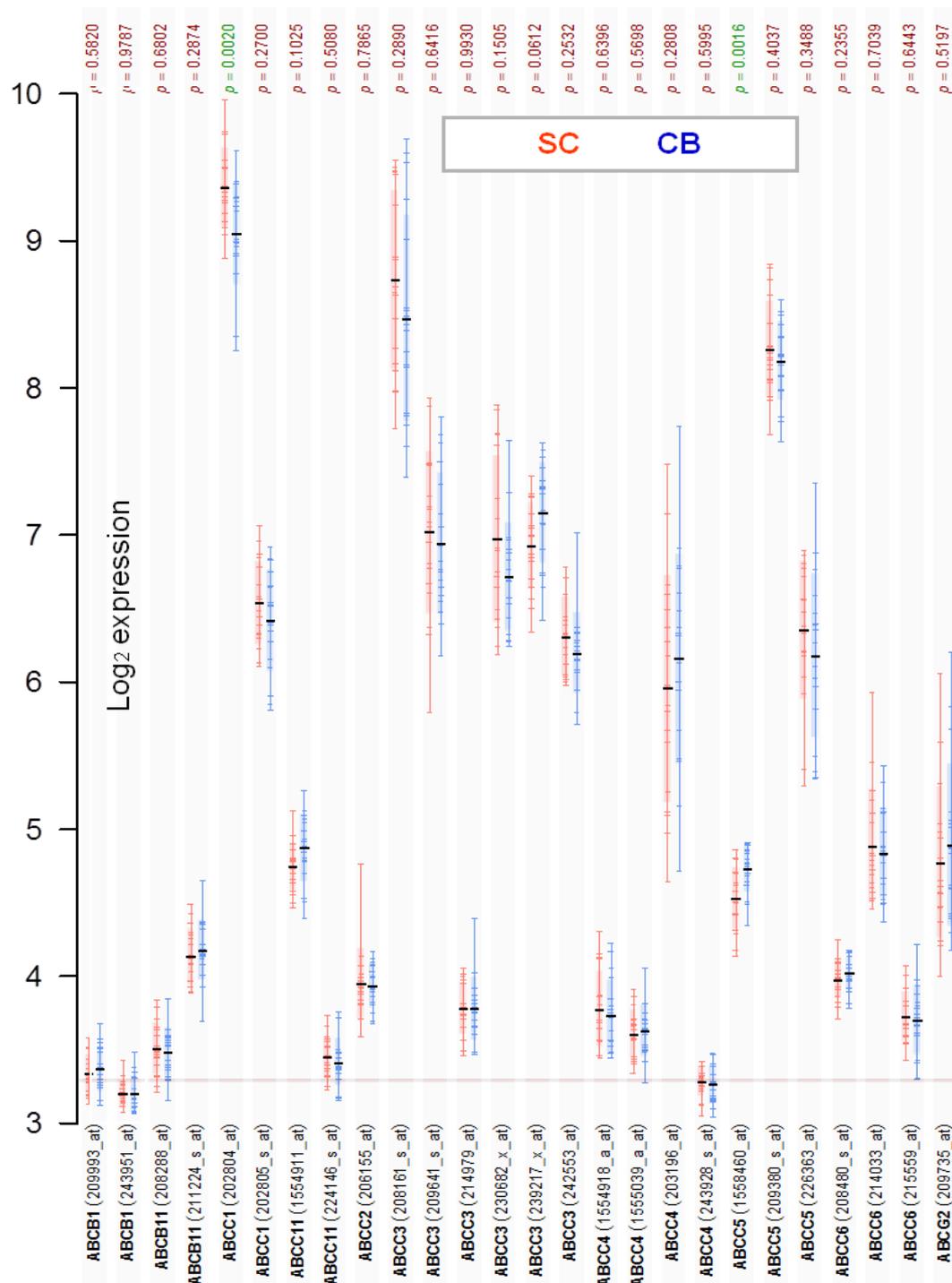
Figure 3-25 Expression of ABC-transporters at mRNA level. Microarray data performed with primary malignant and benign SCs and CBs were obtained from Birnie et al. 2008 [109] and specifically analysed for mRNA-expression levels of ABC-transporters. Each line within one mark presents one patient. P-values marked in green indicate significant differences between the two populations: SC vs. CB for ABCC1 p=0.002; SC vs. CB ABCC5 p=0.0016. Non-significant p-values are shown in brown above the figure. Analysis by Alastair Droop.

3.5.2 Assessment of the functionality of ABC-transporters in primary cells using calcein efflux assays

As described previously, a gene expression analysis of ABC-transporters in malignant and benign primary samples revealed that SCs and CBs expressed various ABC-transporters. However, the microarray-derived expression data did not necessarily reflect the cells' capability to efflux chemotherapeutic drugs, as the ABC-transporters might not be expressed at protein level or not be functional, if expressed. For this reason, a calcein efflux assay was applied to research the function of ABC-transporters in SCs, TAs and CBs. The method is based on the uptake of calcein-am into the cell cytoplasm and its metabolism into the green fluorescent substance calcein (Figure 3-26). A decrease of calcein in the cytoplasm can then be correlated with functional ABC-transporters that are able to expel undesirable substances. Among different fluorescent substances available, calcein was considered as a suitable reagent for several reasons: the substance is highly fluorescent, which is an advantage when detecting small cell numbers. Additionally, it is transported by ABCC1 (calcein) and ABCB1 (calcein-am) [280]. Particularly, ABCC1 was of interest, as it is an etoposide-transporting resistance protein that was found to be significantly higher expressed in malignant and benign SCs. Substances that are fluorescent without prior metabolism such as doxorubicin, daunorubicin and mitoxantrone, were not used, as they have been found to lack sensitivity due to poor fluorescent properties and the risk of measuring a significant number of false negative results [281].
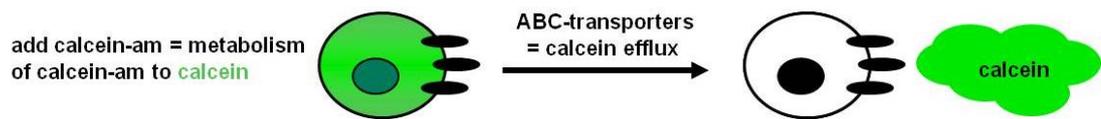
Figure 3-26 Use of calcein to assess the functionality of ABC-transporters. Cells were incubated with calcein-am which is shortly after its uptake, metabolized into green fluorescent calcein. Cells that express functional ABC-transporters are able to efflux calcein and should therefore be less calcein positive.

3.5.2.1 Suitability of the plate reader to measure calcein efflux and rejection of other methods

We tested different approaches to measure calcein efflux in primary prostate cell populations (Table 3-1). The initially chosen methods, flow cytometry and immunofluorescence microscopy, were rejected as they were difficult to conduct due to several technical disadvantages. The main difficulty with immuofluorescence microscopy was the inconsistent calcein signal within the wells where the cells were kept: the calcein signal varied strongly, depending on the position of the cells within the well. There were patches of cells that were able to metabolize the calcein-am to a greater extent than others. When capturing images of 100 cells per well at different time points, it was difficult to exclude the possibility that a change in the signal was not solely based on the technical variability within the wells. Furthermore, taking images of 3 x 100 cells (SCs, TAs and CBs) was a time-consuming procedure and did not allow measurement of the signal in different wells at exactly the same time point. The disadvantage of using flow cytometry for calcein efflux assessment was a constantly poor CD133 staining for SCs, which did not allow the collection of the required minimum of 100 cells for the SC population.

In view of these disadvantages, we used a plate reader as an alternative. To examine the suitability of the plate reader for measuring calcein, 100 to 15 000 unselected primary prostate cells were incubated with calcein-am (Figure 3-27 A and B). The subsequent measurement by the plate reader showed that the number of seeded cells per well was proportional to the detected fluorescence signal.

Methods →	IF	FACS	Plate reader
Advantages	•Low cell number required	•Low cell number required	•Takes the entire well into account for all time points •Measures all wells simultaneously
Disadvantages	•Can not measure all wells simultaneously •Variability of fluorescence intensity in wells are not taken into account	•Poor CD133 staining	•Higher cells numbers required as for immunofluorescence microscopy and flow cytometry
Proceeded with method?	No	No	Yes

Table 3-1 Advantages and disadvantages of different methods to measure calcein.

Since the plate reader was able to detect calcein in cells and took the entire well into account, it was concluded to be a suitable quantitative method. To assess whether selected populations of primary cells were able to exclude calcein, SCs, TAs and CBs were seeded and the calcein signal was measured directly after incubation with calcein-am (15 min) and after 1 h, 2 h and 3 h (Figure 3-27 C and D). The initial signal measured (15 min) was between 30 000 and 45 000 units for the three different cell populations. After 1 h the signal was significantly reduced to 15 000 to 25 000 units, resulting in the (subsequently discovered to be misleading) conclusion that all of the three cell types were highly capable of calcein extrusion. At 2 h and 3 h the signal was reduced further. This initial experiment led to the decision to conduct further calcein efflux assays with the same method. However, it was subsequently observed that the decrease of the signal and in particular the change between 15 min and 1 h, was highly affected by an artefact resulting from the required washing steps: measuring between different time points required washing steps in between, to exclude the possibility of measuring calcein in the media instead of calcein inside the cells. Unexpectedly, the washing steps led to a loss of cells, even though the washing steps were

gently performed with PBS. This was unexpected as the cells have a high affinity for collagen I-coated plates and are therefore strongly adherent. However, the loss of cells during different washing steps significantly influenced the measured signal, to the extent that a decrease of the signal due to efflux or a loss of cells through the washing, were indistinguishable.

A

Detection of calcein in primary cells

Fluorescence intensity (× 1000)

Cell number

B

Visualization of calcein in primary cells

C

Use of calcein to measure efflux:
1x set of wells per cell type to measure the same well at 4 time points

96-well plate

CB ◯ ◯ ◯
TA ◯ ◯ ◯
SC   ◯

Add calcein-am

CB ● ● ●
TA ● ● ●
SC   ●

Measure at 15min 1h, 2h, 3h and wash before each measurement

D

Measurement of calcein in primary cells

SC TA CB

Fluorecence intensity (× 1000)

The steep decrease between 15min to 1h was later found to be an artefact

15min   1h   2h   3h

Figure 3-27 Suitability of plate reader to measure calcein in primary cells. (A) The indicated numbers of unselected primary cells were plated in triplicate on collagen I-coated 96-well plates and left o/n to adhere. Cells were incubated with calcein-am for 15 min and washed with PBS. Wells were filled with KSFM and the calcein was measured by a plate reader. Each bar represents the average of one triplicate. (B) Calcein signal of unselected cells detected by immunofluorescence microscopy. (C) Schematic presentation of the method used in D. (D) Primary cells (H054/11) were selected. CBs and TAs were seeded in 1 x triplicate on collagen I-coated 96-well plates. The entire SC yield was plated at one well. The selected populations were left for 2 h to adhere and cells were incubated for 15 min with calcein-am-containing media. The calcein signal was measured in the same well(s) directly (15 min) and after 1 h, 2 h and 3 h. Each time point represents the calcein signal for one cell population at the indicated times. Standard deviations for each mark are listed in the appendix.

3.5.2.2 Determination of cell loss due to different washing methods

There were two main ways to use calcein. In Figure 3-27 C and D calcein was used to measure efflux. However, due to the previously described difficulties calcein was used in a second way: to determine the loss of cells on collagen I-coated 96-well plates due to required washing steps. In comparison the two methods used with calcein were:

> **Method 1: Use calcein to measure efflux**
>
> Plate cells → add calcein → wash → measure

> **Method 2: Use calcein to determine effect of washes on cell loss**
>
> Plate cells → wash → add calcein → measure

Figure 3-28 refers to method 2 and a detailed schematic presentation of the experimental set up is shown in Figure 3-28 A. Unselected populations were plated on collagen I –coated 96-well plates and left to adhere for 2 h (Figure 3-28 B and C) or o/n (Figure 3-28 D and E). Cells were washed using a vacuum pump (B, D) or alternatively with a pipette (C, E). The different washes (wash 1, wash 2, wash 3, wash 4) equal the number of washes in a calcein <u>efflux</u> experiment: wash 1 equals the washes at the 15 min point, wash 2 the 1 h time point, wash 3 the 2 h time point and wash 4 the 3 h time point. Regardless of the type of method applied for washing (vacuum pump or pipette) or the allowed time for adherence (2 h or o/n), the calcein signal decreased with increasing washes. These findings suggested that the washes resulted in a loss of cells leading to an artefact (as shown in Figure 3-27 D). It was therefore not possible to distinguish between a decrease of the signal due to calcein efflux or due to reduction of cells on the plates due to washing.

Use of calcein to quantify cells:
4 x sets of wells receive a different number of washes
and are measured at the same time point to quantify the
cells remaining after the washes

Apply the number of washes that equal the

96-well plate

○ ○ ○ ...15min time point

○ ○ ○ ...1h time point

○ ○ ○ ...2h time point

○ ○ ○ ...3h time point

Add calcein-am

● ● ●

● ● ●

● ● ●

● ● ●

Measure all wells at the same time
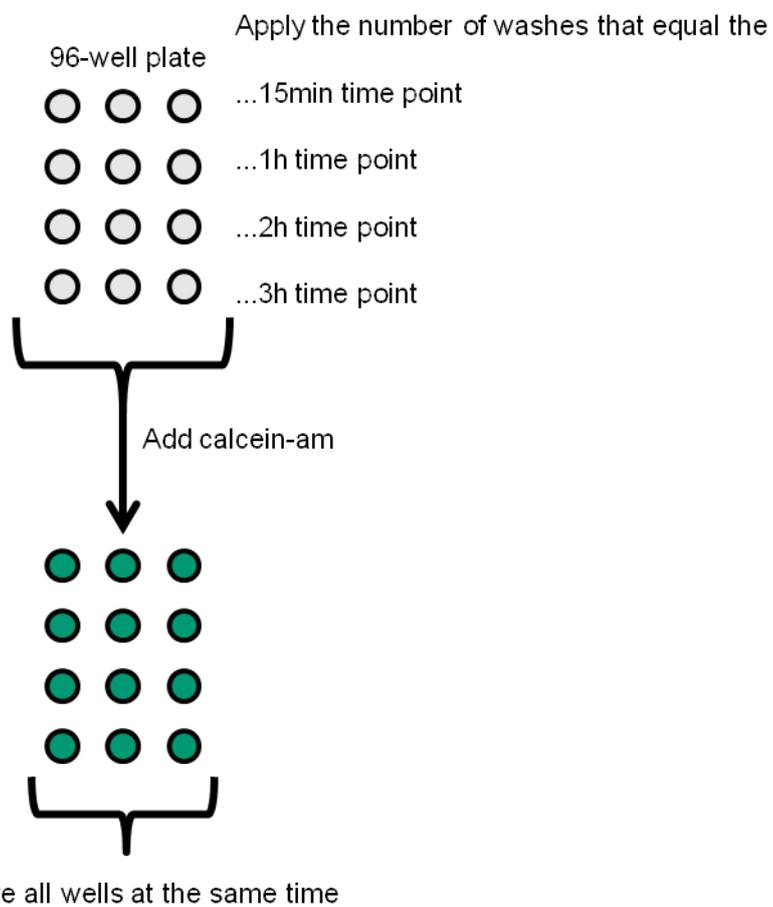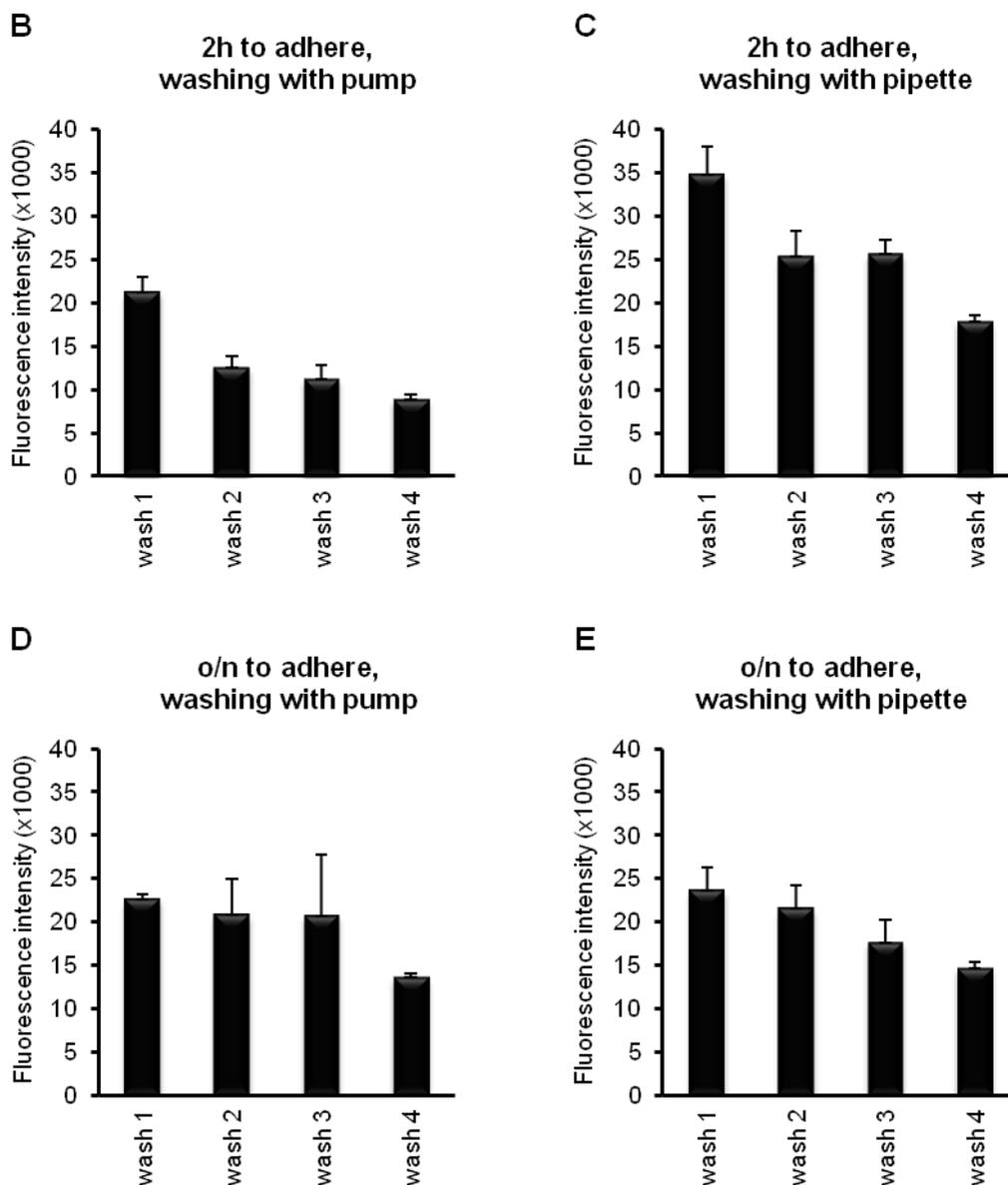
Figure 3-28 Impact of different washing methods on the cell number in the collagen-coated 96-well plates. (A) Schematic presentation of the method used in B-E. (B-E) Unselected primary cells (H069/11) were plated as triplicates on collagen-coated 96-well plates and washed as indicated. Cells were left to adhere for 2 h (B, C) or o/n (D, E). Wells were washed with the same number of washes as used in Figure 3-27 by a vacuum pump (B, D) or with a pipette (C, E). After applying the washes calcein-am-containing media was added and left for 15 min to determine cells remaining after washing and measured by a plate reader. Wash 1 equals the washes at the 15 min time point, wash 2 at the 1 h time point, wash 3 at the 2 h time point and wash 4 at the 3 h time point. Each bar represents the average measured for 1 triplicate.

3.5.2.3 Minimization and prevention of cell loss when conducting calcein efflux assays

Due to the previously described results, there were two main ways to minimize or even prevent the loss of cells affecting the fluorescent signal significantly:

(i) Firstly, a comparison of time points that had a minimum number of washes between them e.g. by comparing the values in Figure 3-27 C using the 2 h time point and the 3 h time point as there was only one washing cycle in between. However, to use the 15 min time point for comparison to any other value in the time course would not have been suitable, as the loss of cells after the 15 min time point was very high (see Figure 3-28 B, C).

(ii) A method that entirely excluded the possibility of a decrease of signal due to a loss of cells caused by washing was the one used in Figure 3-29. In this approach TAs and CBs were plated in 2 x triplicates. Both triplicates were incubated for 15 min with calcein-am-containing media. One triplicate was measured directly after the end of the incubation time, the other triplicate was measured after 3 h. The number of washes was kept constant between the different sets of wells. Due to the SCs being such a very rare population, it was not possible to plate them as triplicates. The maximum number of SC replicate wells was therefore two, but only for samples that contained a high number of SCs. For those with a poor SC yield this method could not be used. Responses in selected populations of the malignant samples H035/11 and H131/11 were measured with the above mentioned method. Interestingly, in all cell populations, there was an increase of signal between the 15 min and the 3 h time point. This finding led to the design of a further experimental set up as described below.
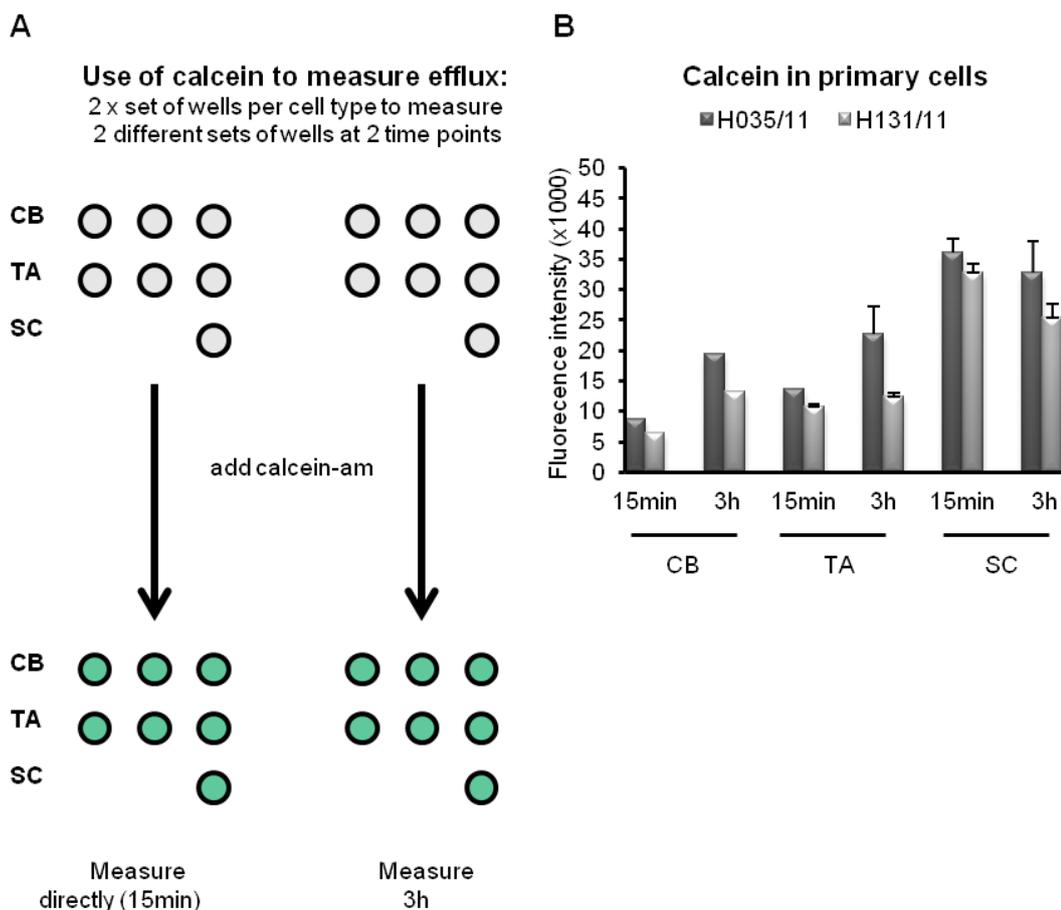
Figure 3-29 The time points 15 min and 3 h are not suitable to measure calcein efflux in selected primary cells. (A) Schematic presentation of the method used in B. (B) CBs and TAs were seeded in 2 x triplicates (15 min, 3 h) on well collagen-coated 96-well plates. The entire SC yield was divided between two wells. The selected populations were left o/n to adhere. Cells were incubated for 15 min with calcein-am-containing media, with PBS and the calcein signal was measured directly (15 min) or after 3 h to allow the detection of calcein efflux by the plate reader Each bar represents the average of one triplicate.

3.5.2.4 Determination of calcein efflux in unselected primary cells and RD-ES cells

The observation of an increase of the signal in all cell populations between 15 min and 3 h as presented in Figure 3-29 led to the design of a further experimental improvement. This was based on the assumption that all cell types might metabolize more calcein-am into calcein than effluxing calcein, in particular in the first 1 or 2 h when there might have still been a distinct amount of calcein-am left in the cytoplasm. Thus calcein had not been metabolized when measuring at earlier time points. Only after most of the calcein-am molecules in the cytoplasm were metabolized, should an efflux have been detectable (if it existed). For this reason, unselected populations of the malignant primary sample H054/11 and benign sample Y023/11 were plated in four triplicates (Figure 3-30 A and B). After incubation with calcein-am, each triplicate was left for different times before measurement. In both samples the following trend was observed: the balance between production of calcein and its efflux changed after 2 h. Before this time point the metabolism into calcein was more dominant, so that a decrease of the signal could not be detected, even if it was likely that there was some efflux present also within the first 2 h. At 2 h most of the calcein-am in the cytoplasm seemed to be used up and an efflux was detected between 2 h and 3 h. Here, the numbers of the fluorescent signal in samples H054/11 and Y023/11 rose from 15 min to 1 h and 2 h. After reaching this maximum, the signal decreased at 3 h. To confirm the suitability of the plate reader method to detect calcein efflux, the ABC-transporter expressing cell line ES-RD was used (Figure 3-30 C). Similar to primary cells, an increase of the signal was initially detected. After peaking at 2 h, the signal decreased due to calcein efflux. This trend was confirmed by

repeating the experiment (Figure 3–30 C, green bars).These results enabled a re-analysis of a data set acquired earlier.

A

Calcein efflux sample H054/11

B

Calcein efflux sample Y023/11

C

Calcein signal in RD-ES cells

■ Test 1　■ Repeat
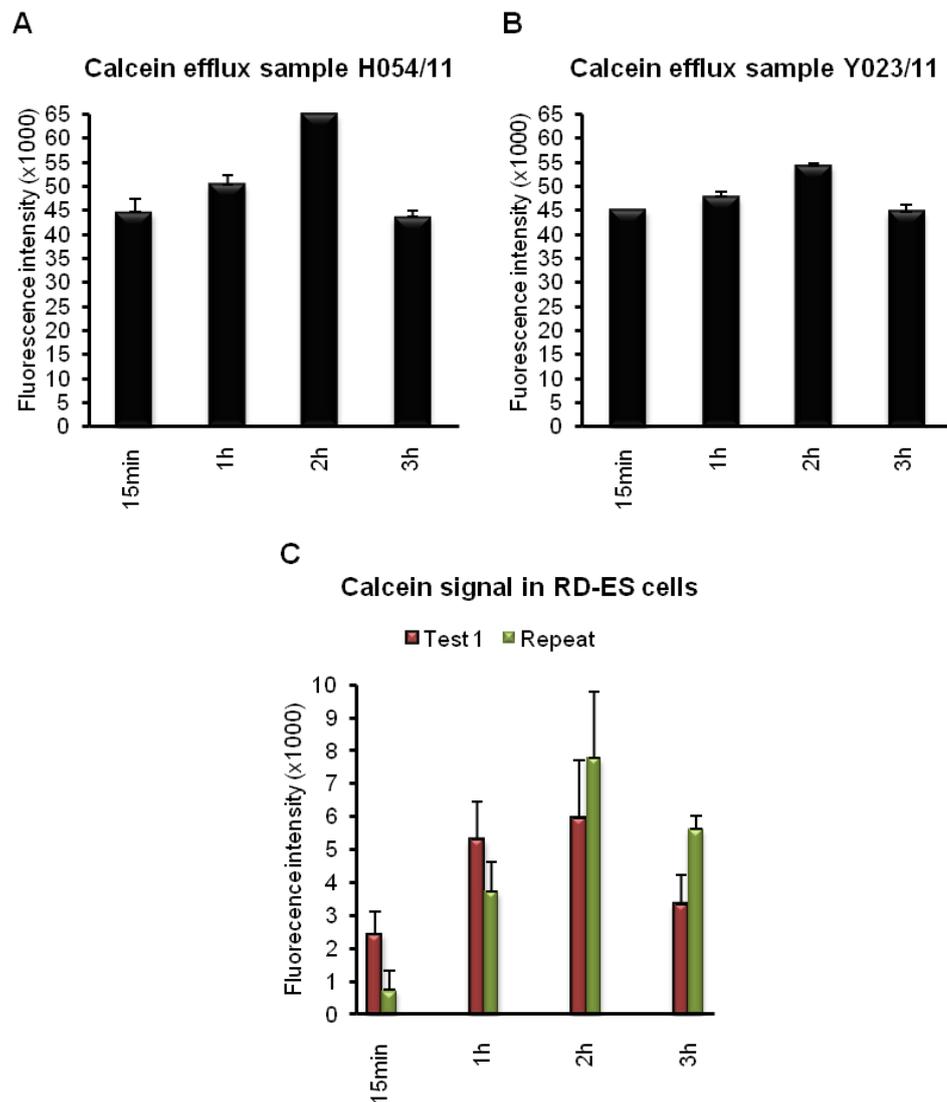
Figure 3-30 Unselected populations of primary cells and RD-ES cells are able to efflux calcein. (A, B) Unselected primary cells (H054/11, Y023/11) were plated as 4 x triplicates (15 min, 1 h, 2 h and 3 h) on collagen I-coated 96-well plates and left o/n to adhere. Cells were incubated with calcein-am for 15 min. Calcein-am-containing media was washed off with PBS, replaced by KSFM and measured directly (15 min) or left to allow efflux for the indicated time points (1 h, 2 h, 3 h). (C) Calcein efflux of RD-ES cells. Each bar represents the average of one triplicate. The experimental set up is similar to that shown in 3-29 A.

3.5.2.5 Measurement of calcein efflux in primary cells

The findings in Figures 3-27 to 3-30 directed a re-analysis of a set of data that was measured according to the strategy in Figure 3-27 C. It was produced earlier by using a vacuum pump for washes and allowing the cells to adhere for 2 h. Hence, Figure 3-31 was created based on the following considerations:

(i) The loss of cells when washing with a vacuum pump and allowing the cells to adhere for 2 h was relatively low, in particular when only comparing time points that did not have more than one wash in between them (only the difference between 15 min and 1 h would have been too high), (Figure 3-28 B).

(ii) According to Figure 3-30 A and B calcein efflux was detectable after 2 h.

The change of the calcein signal in SCs, TAs and CBs is most likely due to efflux of calcein, even when taking into consideration that a slight loss of cells might have played a role for the decrease of the signal (Figure 3-31). When normalizing the signal measured at the 3 h time point to the one at the 2 h time point by setting the 2 h time point measured for each population to 100% no significant different efflux capabilities were found among the populations. This result suggests that enhanced drug efflux is not the dominant resistance mechanism in SCs from malignant and benign prostate tissues.
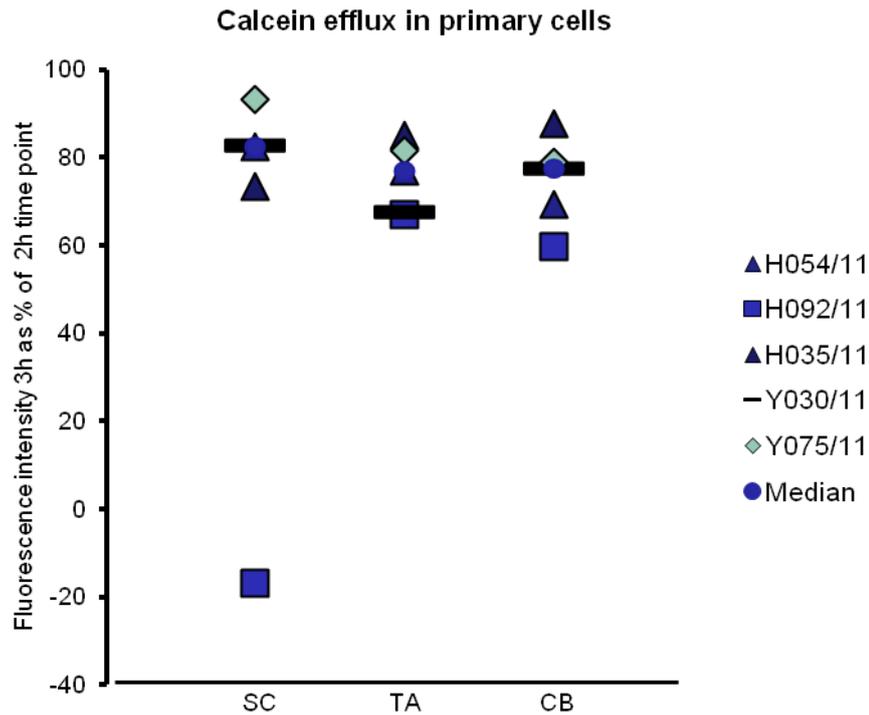
Figure 3-31 SCs do not display an enhanced efflux in comparison to TAs and CBs. The detection of calcein efflux was conducted as shown in Figure 3-27 C and D. CBs and TAs were seeded as 1 x triplicates on collagen-coated 96-well plates. The entire SC yield was plated on one well. The selected populations were left for 2 h to adhere and cells were incubated for 15 min with calcein-containing media. Cells were washed with PBS and the calcein signal was measured in the same well(s) after 2 h and after 3 h. The fluorescence intensity measured after 2 h was set to 100% and the intensity at 3 h calculated in percentile relation to this value. Each symbol represents the calcein signal for one cell population of one patient. Standard deviations for each data point and the non-significant p-values are listed in the appendix.

Chapter IV

DISCUSSION

4. DISCUSSION

In summary our results indicate that SCs from malignant and benign prostate tissues are better protected against DNA damage than TAs and CBs. The colony forming efficiency was less affected in SCs after exposure to DNA damaging conditions. Following this observation we examined potential mechanisms of the increased therapy-resistance and investigated ABC-transporters, cellular quiescence, apoptotic susceptibility and autophagy in prostate primary cells. We found that ABC-transporters were expressed at mRNA level in SCs and CBs, but these seemed not to be causative for the enhanced therapy-resistance in SCs. However, the assessment of cellular quiescence, a frequent obstacle in cancer therapy, revealed that a higher proportion of SCs was in a dormant stage. This might be one of the key factors leading to an increased resistance. Unlike prostate cell lines, primary prostate epithelial cells seemed to lack the ability to undergo apoptosis after exposure to etoposide. Preliminary data suggest that autophagy might be an escape mechanism to apoptosis.

4.1 Assessment of DNA damage in prostate cell populations following etoposide treatment

When we employed both comet assays and staining for γH2A.X expression to assess DNA damage in SCs and differentiated cells from malignant and benign prostate tissues, by both methods the SCs were less susceptible to etoposide-induced DNA damage than their differentiated counterparts.

4.1.1 Comparison of neutral and alkaline comet assays as methods to detect DNA damage in primary cells

Neutral comet assays did not detect high levels of DNA damage, whereas alkaline comet assays were suitable for this purpose. This finding concurs with results from other groups that used alkaline comet assays as the

preferred version to detect DNA damage following etoposide treatment. For example Watters et al 2009, used alkaline comet assays as the method of choice after treating immortalized wild-type mouse embryonic fibroblasts with etoposide [143]. In another study neutral constant field gel electrophoresis (CFGE) did not detect a high amount of etoposide induced DNA damage in SV40 transformed fibroblasts, but alkaline CFGEs were a suitable technique [166]. By combining these methods the authors found that in their system, only 3% of the DNA strand breaks caused by etoposide were indeed DSBs. This observation is the most likely explanation why in neutral comet assays with primary cells only a moderate % of DNA in tail was identified in these studies.

4.1.2 Observation of different γH2A.X phenotypes

The previously described comet assays provide a direct measurement of DNA damage. In contrast, the identification of DNA damage by the histone variant γH2A.X is an indirect and more sensitive method. In addition to classical discernible γH2A.X foci, we also found cells with a pan-nuclear distribution of the marker. This finding is also in accordance with a previous study in our lab that assessed prostate primary cells for up-regulation of γH2A.X after irradiation. In this case, a pan-nuclear γH2A.X staining was found occasionally, but as this study used a different source of DNA damage, the predominant type of foci observed were classical foci (personal communication with F.M. Frame). A pan-nuclear γH2A.X pattern after etoposide treatment has also been identified by other groups. For example, in RKO cells (colon cancer) the same pattern was found after exposure to etoposide [275]. The authors interpreted their finding as a question of drug concentration and software adjustment. A pan-nuclear γH2A.X pattern after etoposide treatment has also been reported after treatment of mouse

embryonic fibroblasts [143]. Further sources of damage such as UV irradiation are also known to cause a pan-nuclear γH2A.X distribution [282, 283]. Its meaning is mostly unknown, but some studies correlated the appearance with S-Phase cells [276, 284]. If this holds true, a higher percentage of malignant prostate primary TAs would be in the S-Phase, which agrees with the nature of TAs and is furthermore supported by our Ki67 staining, where a significantly higher number of TAs were in cycle. Presumably the unwound and open DNA during S-Phase is a cause for the pan-nuclear γH2A.X pattern.

4.1.3 Higher resistance to etoposide-induced DNA damage in SCs

The higher resistance to etoposide-induced DNA damage in SCs is in accordance with data from other studies and can be interpreted as a first hint of more successful survival for SCs. Pedriatic brain tumour neurospheres, which are enriched for CD133+Sox2+ CSCs, displayed a higher resistance to etoposide in comparison to monolayers, as shown by alkaline comet assays [285]. Another study showed that Hs578T cells (breast cancer) could be sensitized to drugs such as etoposide and doxorubicin: After treatment with salinomycin, the cells showed a higher amount of DNA breakage as assessed by comet assays and markers of DNA damage such as γH2A.X and 53BP1 [286]. As salinomycin has been shown to specifically inhibit CSCs [287], it would have been interesting to test this drug on prostate SCs. However, when human embryonic and induced pluripotent stem cells were exposed to etoposide to test their genomic stability, an inverse finding was revealed [288]. The pluripotent cells were more susceptible to DNA damage, in comparison to more differentiated cells. The authors did not assess possible reasons for their observation, but one

explanation might be that the embryonic SC were not quiescent [288], as CSC sometimes are [289, 290].

4.1.4 The DNA damage response in the prostate

Our data match studies on cultured prostate tissues derived from radical prostatectomy specimens that were cored at the unaffected lobe [291]. In the basal compartment, phosphorylation of H2A.X upon irradiation, etoposide or daunomycin treatment was fast, transient and dependent on ATM, but these responses were only moderate in luminal cells [291]. The authors correlated these differential DNA damage responses with distinct chromatin marks [291]. Basal cells contained higher levels of euchromatin, which is more accessible for repair complexes, whereas the DNA in luminal cells was packed in heterochromatin [291]. This study agrees with our finding in respect to the up-regulation of γH2A.X following etoposide treatment in TAs, which are located in the basal compartment. However, the previously described study did not specifically assess the prostate SCs which showed a differential response in our experiments. In this case, our study has gone deeper in understanding the DNA damage response by taking into account the hierarchy of the prostate epithelium and the different subpopulations. The higher resistance to DNA damage of primary malignant and benign prostate SCs in comparison to more differentiated cells has also been found when using irradiation (personal communication with F.M. Frame). Interestingly, in malignant and benign SCs the presence of heterochromatin was identified, which might provide an explanation for the lower γH2A.X levels (personal communication with F.M. Frame).

4.1.5 Conclusions: γH2A.X up-regulation after treatment

The up-regulation of γH2A.X after treatment is an indicator of DNA strand breaks, which result in different outcomes for the cell (cell cycle arrest,

repair or apoptosis). Whereas in the literature γH2A.X is often described as a specific DSB marker [166, 277] recent findings suggest that it also responds to different types of DNA damage such as SSBs [276]. Hence, it is likely that both malignant and benign prostate cells up-regulate γH2A.X not only by etoposide-induced DSBs, but also due to SSBs. A back-up for the assumption that primary prostate cells up-regulate γH2A.X due to SSBs, were the specific experiments, using a treatment condition that causes SSBs (excess thymidine): here we also observed an up-regulation of γH2A.X with SCs showing more resistance to DNA damage.

A clearance of foci is correlated with repair. We monitored a reduction in the percentage of γH2A.X positive cells, as well as foci per cell in malignant and benign TAs after 24 h. In malignant and benign SCs we mainly observed a decrease of foci per cell. However, it was hard to compare repair in SCs and TAs directly, as they sustained different amounts of DNA damage and had therefore a different distance to the baseline. To test repair in SCs it would have been necessary to use a more aggressive treatment. However, other groups have observed a more efficient repair e.g. in brain tumour CSCs [285].

The appearance of γH2A.X is usually seen as a sign of the genotoxic endpoint for the cells. Evaluating γH2A.X has been suggested as a standard in-vitro genotoxicity test to complement micronucleus assays, comet assays and mutation frequency tests [143]. According to Muslimovic et al. 10% of the etoposide-induced DSBs resulted in γH2A.X phosphorylation and these were closely related to toxicity [166]. A consequence of reaching the genotoxic endpoint is often apoptotic cell death e.g. after incubation with etoposide [292]. Our results confirm this observation in part. Indeed, for a high proportion of our cells, the appearance of γH2A.X foci could be

interpreted as a genotoxic endpoint, but we cannot confirm that this genotoxic endpoint results in apoptosis. The question remains as to why SCs acquired less DNA damage than more differentiated cells. Among many different reasons the stage of the cell cycle might play on important role. All these possibilities will be discussed.

4.2 Clonogenic recovery of primary prostate epithelial cells

Clonogenic assays are a meaningful tool to reveal information about the recovery of cells that have been exposed to various treatments. We found that the clonogenic potential of SCs, in particular from malignant tissues, was less affected following etoposide treatment than those of TAs derived from the same tissue. The same trend was confirmed when using irradiation to treat selected populations of primary prostate epithelial cells (personal communication with F.M. Frame). Interestingly, benign samples often failed to produce colonies, even when left untreated. Hence, only two clonogenic assays conducted with BPH derived cells were evaluated. We assume that this was based on the fact that cancer cells are proliferating faster and have therefore a higher clonogenicity than BPH cells. The two BPH samples capable of colony formation were those that were most Ki67 positive among the benign samples in our study.

These observations of SCs of malignant origin being more resistant to drugs such as etoposide was also seen when using SCs from other sources and agrees with our data. For examples spheres grown from cultured brain tumour cells that were enriched for SC-like cells showed a higher clonogenic recovery after etoposide treatment than monolayers which only contained a low number of SC-like cells [285]. CD44+CD24- breast CSCs enriched cell lines were seen to have a higher viability after treatment with chemotherapeutic drugs than populations containing only a low proportion

of CSCs [287]. Out of 16 000 agents only salinomycin targeted the CSC population specifically and decreased their survival *in vitro* and *in vivo* [287]. Furthermore, the authors found that the common chemotherapeutic agent paclitaxel increased the ability of CD44+CD24- CSCs to form mammospheres 2-fold [287]. In one case when we used a prolonged incubation time of etoposide (3 h instead of 45 min) the TAs were prevented entirely from forming colonies. The SCs were reduced in colony formation, but were still able to form a small number of colonies. This leads to the speculation that these recovering cells might be the ones that are causal for a relapse *in vivo*. Indeed, there are reports about a small fraction of tumour cells that survive therapy, namely minimal residual disease, not only in leukemia, but also lung cancer and breast cancer [293-296]. Our data suggest that minimal residual disease in prostate cancer might be mediated by SCs rather than differentiated cells. The hallmarks that provide the protection specifically for SCs from malignant tissues are very likely to be multifactoral. Examples of protection mechanisms of CSCs, are   cellular dormancy [297, 298], expression of ABC-transporters [266, 267, 280, 281, 299-305] apoptotic resistance [218-220, 306-309], limitation of ROS production [254] or the presence of high levels of heterochromatin (personal communication with F.M. Frame), [291], and enhanced DNA repair [297]. Some of these mechanisms were assessed in this study and will be discussed below. If it holds true that CSCs are the main drivers of tumour recurrence, future strategies to target specifically CSCs are crucial. Some approaches have been already made e.g. high throughput screening to identify agents that target CSCs *in vitro* and *in vivo* [287]. However, there is an urgent need to study these agents more extensively on cells cultured from patient samples instead of cell lines. Nevertheless, there are a few clinical trials for different types of cancer e.g. pancreatic, breast and colon present at the time that

aim to target major signaling pathways in CSCs such as Wnt, Hedgehog or Notch [310].

4.3 Cellular quiescence as a resistance mechanism in SCs derived from malignant prostate tissues

Cellular quiescence or dormancy refers to cells in the G0 phase of the cell cycle. Quiescent cells are an obstacle in cancer therapy, as treatments are usually directed against fast proliferating cells [311]. We assessed the quiescence in selected populations of primary prostate epithelial cells of malignant and benign origin and found that a higher proportion of SCs, in comparison to TAs and CBs, was Ki67 negative. This finding is in accordance with the nature of normal tissue SC that are usually dormant and therefore better protected against DNA damage [297]. This enables SCs to avoid mutations through replication that would diminish the potential for self-renewal and differentiation resulting in the degradation of tissue, ageing phenotypes or cancer [312]. It seems that malignant and benign SCs from the prostate maintain this protection mechanism and are therefore more resistant to DNA damage induced by chemotherapy or irradiation. The higher proportion of SCs (benign and malignant origin) in a quiescent stage was also confirmed by a series of experiments in our group that used Ki67 staining and EdU incorporation (BrdU analogue) on a different set of primary samples (personal communication with F.M. Frame). The mainly quiescent nature of CD133$^+$/$\alpha_2\beta_1$integrin^{high} SCs was also confirmed by [106]. The authors isolated SCs directly from BPH samples and assess Ki67 expression [106]. More than 80% of the SCs were found to be dormant [106]. Data from other groups support the hypothesis that dormancy occurs frequently in CSCs and concur with our results. For example CML-SCs were dormant and it was speculated that this is a likely resistance mechanism against anti-

cancer treatment [313, 314]. Quiescence has also been reported for CSCs from the esophageal, rectal carcinoma, breast and pancreatic tumours [289, 290, 315, 316].

A link between the slow cycling nature of CSC populations and therapy resistance has been demonstrated in the colon, breast, ovaries, and pancreas [247, 249, 251, 316]. Quiescent CSCs survived *in vivo* therapies that killed the bulk tumour cells and required *in vitro* increased doses to decrease viability in comparison to rapidly cycling cells [247, 249, 251, 316]. These findings emphasis how ineffective conventional therapies can be on dormant cells and can provide explanations why tumors that seem to be entirely regressed after treatment can recur [242].

To kill quiescent CSCs successfully, the application of agents that target non-cycling cancer cells must be the alternative. It would have been interesting to assess a substance that acts in a cell cycle independent fashion such as the trk tyrosine kinase inhibitor CEP-751 (KT6587) that has been used to examine the elimination of prostate cancer in animal models [317]. Alternatively, dormant cells could be treated in a manner that encourages them to re-enter the cell cycle. Such an approach was made for hematopoietic SCs that were switched from dormancy to self-renewal following stimulation with G-CSF [298]. This mechanism might offer a novel treatment option and be meaningful for the eradication of malignancy. Indeed, CML-SCs were eliminated *in vitro* by imatinib when pre-treated with G-SCF [318]. However, one of the main challenges for the clinical use of these substances will be to activate specifically CSCs whilst sparing healthy SCs. Targeting healthy SCs would be dangerous for the patient and lead to tissue atrophy or indeed could drive malignancy. At this time there is no

substance available that switches exclusively CSCs from dormancy to an activated stage. Hence, further research into substances and their suitability for clinical use is required.

4.4 Apoptotic inhibition in prostate primary cells

The mechanism of action of our "model drug" etoposide is the induction of apoptosis by inhibiting topoisomerase II [277, 319, 320], even if some studies reported that, paradoxically, etoposide might also reduce the expression of several caspases and Bcl-2 related genes [321]. We found that malignant and benign primary prostate epithelial cells failed to undergo apoptosis following etoposide treatment, whereas the prostate cell lines RC92a/ h-TERT and RC165N/h-TERT were able to do so. This effect seems not only to be observed after etoposide treatment of prostate epithelial primary cells, but also after high doses of irradiation (personal communication with F.M. Frame). Recent reports which addressed the question of apoptotic resistance in prostate cells agree with our findings. A higher susceptibility of prostate cell lines to apoptosis in comparison to primary cells has been seen after treatment with drugs such as docetaxel, mitoxantrone, methotrexate or cisplatin [267]. The immortalization of the cell lines obviously led to genetic changes that altered their response to treatment.

Apoptotic resistance remains one of the main obstacles to successful cancer therapy. Its failure can depend on many molecular factors, for example p53, the members of the Bcl-2 family, NF-KB and beclin1. Bcl-2 overexpression has been linked to a failure of treatment strategies such as radiation, chemotherapeutic drugs (e.g. docetaxel) or androgen deprivation [308, 322]. p53 is frequently mutated in metastatic prostate cancer [68, 323, 324] and its lack of function has been shown to inhibit apoptosis in cell lines and

(primary) prostate cells preventing the success of anti-cancer treatment [307, 325]. The pro-apoptotic regulators Fau and Bcl-G were downregulated in prostate tumours relative to normal prostate tissue and BPH and shown to play a role in apoptotic sensitivity [309]. Also the repair factor γH2A.X, which we found to be up-regulated after etoposide treatment, is thought to play a role in treatment success by maintaining cell cycle arrest and preventing apoptosis [326], even though γH2A.X has also been described as a marker for the genotoxic endpoint of the cell [143].

As we didn't detect apoptosis in primary prostate epithelial cells, we took alternative cellular responses such as senescence, necrosis and autophagy into consideration. As primary prostate epithelial cells displayed enlarged vacuoles after etoposide treatment (experiment conducted for a different study by a former lab member), we decided to test for autophagy as an alternative treatment response. Preliminary findings demonstrated the presence of LC3B positive cells following the administration of etoposide. Indeed, autophagy is known as a resistance mechanism for multiple therapeutic substances in the setting of apoptotic inhibition [218-220]. *In vivo* and *in vitro* work on the prostate cancer cell lines PC-3 and LNCaP has demonstrated autophagy as a mechanism to escape apoptosis [219]. By inhibiting autophagy the authors observed an increased ability of the cells to trigger programmed cell death [219]. It is possible that our primary prostate epithelial cells used autophagy as a resistance mechanism.

In conclusion, the observed apoptotic resistance can rely on many factors. To encourage an apoptotic mechanism in primary prostate epithelial cells, it would probably be necessary to block anti-apoptotic factors before the administration of therapy. As we found cells to be autophagy positive, it would have been interesting to pursue this work e.g. by down-regulating

the autophagy gene beclin1 prior to the treatment. To reveal more detailed information it would also be crucial to assess these impacts on selected populations. Based on previous reports it is likely that SCs are more resistant to apoptosis [109, 113, 327] e.g. through expression of NF-κB [109, 113]. The differential findings concerning the apoptotic sensitivity in cell lines vs. primary cells confirm the importance of the use of cells from primary tissues for research.

4.5 The role of ABC-transporters in mediating therapy-resistance

4.5.1 Gene expression analysis of ABC-transporters

ABC multidrug transporters are expressed in many human tumours. They are a major cause of chemoresistance and have also been identified in prostate cell lines and primary prostate cells [266, 267, 299, 300]. Our gene expression analysis of ABC-transporters in SCs and CBs from malignant and benign primary prostate tissues indicated the presence of ABC-transporters in SCs and CBs, suggesting they might be a factor in therapy failure. Out of the 10 ABC-transporters present on the array ABCB1 (Pg-G), ABCC1 (MRP-1), ABCG2 (MRP), ABCC3 and ABCC6 are known to transport etoposide [279, 280]. In particular ABCB1, ABCC1 and ABCG2 belong to the three major types of ABC-transporters correlated with drug resistance and were therefore of further interest. The ABCB1 gene is expressed in many cancer cells including primary malignant and non-malignant prostate cells [266, 302], whereas other studies revealed that it is not present at the protein level [303, 328]. In our gene expression analysis ABCB1 was found in about 50% of the tested samples, even though its expression at mRNA level was very low in comparison to other ABC-transporters. ABCB1 is therefore unlikely to play a main role in drug resistance. Further etoposide-transporting proteins such as ABCG2, ABCC1, ABCC3 and ABCC6 were

(highly) expressed in all of the samples tested. In particular the expression of ABCG2 and ABCC1 has been reported for primary prostate tissue and prostate cell lines and is in accordance with our results [266, 267, 299, 300]. Interestingly, the etoposide-transporting ABCC1 is more highly expressed in malignant and benign SCs, whereas ABCB5 (which is not known to transport etoposide) is significantly highly expressed in CBs. These data suggest that malignant and benign SCs might be able to eliminate etoposide more efficiently, due to increased ABCC1 expression. However, some ABC-transporters which are not known as etoposide transporting systems might still be able to efflux etoposide, even if not specifically described in the literature. Following this gene expression analysis we decided to pursue a functional assay for ABC-transporters.

4.5.2 Calcein efflux assays to assess the functionality of ABC-transporters in primary prostate tissue

In order to reveal more information about a potential influence of ABC-transporters on drug resistance we applied calcein efflux assays to selected populations of primary prostate cells. Among other advantages (as described in results) calcein was considered as a suitable substance as it is a substrate of ABCC1. The application of calcein efflux assays demonstrated that malignant and benign SCs and their corresponding TAs and CBs were all able to efflux calcein, but SCs did not display enhanced efflux capabilities. A similar trend was observed in a series of experiments carried out by one of our lab members (David Hudson) aimed to define the so-called "side population" with Hoechst 33342 (transported by ABCG2 and ABCB1, but not by ABCC1) in primary malignant and benign prostate cells. This "side population" has been described by other groups as a rare ABCG2-positive population within a total population of cells that has SC characteristics and the ability to efflux fluorescent substances such as dye

cycle violet or Hoechst 33342 more efficiently than non-SCs [299, 300, 304]. However, in the previously described study with Hoechst 33342, our lab could not identify the "side population". The calcein assays and the Hoechst 33342 experiments covered the three main ABC-transporters and no specific efflux capabilities were seen in SCs. Our results suggest that malignant and benign SCs do not harbor increased efflux properties that might be an advantage in therapy survival. Based on these findings, the primary cause for the higher *in vitro* resistance to etoposide observed in malignant and benign SCs compared to their differentiated counterparts probably resides with other factors. Our findings are in contradiction to Brown et al. that has defined a "side population" of ABCG2-expressing malignant and benign prostate cells derived from primary tissues [305]. Possible explanations for these conflicting data might be factors such as a different type of preparation or differential growth conditions.

Even if ABC-transporters were a primary cause for therapy resistance, attempts to improve the therapeutic outcome by inhibiting ABC-transporters have mainly failed in clinical trials. For example, blocking one of the most commonly known drug resistance proteins ABCB1 revealed only disappointing results, due to a lack of confirmation of ABCB1 expression in the tumour tissue prior to the administration of the treatment, lack of evidence of ABCB1 inhibition *in vivo* and ABCB1 inhibitor toxicity [329]. In patients with prostate cancer, ABC-transporters have been shown to influence the clinical outcome e.g. genetic variations in ABCB1 influence the toxicity and success of docetaxel therapy [301]. However, inhibitors of ABC-transporters are not in clinical use for the treatment of prostate cancer. Furthermore, even if blocking of ABC-transporters could be easily achieved

in the clinic, it would be likely that additional mechanisms of therapy-resistance prevent successful treatment.

4.5.3 Limitations of the calcein assay

The performance of calcein assays came with some challenges, which were mainly a consequence of the small SC numbers available, which limited the possibilities of the experimental design. The best option would have been a reagent that was highly fluorescent, transported by the three major ABC-transporters and did not rely on metabolism. All of the available substances on the market such as doxorubicin, daunorubicin, mixatrone, Hoechst 33342 and newer ones such as eFluxx—ID Green and Gold lack at least one of these features [281]. Another general limitation of efflux assays (including calcein assays) needs to be taken into consideration: a substance might be effluxed faster than its measurement in the cytoplasm can be conducted. For example in the case of calcein assays, the non-fluorescent calcein-am could be exported before its metabolism into the fluorescent calcein. However, for our study the risk of this effect is considered to be small, since:

- Calcein-am is a substrate of ABCB1, which was only present in about 50% of our samples and furthermore only weakly expressed.
- The other two main ABC-transporters ABCG2 and ABCC1 do not appear to efflux calcein-am. ABCC1 takes calcein as a substrate but here no differences were observed among the populations.

The available kits for efflux studies are certainly suitable for different kinds of studies, such as those that test efflux before and after application of an inhibitor, but are not ideal when comparing efflux in different cell types, in particular when cell numbers are limited.

In addition to the previously described calcein assays, an interesting type of experiment would be the use of an inhibitor against an efflux pump e.g. agosterol A or raloxifine against ABCC1 (significantly elevated at mRNA level in malignant and benign SCs) and subsequent assessment of calcein levels. A higher amount of calcein in the cytoplasm of inhibitor-treated cells vs. non-inhibitor-treated cells would have confirmed efflux and allowed firmer conclusions about the efficiency of the efflux pump. An inhibitor of ABCB1 e.g. verapamil would block a potential efflux of the non-fluorescent calcein-am. This would have eliminated some previously described issues: when calcein-am is prevented from exiting the cell, an accumulation of fluorescent calcein should be visible after time. The extent of calcein accumulation would allow conclusions regarding the efficiency of the pump when comparing it to a non-inhibitor treated control. However, these studies can only be performed, if a sufficient SC yield is available, which is usually not the case. A further interesting experiment would have been the use of inhibitors in combination with a chemotherapeutic drug, and the subsequent assessment of DNA damage or clonogenic recovery. However, three facts lead to the consideration that malignant and benign SCs are not in advantage due to increase effux capabilities:

- At mRNA level we only found similar expressions of ABC-transporters in benign and malignant SCs and CBs (only ABCC1 and ABCB5 were different)
- The selected populations in our calcein assays did not show significant efflux capabilities
- This finding was backed up by independently performed tests with Hoechst 33342

In view of the finding that functional assays referring to the three main ABC-transporters showed negative results, it was decided to focus on other potential mechanisms of therapy resistance.

4.6 Concluding remarks

In summary, our findings suggest that SCs from malignant and benign prostate tissues are more resistant to treatment than the corresponding TAs and CBs originating from the same outgrowth. Indeed, chemotherapy is not successful for the treatment of advanced prostate cancer, and this resistance might be mediated by surviving CSCs that repopulate the tumour mass. One important factor in therapy resistance might be cellular quiescence, as we can confirm for the SCs isolated from malignant and benign prostate tissues. The role of healthy SCs is to repair and repopulate a tissue after wounding. Therapies that decrease tumour size can be thought of as initiating an injury, to which the CSCs responds by going back into a proliferative stage [33]. In malignant tissue, this response might result in an increase in the tumour initiating or metastasis establishing cell pool [33]. Recently, the FDA in the USA has warned about the use of chemotherapy for the treatment of prostate cancer with inhibitors of 5-alpha reductase, which are designed to targets AR+ luminal cells [33]. Studies suggest that these agents promote poorly differentiated tumours in patients who had a pre-existing tumour [33]. This is the likely response after the elimination of differentiated luminal cells resulting in the promotion of basal-like tumour cells.

Due to this potentially fatal role for CSCs in therapeutic outcome, it is crucial to elucidate their mechanisms of therapy survival further. In addition to quiescence as demonstrated in our study, there might be a wide range of other mechanisms. For instance, it would have been interesting to assess

the role of ROS detoxifying enzymes in SCs isolated from prostate tumours. It would have also been logical to assess the role of autophagy in apoptotic inhibition further. Upon the confirmation of SCs relevance in treatment resistance to conventional therapies a screen to identify agents that specifically target CSCs would have been an important step. The elucidation of these mechanisms and the identification of treatments to block them might be an important future direction for the elimination of prostate tumours.

Appendix

Chapter III Results: Comet assays

Figure 3-5: Alkaline Comet assays less than 50 events. Due to the availability of SCs a lower number of events (lower than 50) had to be analyzed for the alkaline comet assays (cancer and benign samples).

SCs 45 min, 250 µM		
sample	number of cells	data point in graph
H031/10	38	1.36
Y025/09	11	1.6
SCs 3 h, 30µM		
sample	number of cells	data point in graph
H018/09	23	3.09
Y004/09	40	0.662
H035/11	43	1.09

Figure 3-5: p-values determined by Wilcoxon rank sum test for alkaline comet assays (cancer and benign samples). Significant p-values shown in **bold**.

45 min, 30 µM	
SC vs. CB	**p=0.007**
SC vs. TA	**p= <0.001**
CB vs. TA	p=0.257
45 min, 250 µM	
SC vs. CB	p= 0.686
SC vs. TA	**p = 0.0029**
CB vs. TA	p = 0.114
3 h, 30 µM	
SC vs. CB	P = 0.222
SC vs. TA	p = 0.056
CB vs. TA	p = 0.421
3 h, 250 µM	
SC vs. CB	p = 0.667
SC vs. TA	p = 0.667
CB vs. TA	p = 0.667

Figure 3-6 A: p-values determined by Wilcoxon rank sum test for alkaline comet assays (cancer samples). Significant p-values shown in **bold**.

45 min, 30 µM	
SC vs. CB	p= 0.095
SC vs. TA	**p= 0.008**

CB vs. TA	P=0.0421

Figure 3–6 B: p–values for alkaline comet assays determined by Wilcoxon rank sum test (benign samples). Significant p–values shown in **bold.**

45 min, 30 µM	
SC vs. CB	p= 0.056
SC vs. TA	**p= 0.008**
CB vs. TA	P=0.548

Chapter III Results: γH2A.X assays

Figure 3–11: p–values determined by Wilcoxon rank sum test for γH2A.X assays (cancer samples). Significant p–values shown in **bold.**

45 min, 30 µM	
SC vs. TA	**p=0.032**
24 h, 30 µM	
SC vs. TA	p=0.114

Figure 3–12: p–values determined by Wilcoxon rank sum test for γH2A.X assays (benign samples).

45 min, 30 µM	
SC vs. TA	p=0.222
24 h, 30 µM	
SC vs. TA	p=0.310

Figure 3–11 and Figure 3–12: p–values yH2A.X assays determined by paired t–test and Wilcoxon rank sum test to assess repair. Significant p–values are shown in **bold.**

Paired t–test	
Cancer	
SC 45 min vs. SC 24 h	P = 0.222
TA 45 min vs. TA 24 h	P = 0.117
Benign	
SC 45 min vs. SC 24 h	**p=0.047**
TA 45 min vs. TA 24 h	**p=0.047**
Wilcoxon signed rank test	
Cancer	
SC 45 min vs. SC 24 h	P = 0.250
TA 45 min vs. TA 24 h	P = 0.250
Benign	
SC 45 min vs. SC 24 h	P = 0.063

TA 45 min vs. TA 24 h	P = 0.063

Figure 3–13 A–D: p-values determined by Wilcoxon rank sum test for the quantification of different γH2A.X foci types (benign and malignant samples). Significant p-values are shown in **bold**.

Quantification of different foci types	
Cancer 45 min, 30 µM	SC vs. TA
5–10 foci	p = 0.841
>10	**p = 0.032**
PL	p = 0.421
PI	p = 0.548
PS	p = 0.841
Cancer 24 h, 30 µM	SC vs. TA
5–10 foci	p = 1.000
>10	p = 0.100
PL	p = 0.400
PI	p = 0.200
PS	p = 0.200
Benign 45 min, 30 µM	SC vs. TA
5–10 foci	p = 0.310
>10	p = 0.421
PL	p = 1.000
PI	p = 0.421
PS	p = 0.222
Benign 24 h, 30 µM	SC vs. TA
5–10 foci	p = 0.421
>10	p = 0.095
PL	p = 0.841
PI	p = 0.310
PS	p = 0.690

Figure 3–13 A–D: Fold-changes for the quantification of different γH2A.X foci types (benign and cancer samples). The median values graphed in Figure 3–13 A–D are highlighted in pink. The fold changes were calculated by dividing the percentage of γH2A.X positive cells after treatment (45 min or 24 h time point) by the percentage before treatment. A 1-fold change was considered as no change, a fold change > 1 was considered as an increase and a fold change <1 was considered as decrease. When 0 cells were positive for a distinct yH2A.X pattern 0 was replaced by 1 to calculate an approximate fold change.

Cancer: SC; 45 min, 30 µM					
Sample	H035/11	PE665	H054/11	H048/11	H049/11
5 to 10 foci	0.85 to 7.69	0.81 to 3.2	0 to 2.56	0 to 0	2.83 to 0.85

fold change	9.047058824	3.950617284	2.56	1	0.300353357
> 10	4.24 to 6.73	8.87 to 4	8.40 to 10.26	4.85 to 3.85	5.66 to 38.14
fold change	1.587264151	0.450958286	1.221428571	0.793814433	6.734982332
PL	16.10 to 8.65	3.23 to 21.6	3.36 to 7.69	2.91 to 7.69	0.94 to 1.69
fold change	0.537267081	6.687306502	2.288690476	2.642611684	1.79787234
PI	4.24 to 6.73	0.81 to 18.4	15.97 to 10.26	1.94 to 5.77	2.83 to 3.39
fold change	1.587264151	22.71604938	0.642454602	2.974226804	1.197879859
PS	1.69 to 1.92	1.61 to 1.6	0 to 3.85	0 to 0	0 to 12.71
fold change	1.136094675	0.99378882	3.85	1	12.71

Cancer: TA; 45 min, 30 µM					
Sample	H035/11	PE665	H054/11	H048/11	H049/11
5 to 10 foci	2.1 to 4.38	0 to 17.61	1.35 to 5	0 to 1.47	0 to 0
fold change	2.085714286	17.61	3.703703704	1.47	1
> 10	5.6 to 29.2	4.20 to 26.06	6.08 to 45	0 to 9.56	3.5 to 54.14
fold change	5.214285714	6.204761905	7.401315789	9.65	15.46285714
PL	2.8 to 7.3	0 to 10.56	2.70 to 0.83	0 to 7.35	1.4 to 8.27
fold change	2.607142857	10.56	0.307407407	7.35	5.907142857
PI	1.4 to 16.79	0 to 12.68	4.73 to 15	0 to 2.21	0 to 0.75
fold change	11.99285714	12.68	3.171247357	2.21	0.75
PS	1.4 to 1.46	0 to 11.27	0 to 1.67	4.41 to 0	0.7 to 21.05
fold change	1.042857143	11.27	1.67	0.22675737	30.07142857

Cancer: SC; 24 h, 30 µM			
Sample	H035/11	H054/11	H049/11
5 to 10 foci	0.85 to 1.64	0 to 0.98	2.83 to 1.39
fold change	1.929411765	0.98	0.491166078
> 10	4.24 to 0.82	8.40 to 0	5.66 to 0.7
fold change	0.193396226	0.119047619	0.123674912
PL	16.10 to 11.48	3.36 to 5.88	0.94 to 10.42
fold change	0.713043478	1.75	11.08510638
PI	4.24 to 3.28	15.97 to 8.82	2.83 to 9.03
fold change	0.773584906	0.552285535	1.197879859
PS	1.69 to 1.64	0 to 0	0 to 0
fold	0.970414201	1	1

change			

Cancer: TA; 24 h, 30 µM			
Sample	H035/11	H054/11	H049/11
5 to 10 foci	2.1 to 4.03	1.35 to 0	0 to 9.68
fold change	1.919047619	0.740740741	1
> 10	5.6 to 2.42	6.08 to 1.71	3.5 to 7.26
fold change	0.432142857	0.28125	2.074285714
PL	2.8 to 23.39	2.70 to 12.82	1.4 to 21.77
fold change	8.353571429	4.748148148	15.55
PI	1.4 to 12.9	4.73 to 5.13	0 to 13.71
fold change	9.214285714	1.084566596	13.71
PS	1.4 to 3.23	0 to 0	0.7 to 4.03
fold change	2.307142857	1	5.757142857

Benign: SC; 45 min, 30 µM					
Sample	HO53/11	YO25/09	YO30/11	YO23/09	YO31/11
5 to 10 foci	0 to 2.86	0.75 to 0.97	0 to 0	0.81 to 0.75	1.89 to 1.03
fold change	2.86	1.293333333	1	0.925925926	0.825242718
> 10	0.86 to 15.24	3.76 to 5.83	2.44 to 0	4.03 to 18.05	3.77 to 7.22
fold change	17.72093023	1.550531915	0.409836066	4.478908189	1.915119363
PL	5.17 to 9.52	1.50 to 18.45	0 to 7.84	8.87 to 14.29	10.38 to 15.46
fold change	1.84139265	12.3	7.84	1.611048478	1.489402697
PI	8.62 to 6.67	0 to 9.71	6.1 to 2.94	4.03 to 21.05	1.89 to 22.68
fold change	0.773781903	9.71	0.481967213	5.223325062	12
PS	0 to 0	1.5 to 0.97	0 to 0	0 to 0.75	0 to 1.03
fold change	1	0.646666667	1	0.75	1.03

Benign: SC; 24 h,30 µM					
Sample	HO53/11	YO25/09	YO30/11	YO23/09	YO31/11
5 to 10 foci	0 to 5.45	0.75 to 0	0 to 0	0.81 to 2.24	1.89 to 5.97
fold change	5.45	1.333333333	1	2.765432099	3.158730159
> 10	0.86 to 0	3.76 to 0	2.44 to 0	4.03 to 0	3.77 to 0.75

fold change	1.162790698	0.265957447	0.409836066	0.248138958	0.198938992
PL	5.17 to 14.55	1.50 to 9.64	0 to 2.4	8.87 to 11.94	10.38 to 12.69
fold change	2.814313346	6.426666667	2.4	1.346110485	1.222543353
PI	8.62 to 3.64	0 to 2.41	6.1 to 3.2	4.03 to 0.75	1.89 to 16.42
fold change	0.422273782	2.41	0.524590164	0.186104218	8.687830688
PS	0 to 0	1.5 to 0	0 to 0	0 to 0	0 to 0
fold change	1	0.666666667	1	1	1

Benign: TA; 45 min, 30 µM					
Sample	HO53/11	YO25/09	YO30/11	YO23/09	YO31/11
5 to 10 foci	0.83 to 0	6.29 to 3.05	2.4 to 6.02	1.72 to 0.74	11.67 to 0
fold change	1.204819277	0.484896661	2.508333333	0.430232558	0.085689803
> 10	10 to 78.81	1.4 to 9.92	1.2 to 8.27	2.87 to 20.74	5 to 7.53
fold change	7.881	7.085714286	6.891666667	7.226480836	1.506
PL	0.83 to 0	2.8 to 12.98	1.8 to 8.27	5.17 to 11.85	5.83 to 15.07
fold change	1.204819277	4.635714286	4.594444444	2.292069632	2.58490566
PI	0.83 to 4.24	2.1 to 31.3	2.4 to 12.78	8.62 to 29.3	0.83 to 27.4
fold change	5.108433735	14.9047619	5.325	3.399071926	33.01204819
PS	0 to 2.54	0 to 4.58	0.6 to 0	0 to 0	0 to 0.68
fold change	2.54	4.58	1.666666667	1	0.68

Benign: TA; 24 h, 30 µM					
Sample	HO53/11	YO25/09	YO30/11	YO23/09	YO31/11
5 to 10 foci	0.83 to 8	6.29 to 4.51	2.4 to 0	1.72 to 5.13	11.67 to 3.85
fold change	9.638554217	0.723370429	0.416666667	2.98255814	0.329905741
> 10	10 to 3.2	1.4 to 13.53	1.2 to 0	2.87 to 17.09	5 to 3.08
fold change	0.32	9.664285714	0.833333333	5.954703833	0.616
PL	0.83 to 5.6	2.8 to 6.02	1.8 to 10.07	5.17 to 2.56	5.83 to 16.15
fold change	6.746987952	2.15	5.594444444	0.49516441	2.770154374
PI	0.83 to 0.8	2.1 to 9.77	2.4 to 4.32	8.62 to 14.53	0.83 to 13.08
fold change	0.963855422	4.652380952	1.8	1.685614849	15.75903614
PS	0 to 0	0 to 0	0.6 to 2.16	0 to 0.85	0 to 0
fold change	1	1	3.6	0.85	1

Chapter III Results: Clonogenic assays

Figure 3–16 A–C: Detailed information about the colony sizes including STDVs

unselected	Etoposide 45 min , 30 µM			DMSO		
Y030/11			STDV			STDV
	all	0.83	0.29	all	30.17	1.44
	2+	0	0	2+	1	1
	4+	0	0	4+	2,67	0.29
	8+	0.5	0.5	8+	10.5	1.32
	16+	0.33	0.58	16+	9.83	2.02
	32+	0	0	32+	6.17	1.26
	Etoposide 45 min, 250 µM			DMSO		
			STDV		unselected	STDV
	all	0	0	all	33.17	17.56
	2+	0	0	2+	0.33	0.29
	4+	0	0	4+	4.67	2.84
	8+	0	0	8+	9.33	7.59
	16+	0	0	16+	11.17	2.89
	32+	0	0	32+	7.67	4.51
	Etoposide 3 h, 30 µM			DMSO		
			STDV		unselected	STDV
	all	0	0	all	29.5	8.53
	2+	0	0	2+	0.83	1.04
	4+	0	0	4+	5.17	1.15
	8+	0	0	8+	8.5	0
	16+	0	0	16+	9.33	3.82
	32+	0	0	32+	5.67	2.75
	Etoposide 3 h, 250 µM			DMSO		
		unselected	STDV		unselected	STDV
	all	0	0	all	33.5	5.41
	2+	0	0	2+	0.5	0.5
	4+	0	0	4+	5.33	1.15
	8+	0	0	8+	8.33	2.03
	16+	0	0	16+	11	3.5
	32+	0	0	32+	8.33	3.79

Sample	Day 3, DMSO				
PE531	Colony size	TA	SC	TA STDV	SC STDV
	all	13.25	9.51	11.5	4.6
	2+	3.89	3.03	3.53	3.88
	4+	6.98	5.91	6.9	2.2
	8+	2.38	0.56	4.12	0.98
	16+	0	0	0	0
	32+	0	0	0	0
	Day 3, Etoposide 45 min, 30 µM				
	Colony size	TA	SC	TA STDV	SC STDV
	all	0.61	0	1.05	0
	2+	0	0	0	0

Colony size	TA	SC	TA STDV	SC STDV
4+	0.61	0	1.05	0
8+	0	0	0	0
16+	0	0	0	0
32+	0	0	0	0
Day 6, DMSO				
Colony size	TA	SC	TA STDV	SC STDV
all	46.61	46.17	7.94	19.53
2+	0	1.7	0	1.87
4+	1.13	2.73	1.96	1.01
8+	12.41	10.74	5.09	4.73
16+	15.34	11.98	7.37	6.48
32+	16.72	19.02	2.22	6.72
Day 6, Etoposide 45 min, 30 µM				
Colony size	TA	SC	TA STDV	SC STDV
all	4.34	12.21	4.73	3.92
2+	0.52	0	0.9	0
4+	0	0.93	0	1.6
8+	0	4.26	0	1.1
16+	3.82	4.87	3.91	1.01
32+	0	2.14	0	0.55

Sample	Day 4, DMSO				
H035/11	Colony size	TA	SC	TA STDV	SC STDV
	all	0.67	15.38	0.58	10.5
	2+	0	0.38	0	0.66
	4+	0	4.23	0	4.26
	8+	0.33	8.47	0.58	7.46
	16+	0	1.91	0	2.4
	32+	0.33	0.38	0.58	0.66
	Day 4, Etoposide 45 min, 30 µM				
	Colony size	TA	SC	TA STDV	SC STDV
	all	0	0.45	1.05	0
	2+	0	0	0	0
	4+	0	0	0	0
	8+	0	0	0	0
	16+	0	0	0	0
	32+	0	0.45	0	0.78
	Day 8, DMSO				
	Colony size	TA	SC	TA STDV	SC STDV
	all	7.67	14.73	5.03	3.03
	2+	0	0	0	0
	4+	0.33	0	0.58	0
	8+	0	0	0	0
	16+	2.33	2.79	2.52	2.52
	32+	5	11.94	2	1.65
	Day 8, Etoposide 45 min, 30 µM				
		TA	SC	TA STDV	SC STDV
	all	1.67	5.47	1.15	0.95
	2+	0	0.45	0	0.78
	4+	0	0.36	0	0.62
	8+	0.33	0.36	0.58	0.62
	16+	0.33	1.52	0.58	2.62

32+		1	2.79	1	2.42

Figure 3–17 A–C: Detailed information about the colony sizes including STDVs and p-values

Sample	Colony size	%TA colonies normalized to vehicle control	%SC colonies normalized to vehicle control	TA STDV	SC STDV
H035/11	all	21.74	37.13	15.06	6.48
	2+	0	3.06	0	5.3
	4+	0	2.43	0	4.22
	8+	4.35	2.43	7.53	4.22
	16+	4.35	10.29	7.53	17.82
	32+	13.04	18.91	13.04	16.4
PE531	all	9.51	26.45	10.36	8.5
	2+	1.14	0	1.98	0
	4+	0	2	0	3.47
	8+	0	9.26	0	2.4
	16+	8.37	10.55	8.57	2.2
	32+	0	4.63	0	1.2
H087/11	all	10.44	17.16	5.5	11.71
	2+	0	2.52	0	4.36
	4+	2.99	7.33	2.63	7.56
	8+	3.46	2.52	6	4.36
	16+	2.66	0	4.61	0
	32+	1.33	4.8	2.31	4.17
H049/11	all	23.22	22.44	7.04	13.58
	2+	0	2.23	0	1.97
	4+	4.44	4.5	3.88	4
	8+	1.58	5.74	2.74	5.62
	16+	9.68	0.98	0.49	1.7
	32+	7.51	8.98	1.76	13.09
H048/11	all	6.45	11.55	4.39	6.4
	2+	0	0.76	0	1.32
	4+	0.23	2.41	0.41	0.32
	8+	3.06	3.81	2.67	4.43
	16+	1.68	2.28	1.54	3.96
	32+	1.46	2.28	1.27	3.96
H054/11	all	8.61	25.38	2.65	3.1
	2+	0	0	0	0
	4+	1.09	2.7	0.61	2.36
	8+	1.63	10.22	0.18	8.98
	16+	3.2	8.07	2.4	5.1
	32+	2.68	4.4	0.85	1.92
Y062/11	all	33.36	78.81	12.03	75.65
	2+	0	0	0	0
	4+	0	0	0	0
	8+	14.1	53.67	15.5	46.76
	16+	3.82	0	6.61	0
	32+	15.44	25.14	17.78	43.55

Y031/11	all	21.66	1.69	27.45	1.53
	2+	0	0	0	0
	4+	2.74	0	4.74	0
	8+	4.63	0.69	4.3	1.19
	16+	10.13	0.5	14.92	0.86
	32+	4.17	0.5	3.52	0.86
Y030/11	all	6.82	12.94	1.13	3.03
	2+	0	0	0	0
	4+	0	0	0	0
	8+	1.24	5.92	0.91	1.36
	16+	2.79	4.93	1.59	1.97
	32+	2.79	2.09	0.86	2.59

Figure 3-17 A and B: p -values for the clonogenic assays

Sample	SC vs. TA
H035/11	p = 0.400
PE531	p = 0.100
H048/11	p = 0.400
H087/11	p= 0.700
H049/11	p = 1.000
H054/11	p = 0.100
Y062/11	p= 0.700
Y031/11	p = 0.100
Y030/11	p = 0.100

Etoposide 3 h, 30 µM				
Colony size	TA	SC	TA STDV	SC STDV
all	0	7.07	0	12.25
2+	0	0	0	0
4+	0	0	0	0
8+	0	4.72	0	8.17
16+	0	0	0	0
32+	0	2.36	0	0

Chapter III Results: KI67

Figure 3-19 A-B: p-values for Ki67 assessment. Significant p-values are shown in **bold.**

Malignant	
TA vs. SC	**P = 0.016**
CB vs. SC	**P = 0.008**
CB vs. TA	p = 0.310
Benign	
TA vs. SC	P=0.065

CB vs. SC	P=0.065
CB vs. TA	p=0.31

Chapter III Results: MTS assay

Figure 3-20: Concentrations for MTS assay

Concentration→ Replication inhibitor↓						
Camptothecin	32µM	12.8µM	5.1µM	2µM	0.8µM	0.32µM
Carboplatin	64µM	25.6µM	10.2µM	4.1µM	1.6µM	0.6µM
Docetaxel	12.8µM	5.12µM	2µM	0.8µM	0.32µM	0.128µM
Doxorubicin	12.8µM	5.12µM	2µM	0.8µM	0.32µM	0.128µM
Etoposide	64µM	25.6µM	10.2µM	4.1µM	1.6µM	0.6µM
DMSO (carrier)	1:1562	1:3906	1:9762	1:24406	1:61015	1:152539

Chapter III: Calcein efflux assays

Figure 3-27 D: STDVs for calcein efflux

STDVs of the triplicates measured for H054/11				
	15 min	1 h	2 h	3 h
CB	1131.8491	2483.0989	1826.0665	949.28763
TA	5763.4303	4613.0499	4088.4203	4281.2879

Figure 3-31: STDVs for calcein efflux and p-values

H054/11	STDV
TA	26.683004
CB	7.6389123
H092/11	STDV
TA	11.352347
CB	21.206506
H035/11	STDV
TA	12.294343
CB	18.578056
Y030/11	STDV
TA	12.268419
CB	4.9243582
Y075/11	STDV

TA	14.040624
CB	11.879222

SC vs. TA	SC vs. CB	TA vs. CB
P = 0.690	P = 0.690	P = 1.000

Permission from Elsevier for Figure 1–1

Order Completed

Thank you very much for your order.

This is a License Agreement between Sandra Klein ("You") and Nature Publishing Group ("Nature Publishing Group"). The license consists of your order details, the terms and conditions provided by Nature Publishing Group, and the payment terms and conditions.

Get the printable license.

License Number	3095590502025
License date	Feb 24, 2013
Licensed content publisher	Nature Publishing Group
Licensed content publication	Nature Reviews Cancer
Licensed content title	Inflammation in prostate carcinogenesis
Licensed content author	Angelo M. De Marzo, Elizabeth A. Platz, Siobhan Sutcliffe, Jianfeng Xu, Henrik Gronberg et al.
Licensed content date	Apr 1, 2007
Type of Use	reuse in a thesis/dissertation
Volume number	7
Issue number	4
Requestor type	non-commercial (non-profit)
Format	print and electronic
Portion	figures/tables/illustrations
Number of figures/tables /illustrations	1
High-res required	no
Figures	Figure 1
Author of this NPG article	no
Your reference number	
Title of your thesis / dissertation	Comparison of the DNA damage response and mechanisms of treatment resistance in stem cells originating from malignant and benign prostate tissues and their differentiated counterparts
Expected completion date	Feb 2013
Estimated size (number of pages)	203
Total	0.00 GBP

Permission from Elsevier for Figure 1-2

Supplier	Elsevier Limited The Boulevard,Langford Lane Kidlington,Oxford,OX5 1GB,UK
Registered Company Number	1982084
Customer name	Sandra Klein
Customer address	School Lane York, UK YO10
License number	2974210783813
License date	Aug 22, 2012
Licensed content publisher	Elsevier
Licensed content publication	European Journal of Cancer
Licensed content title	Prostate cancer stem cells
Licensed content author	Anne T. Collins,Norman J. Maitland
Licensed content date	June 2006
Licensed content volume number	42
Licensed content issue number	9
Number of pages	6
Start Page	1213
End Page	1218
Type of Use	reuse in a thesis/dissertation
Portion	figures/tables/illustrations
Number of figures/tables /illustrations	1
Format	both print and electronic
Are you the author of this Elsevier article?	No
Will you be translating?	No
Order reference number	
Title of your thesis/dissertation	Comparison of the DNA damage response and mechanisms of treatment resistance in stem cells originating from malignant and benign prostate tissues and their differentiated counterparts
Expected completion date	Aug 2012
Estimated size (number of pages)	200
Elsevier VAT number	GB 494 6272 12
Permissions price	0.00 GBP
VAT/Local Sales Tax	0.0 USD / 0.0 GBP
Total	0.00 GBP

Permission from Elsevier for Figure 1–4

Supplier	Elsevier Limited The Boulevard,Langford Lane Kidlington,Oxford,OX5 1GB,UK
Registered Company Number	1982084
Customer name	Sandra Klein
Customer address	School Lane
	York, UK YO10
License number	2971910576053
License date	Aug 18, 2012
Licensed content publisher	Elsevier
Licensed content publication	Pattern Recognition Letters
Licensed content title	Prostate cancer grading: Gland segmentation and structural features
Licensed content author	Kien Nguyen,Bikash Sabata,Anil K. Jain
Licensed content date	1 May 2012
Licensed content volume number	33
Licensed content issue number	7
Number of pages	11
Start Page	951
End Page	961
Type of Use	reuse in a thesis/dissertation
Portion	figures/tables/illustrations
Number of figures/tables/illustrations	1
Format	both print and electronic
Are you the author of this Elsevier article?	No
Will you be translating?	No
Order reference number	
Title of your thesis/dissertation	Comparison of the DNA damage response and mechanisms of treatment resistance in stem cells originating from malignant benign prostate tissues and their differentiated counterparts
Expected completion date	Aug 2012
Estimated size (number of pages)	200
Elsevier VAT number	GB 494 6272 12
Permissions price	0.00 USD
VAT/Local Sales Tax	0.0 USD / 0.0 GBP

References

1.	Cunha, G.R., et al., *The endocrinology and developmental biology of the prostate.* Endocr Rev, 1987. **8**(3): p. 338-62.
2.	McNeal, J.E., *The zonal anatomy of the prostate.* Prostate, 1981. **2**(1): p. 35-49.
3.	Swift, S.L., *A novel approach to prostate cancer gene therapy: targeting neurotensin receptors with baculovirus*, in *Department of Biology*2008, University of York: York. p. 272.
4.	Collins, A.T. and N.J. Maitland, *Prostate cancer stem cells.* Eur J Cancer, 2006. **42**(9): p. 1213-8.
5.	Lilja, H. and P.A. Abrahamsson, *Three predominant proteins secreted by the human prostate gland.* Prostate, 1988. **12**(1): p. 29-38.
6.	Berry, P.A., N.J. Maitland, and A.T. Collins, *Androgen receptor signalling in prostate: effects of stromal factors on normal and cancer stem cells.* Mol Cell Endocrinol, 2008. **288**(1-2): p. 30-7.
7.	Sar, M., et al., *Immunohistochemical localization of the androgen receptor in rat and human tissues.* Endocrinology, 1990. **127**(6): p. 3180-6.
8.	Maitland, N.J. and A.T. Collins, *Prostate cancer stem cells: a new target for therapy.* J Clin Oncol, 2008. **26**(17): p. 2862-70.
9.	Kyprianou, N. and J.T. Isaacs, *Activation of programmed cell death in the rat ventral prostate after castration.* Endocrinology, 1988. **122**(2): p. 552-62.
10.	Bonkhoff, H. and K. Remberger, *Widespread distribution of nuclear androgen receptors in the basal cell layer of the normal and hyperplastic human prostate.* Virchows Arch A Pathol Anat Histopathol, 1993. **422**(1): p. 35-8.
11.	Collins, A.T., et al., *Identification and isolation of human prostate epithelial stem cells based on alpha(2)beta(1)-integrin expression.* J Cell Sci, 2001. **114**(Pt 21): p. 3865-72.
12.	English, H.F., R.J. Santen, and J.T. Isaacs, *Response of glandular versus basal rat ventral prostatic epithelial cells to androgen withdrawal and replacement.* Prostate, 1987. **11**(3): p. 229-42.
13.	Moore, K.A. and I.R. Lemischka, *Stem cells and their niches.* Science, 2006. **311**(5769): p. 1880-5.
14.	Schofield, R., *The relationship between the spleen colony-forming cell and the haemopoietic stem cell.* Blood Cells, 1978. **4**(1-2): p. 7-25.
15.	Hudson, D.L., et al., *Proliferative heterogeneity in the human prostate: evidence for epithelial stem cells.* Lab Invest, 2000. **80**(8): p. 1243-50.
16.	Robinson, E.J., D.E. Neal, and A.T. Collins, *Basal cells are progenitors of luminal cells in primary cultures of differentiating human prostatic epithelium.* Prostate, 1998. **37**(3): p. 149-60.
17.	Bonkhoff, H. and K. Remberger, *Differentiation pathways and histogenetic aspects of normal and abnormal prostatic growth: a stem cell model.* Prostate, 1996. **28**(2): p. 98-106.
18.	Lang, S.H., et al., *Experimental prostate epithelial morphogenesis in response to stroma and three-dimensional matrigel culture.* Cell Growth Differ, 2001. **12**(12): p. 631-40.
19.	Oldridge, E.E., et al., *Prostate cancer stem cells: Are they androgen-responsive?* Mol Cell Endocrinol, 2012. **360**(1-2): p. 14-24.
20.	Bonkhoff, H., U. Stein, and K. Remberger, *Endocrine-paracrine cell types in the prostate and prostatic adenocarcinoma are postmitotic cells.* Hum Pathol, 1995. **26**(2): p. 167-70.

21. di Sant'Agnese, P.A., *Neuroendocrine differentiation in carcinoma of the prostate. Diagnostic, prognostic, and therapeutic implications.* Cancer, 1992. **70**(1 Suppl): p. 254-68.

22. Condon, M.S. and M.C. Bosland, *The role of stromal cells in prostate cancer development and progression.* In Vivo, 1999. **13**(1): p. 61-5.

23. De Marzo, A.M., et al., *Inflammation in prostate carcinogenesis.* Nature reviews. Cancer, 2007. **7**(4): p. 256-69.

24. McNeal, J.E., *Origin and evolution of benign prostatic enlargement.* Invest Urol, 1978. **15**(4): p. 340-5.

25. McNeal, J.E., *Normal histology of the prostate.* Am J Surg Pathol, 1988. **12**(8): p. 619-33.

26. McNeal, J.E., et al., *Zonal distribution of prostatic adenocarcinoma. Correlation with histologic pattern and direction of spread.* Am J Surg Pathol, 1988. **12**(12): p. 897-906.

27. Bostwick, D.G., et al., *Prostatic intraepithelial neoplasia and well differentiated adenocarcinoma maintain an intact basement membrane.* Pathol Res Pract, 1995. **191**(9): p. 850-5.

28. Sakr, W.A., et al., *The frequency of carcinoma and intraepithelial neoplasia of the prostate in young male patients.* J Urol, 1993. **150**(2 Pt 1): p. 379-85.

29. Braun, M. and S. Perner, *[High-grade prostatic intraepithelial neoplasia: the only accepted prostate cancer precursor lesion].* Pathologe, 2011. **32 Suppl 2**: p. 237-41.

30. Zynger, D.L. and X. Yang, *High-grade prostatic intraepithelial neoplasia of the prostate: the precursor lesion of prostate cancer.* Int J Clin Exp Pathol, 2009. **2**(4): p. 327-38.

31. Jemal, A., et al., *Cancer statistics, 2003.* CA Cancer J Clin, 2003. **53**(1): p. 5-26.

32. Jemal, A., et al., *Cancer statistics, 2005.* CA Cancer J Clin, 2005. **55**(1): p. 10-30.

33. Klein, S., *Treatment resistance in prostate cancer: a stem cell perspective*, in *Stem cells and regenerative medicine*2012, Springer.

34. Isaacs, W., A. De Marzo, and W.G. Nelson, *Focus on prostate cancer.* Cancer Cell, 2002. **2**(2): p. 113-6.

35. Sakr, W.A., et al., *High grade prostatic intraepithelial neoplasia (HGPIN) and prostatic adenocarcinoma between the ages of 20-69: an autopsy study of 249 cases.* In Vivo, 1994. **8**(3): p. 439-43.

36. Boring, C.C., et al., *Cancer statistics, 1994.* CA Cancer J Clin, 1994. **44**(1): p. 7-26.

37. Sonn, G.A., W. Aronson, and M.S. Litwin, *Impact of diet on prostate cancer: a review.* Prostate Cancer Prostatic Dis, 2005. **8**(4): p. 304-10.

38. Hudson, M.A., R.R. Bahnson, and W.J. Catalona, *Clinical use of prostate specific antigen in patients with prostate cancer.* J Urol, 1989. **142**(4): p. 1011-7.

39. Brawer, M.K., *Prostate-specific antigen: current status.* CA Cancer J Clin, 1999. **49**(5): p. 264-81.

40. Levesque, M., et al., *Immunoreactive prostate-specific antigen in lung tumors.* J Clin Lab Anal, 1995. **9**(6): p. 375-9.

41. Baron, J.C., et al., *Prostate-specific antigen in prostatic cancer.* Am J Clin Oncol, 1988. **11 Suppl 2**: p. S75-6.

42. Ferrero Doria, R., et al., *[Impact of prostatic benign hyperplasia and prostatic inflammation on the increase of prostate specific antigen levels].* Actas Urol Esp, 1997. **21**(2): p. 100-4.

43. Thompson, I.M., et al., *Prevalence of prostate cancer among men with a prostate-specific antigen level < or =4.0 ng per milliliter.* N Engl J Med, 2004. **350**(22): p. 2239-46.

44. Gleason, D.F., *Classification of prostatic carcinomas.* Cancer chemotherapy reports. Part 1, 1966. **50**(3): p. 125-8.

45. Pierorazio, P., *Preoperative characteristics of high-Gleason disease predictive of favourable pathological and clinical outcomes at radical prostatectomy.* BJU Int, 2012.

46. Nguyen, K., *Prostate cancer grading: Gland segmentation and structural features.* Pattern Recognition Letters, 2011. **33**(7): p. 951.

47. Kollmeier, M.A. and M.J. Zelefsky, *Brachytherapy for clinically localized prostate cancer: optimal patient selection.* Archivos espanoles de urologia, 2011. **64**(8): p. 847-857.

48. Koontz, B.F. and W.R. Lee, *External beam radiation therapy for clinically localized prostate cancer: when and how we optimize with concurrent hormonal deprivation.* Archivos espanoles de urologia, 2011. **64**(8): p. 858-864.

49. Duchesne, G., *Localised prostate cancer - current treatment options.* Australian family physician, 2011. **40**(10): p. 768-71.

50. Massard, C., E. Deutsch, and J.C. Soria, *Tumour stem cell-targeted treatment: elimination or differentiation.* Ann Oncol, 2006. **17**(11): p. 1620-4.

51. Gomella, L.G., et al., *Hormone therapy in the management of prostate cancer: evidence-based approaches.* Therapeutic advances in urology, 2010. **2**(4): p. 171-81.

52. Garcia, J.A. and B.I. Rini, *Castration-resistant prostate cancer: Many treatments, many options, many challenges ahead.* Cancer, 2011.

53. Garcia, J.A., et al., *Gemcitabine and docetaxel in metastatic, castrate-resistant prostate cancer: results from a phase 2 trial.* Cancer, 2011. **117**(4): p. 752-7.

54. Seruga, B. and I.F. Tannock, *Chemotherapy-based treatment for castration-resistant prostate cancer.* Journal of clinical oncology : official journal of the American Society of Clinical Oncology, 2011. **29**(27): p. 3686-94.

55. Sartor, O., et al., *Novel Therapeutic Strategies for Metastatic Prostate Cancer in the Post-Docetaxel Setting.* The oncologist, 2011.

56. Jones, J.S., *Radiorecurrent Prostate Cancer: An Emerging and Largely Mismanaged Epidemic.* European Urology, 2011.

57. Catton, C., et al., *Recurrent prostate cancer following external beam radiotherapy: follow-up strategies and management.* The Urologic clinics of North America, 2003. **30**(4): p. 751-63.

58. Ishkanian, A.S., et al., *Array CGH as a potential predictor of radiocurability in intermediate risk prostate cancer.* Acta oncologica, 2010. **49**(7): p. 888-94.

59. Zafarana, G. and R.G. Bristow, *Tumor senescence and radioresistant tumor-initiating cells (TICs): let sleeping dogs lie!* Breast cancer research : BCR, 2010. **12**(4): p. 111.

60. Gerritsen, W.R. and P. Sharma, *Current and Emerging Treatment Options for Castration-Resistant Prostate Cancer: A Focus on Immunotherapy.* Journal of clinical immunology, 2011.

61. Madan, R.A., et al., *Therapeutic vaccines in metastatic castration-resistant prostate cancer: principles in clinical trial design.* Expert opinion on biological therapy, 2010. **10**(1): p. 19-28.

62. Rivera-Gonzalez, G.C., et al., *Baculoviruses as gene therapy vectors for human prostate cancer.* Journal of invertebrate pathology, 2011. **107 Suppl**: p. S59-70.

63. Lindner, U., J. Trachtenberg, and N. Lawrentschuk, *Focal therapy in prostate cancer: modalities, findings and future considerations.* Nature reviews. Urology, 2010. **7**(10): p. 562-71.

64. (http://cancerhelp.cancerresearchuk.org/type/prostate-cancer/treatment/the-stages-of-prostate-cancer), C.R.U. 2012.

65. Lerner, I., et al., *Function of heparanase in prostate tumorigenesis: potential for therapy.* Clin Cancer Res, 2008. **14**(3): p. 668-76.

66. Cunha, G.R., et al., *Estrogenic effects on prostatic differentiation and carcinogenesis.* Reprod Fertil Dev, 2001. **13**(4): p. 285-96.

67. Abate-Shen, C. and M.M. Shen, *Molecular genetics of prostate cancer.* Genes Dev, 2000. **14**(19): p. 2410-34.

68. Dong, J.T., *Prevalent mutations in prostate cancer.* J Cell Biochem, 2006. **97**(3): p. 433-47.

69. Cerveira, N., et al., *TMPRSS2-ERG gene fusion causing ERG overexpression precedes chromosome copy number changes in prostate carcinomas and paired HGPIN lesions.* Neoplasia, 2006. **8**(10): p. 826-32.

70. Demichelis, F., et al., *TMPRSS2:ERG gene fusion associated with lethal prostate cancer in a watchful waiting cohort.* Oncogene, 2007. **26**(31): p. 4596-9.

71. Nakayama, M., et al., *GSTP1 CpG island hypermethylation as a molecular biomarker for prostate cancer.* J Cell Biochem, 2004. **91**(3): p. 540-52.

72. Pulukuri, S.M., et al., *Epigenetic inactivation of the tissue inhibitor of metalloproteinase-2 (TIMP-2) gene in human prostate tumors.* Oncogene, 2007. **26**(36): p. 5229-37.

73. DeClerck, Y.A., et al., *Inhibition of invasion and metastasis in cells transfected with an inhibitor of metalloproteinases.* Cancer Res, 1992. **52**(3): p. 701-8.

74. Taipale, J. and P.A. Beachy, *The Hedgehog and Wnt signalling pathways in cancer.* Nature, 2001. **411**(6835): p. 349-54.

75. Preston, S.L., et al., *The new stem cell biology: something for everyone.* Mol Pathol, 2003. **56**(2): p. 86-96.

76. Spangrude, G.J., S. Heimfeld, and I.L. Weissman, *Purification and characterization of mouse hematopoietic stem cells.* Science, 1988. **241**(4861): p. 58-62.

77. Raff, M., *Adult stem cell plasticity: fact or artifact?* Annu Rev Cell Dev Biol, 2003. **19**: p. 1-22.

78. Chen, Z., H.M. Sun, and X.Y. Yuan, *[Identification of human corneal epithelial stem cells].* Zhonghua Yan Ke Za Zhi, 2005. **41**(11): p. 1014-9.

79. Alvarez-Buylla, A., B. Seri, and F. Doetsch, *Identification of neural stem cells in the adult vertebrate brain.* Brain Res Bull, 2002. **57**(6): p. 751-8.

80. Wang, Y., et al., *Cell differentiation lineage in the prostate.* Differentiation, 2001. **68**(4-5): p. 270-9.

81. Androutsellis-Theotokis, A., et al., *Notch signalling regulates stem cell numbers in vitro and in vivo.* Nature, 2006. **442**(7104): p. 823-6.

82. Das, A.V., et al., *The canonical Wnt pathway regulates retinal stem cells/progenitors in concert with Notch signaling.* Dev Neurosci, 2008. **30**(6): p. 389-409.

83. Kalani, M.Y., et al., *Wnt-mediated self-renewal of neural stem/progenitor cells.* Proc Natl Acad Sci U S A, 2008. **105**(44): p. 16970-5.

84. Liu, S., et al., *Hedgehog signaling and Bmi-1 regulate self-renewal of normal and malignant human mammary stem cells.* Cancer Res, 2006. **66**(12): p. 6063-71.

85. Clarke, M.F., et al., *Cancer stem cells--perspectives on current status and future directions: AACR Workshop on cancer stem cells.* Cancer Res, 2006. **66**(19): p. 9339-44.

86. Clarke, M.F., *Cancer Stem Cells—Perspectives on Current Status and Future Directions: AACR Workshop on Cancer Stem Cells.* Cancer Res, 2006. **99**(19): p. 9339-9344.

87. Collins, A.T., et al., *Prospective identification of tumorigenic prostate cancer stem cells.* Cancer Res, 2005. **65**(23): p. 10946-51.

88. Bonnet, D. and J.E. Dick, *Human acute myeloid leukemia is organized as a hierarchy that originates from a primitive hematopoietic cell.* Nat Med, 1997. **3**(7): p. 730-7.

89. Boiko, A.D., et al., *Human melanoma-initiating cells express neural crest nerve growth factor receptor CD271.* Nature, 2010. **466**(7302): p. 133-7.

90. Bussolati, B., et al., *Identification of a tumor-initiating stem cell population in human renal carcinomas.* Faseb J, 2008. **22**(10): p. 3696-705.

91. Eramo, A., et al., *Identification and expansion of the tumorigenic lung cancer stem cell population.* Cell Death Differ, 2008. **15**(3): p. 504-14.

92. Ginestier, C., et al., *ALDH1 is a marker of normal and malignant human mammary stem cells and a predictor of poor clinical outcome.* Cell Stem Cell, 2007. **1**(5): p. 555-67.

93. Ma, S., et al., *Identification and characterization of tumorigenic liver cancer stem/progenitor cells.* Gastroenterology, 2007. **132**(7): p. 2542-56.

94. Rutella, S., et al., *Cells with characteristics of cancer stem/progenitor cells express the CD133 antigen in human endometrial tumors.* Clin Cancer Res, 2009. **15**(13): p. 4299-311.

95. Zhang, S., et al., *Identification and characterization of ovarian cancer-initiating cells from primary human tumors.* Cancer Res, 2008. **68**(11): p. 4311-20.

96. Chan, K.S., et al., *Identification, molecular characterization, clinical prognosis, and therapeutic targeting of human bladder tumor-initiating cells.* Proc Natl Acad Sci U S A, 2009. **106**(33): p. 14016-21.

97. Chiou, S.H., et al., *Identification of CD133-positive radioresistant cells in atypical teratoid/rhabdoid tumor.* PLoS One, 2008. **3**(5): p. e2090.

98. Prince, M.E., et al., *Identification of a subpopulation of cells with cancer stem cell properties in head and neck squamous cell carcinoma.* Proc Natl Acad Sci U S A, 2007. **104**(3): p. 973-8.

99. Schatton, T., et al., *Identification of cells initiating human melanomas.* Nature, 2008. **451**(7176): p. 345-9.

100. Al-Hajj, M., et al., *Therapeutic implications of cancer stem cells.* Curr Opin Genet Dev, 2004. **14**(1): p. 43-7.

101. Ricci-Vitiani, L., et al., *Identification and expansion of human colon-cancer-initiating cells.* Nature, 2007. **445**(7123): p. 111-5.

102. Singh, S.K., et al., *Identification of a cancer stem cell in human brain tumors.* Cancer Res, 2003. **63**(18): p. 5821-8.

103. Singh, S.K., et al., *Identification of human brain tumour initiating cells.* Nature, 2004. **432**(7015): p. 396-401.

104. Isaacs, J.T. and D.S. Coffey, *Etiology and disease process of benign prostatic hyperplasia.* Prostate Suppl, 1989. **2**: p. 33-50.

105. Isaacs, J.T., *Control of cell proliferation and cell death in the normal and neoplastic prostate: a stem cell model*, in *Benign Prostate Hyperplasia*, C.D. Rodgers CH, Gunha G, Grayhack JT, Hinman Jr F, Horton R, Editor 1987, NIH No.87-2881: Bethesda, MD. p. 85-94.

106. Richardson, G.D., et al., *CD133, a novel marker for human prostatic epithelial stem cells.* J Cell Sci, 2004. **117**(Pt 16): p. 3539-45.

107. Maitland, N.J., et al., *Prostate cancer stem cells: Do they have a basal or luminal phenotype?* Hormone and Cancer, 2010.

108. Oldridge, E.E., et al., *Prostate cancer stem cells: Are they androgen-responsive?* Molecular and cellular endocrinology, 2011.

109. Birnie, R., et al., *Gene expression profiling of human prostate cancer stem cells reveals a pro-inflammatory phenotype and the importance of extracellular matrix interactions.* Genome Biol, 2008. **9**(5): p. R83.

110. Fodde, R. and T. Brabletz, *Wnt/beta-catenin signaling in cancer stemness and malignant behavior.* Curr Opin Cell Biol, 2007. **19**(2): p. 150-8.

111. Verras, M. and Z. Sun, *Roles and regulation of Wnt signaling and beta-catenin in prostate cancer.* Cancer Lett, 2006. **237**(1): p. 22-32.

112. Dai, J., et al., *Prostate cancer induces bone metastasis through Wnt-induced bone morphogenetic protein-dependent and independent mechanisms.* Cancer Res, 2008. **68**(14): p. 5785-94.

113. Rajasekhar, V.K., et al., *Tumour-initiating stem-like cells in human prostate cancer exhibit increased NF-kappaB signalling.* Nature communications, 2011. **2**: p. 162.

114. Maitland, N.J. and A.T. Collins, *Cancer stem cells - A therapeutic target?* Current Opinion in Molecular Therapeutics, 2010. **12**(6): p. 662-673.

115. Taylor, R.A., R. Toivanen, and G.P. Risbridger, *Stem cells in prostate cancer: treating the root of the problem.* Endocrine-related cancer, 2010. **17**(4): p. R273-85.

116. Humphrey, P.A., *Diagnosis of adenocarcinoma in prostate needle biopsy tissue.* Journal of clinical pathology, 2007. **60**(1): p. 35-42.

117. Kasper, S., *Exploring the Origins of the Normal Prostate and Prostate Cancer Stem Cell.* Stem Cell Rev, 2008. **4**(4): p. 329.

118. Goldstein, A.S., et al., *Identification of a cell of origin for human prostate cancer.* Science, 2010. **329**(5991): p. 568-71.

119. Goldstein, A.S., T. Stoyanova, and O.N. Witte, *Primitive origins of prostate cancer: in vivo evidence for prostate-regenerating cells and prostate cancer-initiating cells.* Mol Oncol, 2010. **4**(5): p. 385-96.

120. Patrawala, L., et al., *Highly purified CD44+ prostate cancer cells from xenograft human tumors are enriched in tumorigenic and metastatic progenitor cells.* Oncogene, 2006. **25**(12): p. 1696-708.

121. Patrawala, L., et al., *Hierarchical organization of prostate cancer cells in xenograft tumors: the CD44+alpha2beta1+ cell population is enriched in tumor-initiating cells.* Cancer Res, 2007. **67**(14): p. 6796-805.

122. Trerotola, M., et al., *CD133, Trop-2 and alpha2beta1 integrin surface receptors as markers of putative human prostate cancer stem cells.* Am J Transl Res, 2010. **2**(2): p. 135-44.

123. Risbridger, G.P. and R.A. Taylor, *The complexities of identifying a cell of origin for human prostate cancer.* Asian journal of andrology, 2011. **13**(1): p. 118-9.

124. Frame, F.M. and N.J. Maitland, *Cancer Stem Cells, Models of Study and Implications of Therapy Resistance Mechanisms*, in *Human Cell Transformation - Role of Stem Cells and the Microenvironment* J.S. Rhim and R. Kremer, Editors. 2011, Springer Science + Business Media, LLC. p. 105-118.

125. Kenmore, D., *Investigation into the DNA damage induced cell cycle checkpoint responses of karyotypically normal and culture-adapted human embryonic stem cells* in *Institute for Cancer Studies*2011, University of Sheffield: Sheffield.

126. Leach, F.S., et al., *Mutations of a mutS homolog in hereditary nonpolyposis colorectal cancer.* Cell, 1993. **75**(6): p. 1215-25.

127. Savitsky, K., et al., *A single ataxia telangiectasia gene with a product similar to PI-3 kinase.* Science, 1995. **268**(5218): p. 1749-53.

128. Weeda, G., et al., *A presumed DNA helicase encoded by ERCC-3 is involved in the human repair disorders xeroderma pigmentosum and Cockayne's syndrome.* Cell, 1990. **62**(4): p. 777-91.

129. Hande, K.R., *Etoposide: four decades of development of a topoisomerase II inhibitor.* Eur J Cancer, 1998. **34**(10): p. 1514-21.

130. Wall, M.E., *Plant antitumor agents. I. The isolation and structure of camptothecin, a novel alkaloidal leukemia and tumor inhibitor from camptotheca acuminate*

. J. Am. Chem. Soc, 1966. **88**(16): p. 3888–3890.

131. Ulukan, H. and P.W. Swaan, *Camptothecins: a review of their chemotherapeutic potential.* Drugs, 2002. **62**(14): p. 2039-57.

132. Roland, P.S., *Ototoxicity*2004: BC Decker Inc. 221.

133. Knox, R.J., *Mechanism of cytotoxicity of anticancer platinum drugs: evidence that cis-diamminedichloroplatinum(II) and cis-diammine-(1,1-cyclobutanedicarboxylato)platinum(II) differ only in the kinetics of their interaction with DNA.* Cancer Res, 1986. **46**: p. 1972-1979.

134. Fornari, F.A., et al., *Interference by doxorubicin with DNA unwinding in MCF-7 breast tumor cells.* Mol Pharmacol, 1994. **45**(4): p. 649-56.

135. Momparler, R.L., et al., *Effect of adriamycin on DNA, RNA, and protein synthesis in cell-free systems and intact cells.* Cancer Res, 1976. **36**(8): p. 2891-5.

136. Montero, A., et al., *Docetaxel for treatment of solid tumours: a systematic review of clinical data.* Lancet Oncol, 2005. **6**(4): p. 229-39.

137. Eriksson, S., L. Thelander, and M. Akerman, *Allosteric regulation of calf thymus ribonucleoside diphosphate reductase.* Biochemistry, 1979. **18**(14): p. 2948-52.

138. Bjursell, G. and P. Reichard, *Effects of thymidine on deoxyribonucleoside triphosphate pools and deoxyribonucleic acid synthesis in Chinese hamster ovary cells.* J Biol Chem, 1973. **248**(11): p. 3904-9.

139. Banin, S., et al., *Enhanced phosphorylation of p53 by ATM in response to DNA damage.* Science, 1998. **281**(5383): p. 1674-7.

140. Lee, J.H. and T.T. Paull, *ATM activation by DNA double-strand breaks through the Mre11-Rad50-Nbs1 complex.* Science, 2005. **308**(5721): p. 551-4.

141. Cimprich, K.A. and D. Cortez, *ATR: an essential regulator of genome integrity.* Nat Rev Mol Cell Biol, 2008. **9**(8): p. 616-27.

142. Paull, T.T., et al., *A critical role for histone H2AX in recruitment of repair factors to nuclear foci after DNA damage.* Current biology : CB, 2000. **10**(15): p. 886-95.

143. Watters, G.P., et al., *H2AX phosphorylation as a genotoxicity endpoint.* Mutat Res, 2009. **679**(1-2): p. 50-8.

144. Khosravi, R., et al., *Rapid ATM-dependent phosphorylation of MDM2 precedes p53 accumulation in response to DNA damage.* Proc Natl Acad Sci U S A, 1999. **96**(26): p. 14973-7.

145. Lim, D.S., et al., *ATM phosphorylates p95/nbs1 in an S-phase checkpoint pathway.* Nature, 2000. **404**(6778): p. 613-7.

146. Xu, B., et al., *Phosphorylation of serine 1387 in Brca1 is specifically required for the Atm-mediated S-phase checkpoint after ionizing irradiation.* Cancer Res, 2002. **62**(16): p. 4588-91.

147. Petermann, E. and K.W. Caldecott, *Evidence that the ATR/Chk1 pathway maintains normal replication fork progression during unperturbed S phase.* Cell Cycle, 2006. **5**(19): p. 2203-9.

148. Byun, T.S., et al., *Functional uncoupling of MCM helicase and DNA polymerase activities activates the ATR-dependent checkpoint.* Genes Dev, 2005. **19**(9): p. 1040-52.

149. Walter, J. and J. Newport, *Initiation of eukaryotic DNA replication: origin unwinding and sequential chromatin association of Cdc45, RPA, and DNA polymerase alpha.* Mol Cell, 2000. **5**(4): p. 617-27.

150. Dart, D.A., et al., *Recruitment of the cell cycle checkpoint kinase ATR to chromatin during S-phase.* J Biol Chem, 2004. **279**(16): p. 16433-40.

151. Zou, L. and S.J. Elledge, *Sensing DNA damage through ATRIP recognition of RPA-ssDNA complexes.* Science, 2003. **300**(5625): p. 1542-8.

152. Parrilla-Castellar, E.R., S.J. Arlander, and L. Karnitz, *Dial 9-1-1 for DNA damage: the Rad9-Hus1-Rad1 (9-1-1) clamp complex.* DNA Repair (Amst), 2004. **3**(8-9): p. 1009-14.

153. Delacroix, S., et al., *The Rad9-Hus1-Rad1 (9-1-1) clamp activates checkpoint signaling via TopBP1.* Genes Dev, 2007. **21**(12): p. 1472-7.

154. Lee, J., A. Kumagai, and W.G. Dunphy, *The Rad9-Hus1-Rad1 checkpoint clamp regulates interaction of TopBP1 with ATR.* J Biol Chem, 2007. **282**(38): p. 28036-44.

155. Guo, Z., et al., *Requirement for Atr in phosphorylation of Chk1 and cell cycle regulation in response to DNA replication blocks and UV-damaged DNA in Xenopus egg extracts.* Genes Dev, 2000. **14**(21): p. 2745-56.

156. Liu, Q., et al., *Chk1 is an essential kinase that is regulated by Atr and required for the G(2)/M DNA damage checkpoint.* Genes Dev, 2000. **14**(12): p. 1448-59.

157. Zhao, H. and H. Piwnica-Worms, *ATR-mediated checkpoint pathways regulate phosphorylation and activation of human Chk1.* Mol Cell Biol, 2001. **21**(13): p. 4129-39.

158. Roos, W.P. and B. Kaina, *DNA damage-induced cell death by apoptosis.* Trends Mol Med, 2006. **12**(9): p. 440-50.

159. Jackson, S.P. and J. Bartek, *The DNA-damage response in human biology and disease.* Nature, 2009. **461**(7267): p. 1071-8.

160. Emanuel, P. and N. Scheinfeld, *A review of DNA repair and possible DNA-repair adjuvants and selected natural anti-oxidants.* Dermatol Online J, 2007. **13**(3): p. 10.

161. Lieber, M.R., et al., *Mechanism and regulation of human non-homologous DNA end-joining.* Nat Rev Mol Cell Biol, 2003. **4**(9): p. 712-20.

162. West, S.C., *Molecular views of recombination proteins and their control.* Nat Rev Mol Cell Biol, 2003. **4**(6): p. 435-45.

163. Davies, C.S., *Screening for gamma-ray hypersensitive mutants of Arabidopsis.* Methods Mol Biol, 1999. **113**: p. 41-8.

164. Bradley, M.O. and K.W. Kohn, *X-ray induced DNA double strand break production and repair in mammalian cells as measured by neutral filter elution.* Nucleic Acids Res, 1979. **7**(3): p. 793-804.

165. Pommier, Y., et al., *Repair of and checkpoint response to topoisomerase I-mediated DNA damage.* Mutat Res, 2003. **532**(1-2): p. 173-203.

166. Muslimovic, A., et al., *Numerical analysis of etoposide induced DNA breaks.* PLoS One, 2009. **4**(6): p. e5859.

167. Ame, J.C., et al., *PARP-2, A novel mammalian DNA damage-dependent poly(ADP-ribose) polymerase.* J Biol Chem, 1999. **274**(25): p. 17860-8.

168. Masson, M., et al., *XRCC1 is specifically associated with poly(ADP-ribose) polymerase and negatively regulates its activity following DNA damage.* Mol Cell Biol, 1998. **18**(6): p. 3563-71.

169. Matsumoto, Y. and K. Kim, *Excision of deoxyribose phosphate residues by DNA polymerase beta during DNA repair.* Science, 1995. **269**(5224): p. 699-702.

170. Sancar, A., et al., *Molecular mechanisms of mammalian DNA repair and the DNA damage checkpoints.* Annu Rev Biochem, 2004. **73**: p. 39-85.

171. Kuzminov, A., *Single-strand interruptions in replicating chromosomes cause double-strand breaks.* Proc Natl Acad Sci U S A, 2001. **98**(15): p. 8241-6.

172. Saleh-Gohari, N., et al., *Spontaneous homologous recombination is induced by collapsed replication forks that are caused by endogenous DNA single-strand breaks.* Mol Cell Biol, 2005. **25**(16): p. 7158-69.

173. Thode, S., et al., *A novel pathway of DNA end-to-end joining.* Cell, 1990. **60**(6): p. 921-8.

174. Gottlieb, T.M. and S.P. Jackson, *The DNA-dependent protein kinase: requirement for DNA ends and association with Ku antigen.* Cell, 1993. **72**(1): p. 131-42.

175. Ma, Y., et al., *Hairpin opening and overhang processing by an Artemis/DNA-dependent protein kinase complex in nonhomologous end joining and V(D)J recombination.* Cell, 2002. **108**(6): p. 781-94.

176. Koch, C.A., et al., *Xrcc4 physically links DNA end processing by polynucleotide kinase to DNA ligation by DNA ligase IV.* EMBO J, 2004. **23**(19): p. 3874-85.

177. Lee, J.W., et al., *Implication of DNA polymerase lambda in alignment-based gap filling for nonhomologous DNA end joining in human nuclear extracts.* J Biol Chem, 2004. **279**(1): p. 805-11.

178. Calsou, P., et al., *Coordinated assembly of Ku and p460 subunits of the DNA-dependent protein kinase on DNA ends is necessary for XRCC4-ligase IV recruitment.* J Mol Biol, 2003. **326**(1): p. 93-103.

179. Jazayeri, A., et al., *ATM- and cell cycle-dependent regulation of ATR in response to DNA double-strand breaks.* Nat Cell Biol, 2006. **8**(1): p. 37-45.

180. Ogawa, T., et al., *Similarity of the yeast RAD51 filament to the bacterial RecA filament.* Science, 1993. **259**(5103): p. 1896-9.

181. Sung, P., *Catalysis of ATP-dependent homologous DNA pairing and strand exchange by yeast RAD51 protein.* Science, 1994. **265**(5176): p. 1241-3.

182. Holliday, R., *A mechanism for gene conversion in fungi.* Genet. Res., 1964. **5**: p. 282-304.

183. McIlwraith, M.J., et al., *Human DNA polymerase eta promotes DNA synthesis from strand invasion intermediates of homologous recombination.* Mol Cell, 2005. **20**(5): p. 783-92.

184. Iijima, K., et al., *Dancing on damaged chromatin: functions of ATM and the RAD50/MRE11/NBS1 complex in cellular responses to DNA damage.* J Radiat Res, 2008. **49**(5): p. 451-64.

185. Davies, S.L., et al., *Phosphorylation of the Bloom's syndrome helicase and its role in recovery from S-phase arrest.* Mol Cell Biol, 2004. **24**(3): p. 1279-91.

186. Tibbetts, R.S., et al., *Functional interactions between BRCA1 and the checkpoint kinase ATR during genotoxic stress.* Genes Dev, 2000. **14**(23): p. 2989-3002.

187. Pichierri, P., F. Rosselli, and A. Franchitto, *Werner's syndrome protein is phosphorylated in an ATR/ATM-dependent manner following replication arrest and DNA damage induced during the S phase of the cell cycle.* Oncogene, 2003. **22**(10): p. 1491-500.

188. Li, W., et al., *Absence of BLM leads to accumulation of chromosomal DNA breaks during both unperturbed and disrupted S phases.* J Cell Biol, 2004. **165**(6): p. 801-12.

189. Saha, T., M. Smulson, and E.M. Rosen, *BRCA1 regulation of base excision repair pathway.* Cell Cycle, 2010. **9**(13): p. 2471-2.

190. Weinert, T. and L. Hartwell, *Control of G2 delay by the rad9 gene of Saccharomyces cerevisiae.* J Cell Sci Suppl, 1989. **12**: p. 145-8.

191. Bohnsack, B.L. and K.K. Hirschi, *Nutrient regulation of cell cycle progression.* Annu Rev Nutr, 2004. **24**: p. 433-53.

192. Johnston, G.C., J.R. Pringle, and L.H. Hartwell, *Coordination of growth with cell division in the yeast Saccharomyces cerevisiae.* Exp Cell Res, 1977. **105**(1): p. 79-98.

193. King, K.L. and J.A. Cidlowski, *Cell cycle regulation and apoptosis.* Annu Rev Physiol, 1998. **60**: p. 601-17.

194. Dasika, G.K., et al., *DNA damage-induced cell cycle checkpoints and DNA strand break repair in development and tumorigenesis.* Oncogene, 1999. **18**(55): p. 7883-99.

195. Paulovich, A.G. and L.H. Hartwell, *A checkpoint regulates the rate of progression through S phase in S. cerevisiae in response to DNA damage.* Cell, 1995. **82**(5): p. 841-7.

196. Willis, N. and N. Rhind, *Regulation of DNA replication by the S-phase DNA damage checkpoint.* Cell Div, 2009. **4**: p. 13.

197. Bartek, J. and J. Lukas, *Mammalian G1- and S-phase checkpoints in response to DNA damage.* Curr Opin Cell Biol, 2001. **13**(6): p. 738-47.

198. Molinari, M., et al., *Human Cdc25 A inactivation in response to S phase inhibition and its role in preventing premature mitosis.* EMBO Rep, 2000. **1**(1): p. 71-9.

199. Falck, J., et al., *The ATM-Chk2-Cdc25A checkpoint pathway guards against radioresistant DNA synthesis.* Nature, 2001. **410**(6830): p. 842-7.

200. Xu, B., et al., *Two molecularly distinct G(2)/M checkpoints are induced by ionizing irradiation.* Mol Cell Biol, 2002. **22**(4): p. 1049-59.

201. Brown, E.J. and D. Baltimore, *Essential and dispensable roles of ATR in cell cycle arrest and genome maintenance.* Genes Dev, 2003. **17**(5): p. 615-28.

202. Elmore, S., *Apoptosis: a review of programmed cell death.* Toxicol Pathol, 2007. **35**(4): p. 495-516.

203. Saelens, X., et al., *Toxic proteins released from mitochondria in cell death.* Oncogene, 2004. **23**(16): p. 2861-74.

204. Lavrik, I.N., A. Golks, and P.H. Krammer, *Caspases: pharmacological manipulation of cell death.* J Clin Invest, 2005. **115**(10): p. 2665-72.

205. Chinnaiyan, A.M., *The apoptosome: heart and soul of the cell death machine.* Neoplasia, 1999. **1**(1): p. 5-15.

206. Hill, M.M., et al., *Analysis of the composition, assembly kinetics and activity of native Apaf-1 apoptosomes.* EMBO J, 2004. **23**(10): p. 2134-45.

207. Cory, S. and J.M. Adams, *The Bcl2 family: regulators of the cellular life-or-death switch.* Nat Rev Cancer, 2002. **2**(9): p. 647-56.

208. Matsuoka, S., M. Huang, and S.J. Elledge, *Linkage of ATM to cell cycle regulation by the Chk2 protein kinase.* Science, 1998. **282**(5395): p. 1893-7.

209. Ahn, J.Y., et al., *Threonine 68 phosphorylation by ataxia telangiectasia mutated is required for efficient activation of Chk2 in response to ionizing radiation.* Cancer Res, 2000. **60**(21): p. 5934-6.

210. Fernandez-Capetillo, O., et al., *DNA damage-induced G2-M checkpoint activation by histone H2AX and 53BP1.* Nat Cell Biol, 2002. **4**(12): p. 993-7.

211. Cortez, D., et al., *Requirement of ATM-dependent phosphorylation of brca1 in the DNA damage response to double-strand breaks.* Science, 1999. **286**(5442): p. 1162-6.

212. Schuler, M. and D.R. Green, *Mechanisms of p53-dependent apoptosis.* Biochemical Society transactions, 2001. **29**(Pt 6): p. 684-8.

213. Noda, T., K. Suzuki, and Y. Ohsumi, *Yeast autophagosomes: de novo formation of a membrane structure.* Trends Cell Biol, 2002. **12**(5): p. 231-5.

214. Cohen, J.J., *Programmed cell death in the immune system.* Adv Immunol, 1991. **50**: p. 55-85.

215. Marino, G. and C. Lopez-Otin, *Autophagy: molecular mechanisms, physiological functions and relevance in human pathology.* Cell Mol Life Sci, 2004. **61**(12): p. 1439-54.

216. Mizushima, N., *Autophagy: process and function.* Genes Dev, 2007. **21**(22): p. 2861-73.

217. Kondo, Y., et al., *The role of autophagy in cancer development and response to therapy.* Nat Rev Cancer, 2005. **5**(9): p. 726-34.

218. DiPaola, R.S., et al., *Therapeutic starvation and autophagy in prostate cancer: a new paradigm for targeting metabolism in cancer therapy.* Prostate, 2008. **68**(16): p. 1743-52.

219. Saleem, A., et al., *Effect of dual inhibition of apoptosis and autophagy in prostate cancer.* Prostate, 2012.

220. Huang, S. and F.A. Sinicrope, *Celecoxib-induced apoptosis is enhanced by ABT-737 and by inhibition of autophagy in human colorectal cancer cells.* Autophagy, 2010. **6**(2): p. 256-69.

221. Maiuri, M.C., et al., *Self-eating and self-killing: crosstalk between autophagy and apoptosis.* Nat Rev Mol Cell Biol, 2007. **8**(9): p. 741-52.

222. Dunn, W.A., Jr., *Studies on the mechanisms of autophagy: formation of the autophagic vacuole.* J Cell Biol, 1990. **110**(6): p. 1923-33.

223. Furuno, K., et al., *Immunocytochemical study of the surrounding envelope of autophagic vacuoles in cultured rat hepatocytes.* Exp Cell Res, 1990. **189**(2): p. 261-8.

224. Suzuki, K., et al., *Hierarchy of Atg proteins in pre-autophagosomal structure organization.* Genes Cells, 2007. **12**(2): p. 209-18.

225. Rosenfeldt, M.T. and K.M. Ryan, *The multiple roles of autophagy in cancer.* Carcinogenesis, 2011. **32**(7): p. 955-63.

226. Schmitt, C.A., *Cellular senescence and cancer treatment.* Biochim Biophys Acta, 2007. **1775**(1): p. 5-20.

227. Herbig, U., et al., *Telomere shortening triggers senescence of human cells through a pathway involving ATM, p53, and p21(CIP1), but not p16(INK4a).* Mol Cell, 2004. **14**(4): p. 501-13.

228. d'Adda di Fagagna, F., S.H. Teo, and S.P. Jackson, *Functional links between telomeres and proteins of the DNA-damage response.* Genes Dev, 2004. **18**(15): p. 1781-99.

229. Chen, Q. and B.N. Ames, *Senescence-like growth arrest induced by hydrogen peroxide in human diploid fibroblast F65 cells.* Proc Natl Acad Sci U S A, 1994. **91**(10): p. 4130-4.

230. MacLaren, A., et al., *c-Jun-deficient cells undergo premature senescence as a result of spontaneous DNA damage accumulation.* Mol Cell Biol, 2004. **24**(20): p. 9006-18.

231. von Zglinicki, T., et al., *Human cell senescence as a DNA damage response.* Mech Ageing Dev, 2005. **126**(1): p. 111-7.

232. Elmore, L.W., et al., *Adriamycin-induced senescence in breast tumor cells involves functional p53 and telomere dysfunction.* J Biol Chem, 2002. **277**(38): p. 35509-15.

233. Suzuki, K., et al., *Radiation-induced senescence-like growth arrest requires TP53 function but not telomere shortening.* Radiat Res, 2001. **155**(1 Pt 2): p. 248-253.

234. Han, Z., et al., *Role of p21 in apoptosis and senescence of human colon cancer cells treated with camptothecin.* J Biol Chem, 2002. **277**(19): p. 17154-60.

235. Beausejour, C.M., et al., *Reversal of human cellular senescence: roles of the p53 and p16 pathways.* EMBO J, 2003. **22**(16): p. 4212-22.

236. Dirac, A.M. and R. Bernards, *Reversal of senescence in mouse fibroblasts through lentiviral suppression of p53.* J Biol Chem, 2003. **278**(14): p. 11731-4.

237. Dean, M., T. Fojo, and S. Bates, *Tumour stem cells and drug resistance.* Nat Rev Cancer, 2005. **5**(4): p. 275-84.

238. Ishii, H., et al., *Cancer stem cells and chemoradiation resistance.* Cancer Sci, 2008. **99**(10): p. 1871-7.

239. Rich, J.N., *Cancer stem cells in radiation resistance.* Cancer research, 2007. **67**(19): p. 8980-4.

240. Luo, L.Z., et al., *DNA repair in human pluripotent stem cells is distinct from that in non-pluripotent human cells.* PLoS One, 2012. **7**(3): p. e30541.

241. Krishnamurthy, P., et al., *The stem cell marker Bcrp/ABCG2 enhances hypoxic cell survival through interactions with heme.* J Biol Chem, 2004. **279**(23): p. 24218-25.

242. Moore, N. and S. Lyle, *Quiescent, slow-cycling stem cell populations in cancer: a review of the evidence and discussion of significance.* J Oncol, 2011. **2011**.

243. Scharenberg, C.W., M.A. Harkey, and B. Torok-Storb, *The ABCG2 transporter is an efficient Hoechst 33342 efflux pump and is preferentially expressed by immature human hematopoietic progenitors.* Blood, 2002. **99**(2): p. 507-12.

244. Eyler, C.E. and J.N. Rich, *Survival of the fittest: cancer stem cells in therapeutic resistance and angiogenesis.* J Clin Oncol, 2008. **26**(17): p. 2839-45.

245. Baumann, M., M. Krause, and R. Hill, *Exploring the role of cancer stem cells in radioresistance.* Nat Rev Cancer, 2008. **8**(7): p. 545-54.

246. Morrison, R., et al., *Targeting the mechanisms of resistance to chemotherapy and radiotherapy with the cancer stem cell hypothesis.* J Oncol, 2011. **2011**: p. 941876.

247. Bao, S., et al., *Glioma stem cells promote radioresistance by preferential activation of the DNA damage response.* Nature, 2006. **444**(7120): p. 756-60.

248. Hambardzumyan, D., M. Squatrito, and E.C. Holland, *Radiation resistance and stem-like cells in brain tumors.* Cancer Cell, 2006. **10**(6): p. 454-6.

249. Gao, M.Q., et al., *CD24+ cells from hierarchically organized ovarian cancer are enriched in cancer stem cells.* Oncogene, 2010. **29**(18): p. 2672-80.

250. Mani, S.A., et al., *The epithelial-mesenchymal transition generates cells with properties of stem cells.* Cell, 2008. **133**(4): p. 704-15.

251. Naumov, G.N., et al., *Ineffectiveness of doxorubicin treatment on solitary dormant mammary carcinoma cells or late-developing metastases.* Breast Cancer Res Treat, 2003. **82**(3): p. 199-206.

252. Lim, H.W., et al., *Up-regulation of defense enzymes is responsible for low reactive oxygen species in malignant prostate cancer cells.* Exp Mol Med, 2005. **37**(5): p. 497-506.

253. Graves, J.A., et al., *Regulation of reactive oxygen species homeostasis by peroxiredoxins and c-Myc.* J Biol Chem, 2009. **284**(10): p. 6520-9.

254. Diehn, M., et al., *Association of reactive oxygen species levels and radioresistance in cancer stem cells.* Nature, 2009. **458**(7239): p. 780-3.

255. Hisaoka, T., et al., *[A case of subacute thyroiditis with highly positive thyrotropin receptor antibodies and normal radioiodine uptake].* Nippon Naibunpi Gakkai Zasshi, 1993. **69**(9): p. 997-1002.

256. Ito, K., et al., *Regulation of oxidative stress by ATM is required for self-renewal of haematopoietic stem cells.* Nature, 2004. **431**(7011): p. 997-1002.

257. Ito, K., et al., *Reactive oxygen species act through p38 MAPK to limit the lifespan of hematopoietic stem cells.* Nat Med, 2006. **12**(4): p. 446-51.

258. Miyamoto, K., et al., *Foxo3a is essential for maintenance of the hematopoietic stem cell pool.* Cell Stem Cell, 2007. **1**(1): p. 101-12.

259. Smith, J., et al., *Redox state is a central modulator of the balance between self-renewal and differentiation in a dividing glial precursor cell.* Proc Natl Acad Sci U S A, 2000. **97**(18): p. 10032-7.

260. Tothova, Z., et al., *FoxOs are critical mediators of hematopoietic stem cell resistance to physiologic oxidative stress.* Cell, 2007. **128**(2): p. 325-39.

261. Tsatmali, M., E.C. Walcott, and K.L. Crossin, *Newborn neurons acquire high levels of reactive oxygen species and increased mitochondrial proteins upon differentiation from progenitors.* Brain Res, 2005. **1040**(1-2): p. 137-50.

262. Chuthapisith, S., *Cancer Stem Cells and Chemoresistance*, in *Cancer Stem Cells Theories and Practice*, S. Shostak, Editor 2011, InTech.

263. Chuthapisith, S., et al., *Breast cancer chemoresistance: Emerging importance of cancer stem cells.* Surg Oncol, 2009.

264. Hirschmann-Jax, C., et al., *A distinct "side population" of cells with high drug efflux capacity in human tumor cells.* Proc Natl Acad Sci U S A, 2004. **101**(39): p. 14228-33.

265. Dean, M., *ABC transporters, drug resistance, and cancer stem cells.* J Mammary Gland Biol Neoplasia, 2009. **14**(1): p. 3-9.

266. Sanchez, C., et al., *Expression of multidrug resistance proteins in prostate cancer is related with cell sensitivity to chemotherapeutic drugs.* Prostate, 2009. **69**(13): p. 1448-59.

267.   Sanchez, C., et al., *Chemotherapy sensitivity recovery of prostate cancer cells by functional inhibition and knock down of multidrug resistance proteins.* Prostate, 2011. **71**(16): p. 1810-7.

268.   Ischenko, I., et al., *Cancer Stem Cells: How can we Target them?* Curr Med Chem, 2008. **15**(30): p. 3171-84.

269.   Hambardzumyan, D., et al., *PI3K pathway regulates survival of cancer stem cells residing in the perivascular niche following radiation in medulloblastoma in vivo.* Genes Dev, 2008. **22**(4): p. 436-48.

270.   Iannolo, G., et al., *Apoptosis in normal and cancer stem cells.* Crit Rev Oncol Hematol, 2008. **66**(1): p. 42-51.

271.   Todaro, M., et al., *Apoptosis resistance in epithelial tumors is mediated by tumor-cell-derived interleukin-4.* Cell Death Differ, 2008. **15**(4): p. 762-72.

272.   Francipane, M.G., et al., *Crucial role of interleukin-4 in the survival of colon cancer stem cells.* Cancer Res, 2008. **68**(11): p. 4022-5.

273.   Lou, H. and M. Dean, *Targeted therapy for cancer stem cells: the patched pathway and ABC transporters.* Oncogene, 2007. **26**(9): p. 1357-60.

274.   Miki, J., et al., *Identification of putative stem cell markers, CD133 and CXCR4, in hTERT-immortalized primary nonmalignant and malignant tumor-derived human prostate epithelial cell lines and in prostate cancer specimens.* Cancer Res, 2007. **67**(7): p. 3153-61.

275.   Gallmeier, E., et al., *Novel genotoxicity assays identify norethindrone to activate p53 and phosphorylate H2AX.* Carcinogenesis, 2005. **26**(10): p. 1811-20.

276.   Lobrich, M., et al., *gammaH2AX foci analysis for monitoring DNA double-strand break repair: strengths, limitations and optimization.* Cell Cycle, 2010. **9**(4): p. 662-9.

277.   Montecucco, A. and G. Biamonti, *Cellular response to etoposide treatment.* Cancer Lett, 2007. **252**(1): p. 9-18.

278.   Scholzen, T. and J. Gerdes, *The Ki-67 protein: from the known and the unknown.* J Cell Physiol, 2000. **182**(3): p. 311-22.

279.   Boumendjel, A., *ABC Transporters and Multidrug Resistance*, ed. B. Wang2009: WILEY.

280.   Sharom, F.J., *ABC multidrug transporters: structure, function and role in chemoresistance.* Pharmacogenomics, 2008. **9**(1): p. 105-27.

281.   Lebedeva, I.V., P. Pande, and W.F. Patton, *Sensitive and specific fluorescent probes for functional analysis of the three major types of mammalian ABC transporters.* PLoS One, 2011. **6**(7): p. e22429.

282.   de Feraudy, S., et al., *A minority of foci or pan-nuclear apoptotic staining of gammaH2AX in the S phase after UV damage contain DNA double-strand breaks.* Proc Natl Acad Sci U S A, 2010. **107**(15): p. 6870-5.

283.   Bonner, W.M., et al., *GammaH2AX and cancer.* Nat Rev Cancer, 2008. **8**(12): p. 957-67.

284.   Gagou, M.E., P. Zuazua-Villar, and M. Meuth, *Enhanced H2AX phosphorylation, DNA replication fork arrest, and cell death in the absence of Chk1.* Mol Biol Cell, 2010. **21**(5): p. 739-52.

285.   Hussein, D., et al., *Pediatric brain tumor cancer stem cells: cell cycle dynamics, DNA repair, and etoposide extrusion.* Neuro Oncol, 2011. **13**(1): p. 70-83.

286.   Kim, J.H., et al., *Salinomycin sensitizes cancer cells to the effects of doxorubicin and etoposide treatment by increasing DNA damage and reducing p21 protein.* Br J Pharmacol, 2011. **162**(3): p. 773-84.

287.   Gupta, P.B., et al., *Identification of selective inhibitors of cancer stem cells by high-throughput screening.* Cell, 2009. **138**(4): p. 645-59.

288. Velichko, A.K., et al., *Sensitivity of human embryonic and induced pluripotent stem cells to a topoisomerase II poison etoposide.* Cell Cycle, 2011. **10**(12): p. 2035-7.

289. Chen, Y., et al., *Quiescence and attenuated DNA damage response promote survival of esophageal cancer stem cells.* J Cell Biochem, 2012.

290. Buczacki, S., R.J. Davies, and D.J. Winton, *Stem cells, quiescence and rectal carcinoma: an unexplored relationship and potential therapeutic target.* Br J Cancer, 2011. **105**(9): p. 1253-9.

291. Zhang, Z., et al., *Differential epithelium DNA damage response to ATM and DNA-PK pathway inhibition in human prostate tissue culture.* Cell Cycle, 2011. **10**(20): p. 3545-53.

292. Tanaka, T., et al., *Induction of ATM activation, histone H2AX phosphorylation and apoptosis by etoposide: relation to cell cycle phase.* Cell Cycle, 2007. **6**(3): p. 371-6.

293. Stow, P., et al., *Clinical significance of low levels of minimal residual disease at the end of remission induction therapy in childhood acute lymphoblastic leukemia.* Blood, 2010. **115**(23): p. 4657-63.

294. Wang, L., et al., *[Clinical significance of sequential monitoring minimal residual disease in childhood B-cell acute lymphoblastic leukemia].* Zhonghua Xue Ye Xue Za Zhi, 2011. **32**(6): p. 400-3.

295. Hosch, S.B., P. Scheunemann, and J.R. Izbicki, *Minimal residual disease in non-small-cell lung cancer.* Semin Surg Oncol, 2001. **20**(4): p. 278-81.

296. Ignatiadis, M., C. Sotiriou, and K. Pantel, *Minimal Residual Disease and Circulating Tumor Cells in Breast Cancer: Open Questions for Research.* Recent Results Cancer Res, 2012. **195**: p. 3-9.

297. Blanpain, C., et al., *DNA-damage response in tissue-specific and cancer stem cells.* Cell Stem Cell, 2011. **8**(1): p. 16-29.

298. Wilson, A., et al., *Hematopoietic stem cells reversibly switch from dormancy to self-renewal during homeostasis and repair.* Cell, 2008. **135**(6): p. 1118-29.

299. Mathew, G., et al., *ABCG2-mediated DyeCycle Violet efflux defined side population in benign and malignant prostate.* Cell Cycle, 2009. **8**(7): p. 1053-61.

300. Pascal, L.E., et al., *Molecular and cellular characterization of ABCG2 in the prostate.* BMC urology, 2007. **7**: p. 6.

301. Sissung, T.M., et al., *ABCB1 genetic variation influences the toxicity and clinical outcome of patients with androgen-independent prostate cancer treated with docetaxel.* Clinical cancer research : an official journal of the American Association for Cancer Research, 2008. **14**(14): p. 4543-9.

302. Kawai, K., et al., *Demonstration of MDR1 P-glycoprotein isoform expression in benign and malignant human prostate cells by isoform-specific monoclonal antibodies.* Cancer Lett, 2000. **150**(2): p. 147-53.

303. Van Brussel, J.P., et al., *Expression of multidrug resistance related proteins and proliferative activity is increased in advanced clinical prostate cancer.* J Urol, 2001. **165**(1): p. 130-5.

304. Huss, W.J., et al., *Breast cancer resistance protein-mediated efflux of androgen in putative benign and malignant prostate stem cells.* Cancer research, 2005. **65**(15): p. 6640-50.

305. Brown, M.D., et al., *Characterization of benign and malignant prostate epithelial Hoechst 33342 side populations.* Prostate, 2007. **67**(13): p. 1384-96.

306. Pommier, Y., et al., *Targeting chk2 kinase: molecular interaction maps and therapeutic rationale.* Current pharmaceutical design, 2005. **11**(22): p. 2855-72.

307. Ide, H., et al., *DNA damage response in prostate cancer cells after high-intensity focused ultrasound (HIFU) treatment.* Anticancer Res, 2008. **28**(2A): p. 639-43.

308. Catz, S.D. and J.L. Johnson, *BCL-2 in prostate cancer: a minireview.* Apoptosis : an international journal on programmed cell death, 2003. **8**(1): p. 29-37.

309. Pickard, M.R., et al., *Apoptosis regulators Fau and Bcl-G are down-regulated in prostate cancer.* Prostate, 2010. **70**(14): p. 1513-23.

310. Diaz, A., *Therapeutic Approaches to Target Cancer Stem Cells.* Cancers, 2011. **3**(3): p. 3331-3352.

311. Visvader, J.E. and G.J. Lindeman, *Cancer stem cells in solid tumours: accumulating evidence and unresolved questions.* Nat Rev Cancer, 2008. **8**(10): p. 755-68.

312. Rossi, D.J., et al., *Deficiencies in DNA damage repair limit the function of haematopoietic stem cells with age.* Nature, 2007. **447**(7145): p. 725-9.

313. Aguirre-Ghiso, J.A., *Models, mechanisms and clinical evidence for cancer dormancy.* Nat Rev Cancer, 2007. **7**(11): p. 834-46.

314. Trumpp, A. and O.D. Wiestler, *Mechanisms of Disease: cancer stem cells--targeting the evil twin.* Nature clinical practice. Oncology, 2008. **5**(6): p. 337-47.

315. Pece, S., et al., *Biological and molecular heterogeneity of breast cancers correlates with their cancer stem cell content.* Cell, 2010. **140**(1): p. 62-73.

316. Dembinski, J.L. and S. Krauss, *Characterization and functional analysis of a slow cycling stem cell-like subpopulation in pancreas adenocarcinoma.* Clin Exp Metastasis, 2009. **26**(7): p. 611-23.

317. Dionne, C.A., et al., *Cell cycle-independent death of prostate adenocarcinoma is induced by the trk tyrosine kinase inhibitor CEP-751 (KT6587).* Clin Cancer Res, 1998. **4**(8): p. 1887-98.

318. Jorgensen, H.G., et al., *Intermittent exposure of primitive quiescent chronic myeloid leukemia cells to granulocyte-colony stimulating factor in vitro promotes their elimination by imatinib mesylate.* Clin Cancer Res, 2006. **12**(2): p. 626-33.

319. Kaufmann, S.H. and W.C. Earnshaw, *Induction of apoptosis by cancer chemotherapy.* Exp Cell Res, 2000. **256**(1): p. 42-9.

320. Wang, P., et al., *Role of death receptor and mitochondrial pathways in conventional chemotherapy drug induction of apoptosis.* Cell Signal, 2006. **18**(9): p. 1528-35.

321. Wotawa, A., et al., *Differential influence of etoposide on two caspase-2 mRNA isoforms in leukemic cells.* Cancer Lett, 2002. **185**(2): p. 181-9.

322. Bubendorf, L., et al., *Prognostic significance of Bcl-2 in clinically localized prostate cancer.* The American journal of pathology, 1996. **148**(5): p. 1557-65.

323. Chi, S.G., et al., *p53 in prostate cancer: frequent expressed transition mutations.* J Natl Cancer Inst, 1994. **86**(12): p. 926-33.

324. Gumerlock, P.H., et al., *p53 abnormalities in primary prostate cancer: single-strand conformation polymorphism analysis of complementary DNA in comparison with genomic DNA. The Cooperative Prostate Network.* J Natl Cancer Inst, 1997. **89**(1): p. 66-71.

325. Aimola, P., et al., *Cadmium induces p53-dependent apoptosis in human prostate epithelial cells.* PLoS One, 2012. **7**(3): p. e33647.

326. Kao, J., et al., *gamma-H2AX as a therapeutic target for improving the efficacy of radiation therapy.* Curr Cancer Drug Targets, 2006. **6**(3): p. 197-205.

327. Jin, F., et al., *Influence of Etoposide on anti-apoptotic and multidrug resistance-associated protein genes in CD133 positive U251 glioblastoma stem-like cells.* Brain Res, 2010. **1336**: p. 103-11.

328. Sullivan, G.F., et al., *The expression of drug resistance gene products during the progression of human prostate cancer.* Clin Cancer Res, 1998. **4**(6): p. 1393-403.

329. Leonard, G.D., T. Fojo, and S.E. Bates, *The role of ABC transporters in clinical practice.* The oncologist, 2003. **8**(5): p. 411-24.